NASA CONTRACTOR REPORT

NASA CR-2122

NASA CR-2122

ANALYTICAL AND EXPERIMENTAL INVESTIGATION OF AIRCRAFT METAL STRUCTURES REINFORCED WITH FILAMENTARY COMPOSITES

Phase III - Major Component Development

by L. L. Bryson and J. E. McCarty

Prepared by
BOEING COMMERCIAL AIRPLANE COMPANY
Seattle, Wash. 98124
for Langley Research Center

NATIONAL AERONAUTICS AND SPACE ADMINISTRATION • WASHINGTON, D. C. • NOVEMBER 1973

1. Report No.	2. Government Accession No.	3. Recipient's Catalog No.
NASA CR-2122		

4. Title and Subtitle	5. Report Date
Analytical and Experimental Investigation of Aircraft Metal Structures Reinforced With Filamentary Composites: Phase III, Major Component Development	November 1973
	6. Performing Organization Code
7. Author(s)	8. Performing Organization Report No.
L. L. Bryson and J. E. McCarty	D6-60136-3
	10. Work Unit No.
9. Performing Organization Name and Address	11. Contract or Grant No.
Boeing Commercial Airplane Company P.O. Box 3707 Seattle, Washington 98124	NAS1-8858
	13. Type of Report and Period Covered
12. Sponsoring Agency Name and Address	Contractor report
National Aeronautics and Space Administration Washington, D.C. 20546	14. Sponsoring Agency Code

15. Supplementary Notes

This is a final report.

16. Abstract

Analytical and experimental investigations, performed to establish the feasibility of reinforcing metal aircraft structures with advanced filamentary composites, are reported. Aluminum-boron-epoxy and titanium-boron-epoxy were used in the design and manufacture of three major structural components. The components evaluated were representative of subsonic aircraft fuselage and window belt panels and supersonic aircraft compression panels. Both unidirectional and multidirectional reinforcement concepts were employed. Blade penetration, axial compression, and inplane shear tests were conducted. Composite reinforced structural components designed to realistic airframe structural criteria demonstrated the potential for significant weight savings while maintaining strength, stability, and damage containment properties of all metal components designed to meet the same criteria.

17. Key Words (Suggested by Author(s))	18. Distribution Statement
reinforced metal structures filamentary composites boron-epoxy compression shear damage-containment	Unclassified—Unlimited

19. Security Classif. (of this report)	20. Security Classif. (of this page)	21. No. of Pages	22. Price*
Unclassified	Unclassified	111	Domestic, $4.25 Foreign, $6.75

*For sale by the National Technical Information Service, Springfield, Virginia 22151

FOREWORD

This report was prepared by Boeing Commercial Airplane Company under NASA contract NAS1-8858 and covers the work performed during the period February 1970 to October 1971 on phase III of a three-phase contract. The contract was administered under the direction of R. A. Pride, head of the Composites section, NASA Langley Research Center.

The authors wish to acknowledge the contributions of the following Boeing personnel:

S. Oken R. E. Horton	Structures Staff
C. A. Filippa	Analysis
G. F. Harbord	Manufacturing

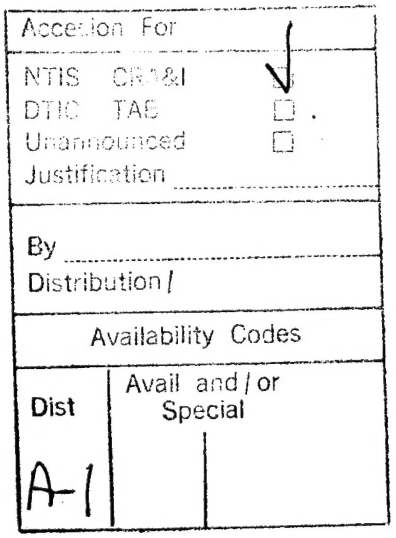

CONTENTS

FIGURES

FIGURES—Concluded

TABLES

ANALYTICAL AND EXPERIMENTAL INVESTIGATION OF AIRCRAFT METAL STRUCTURES REINFORCED WITH FILAMENTARY COMPOSITES

Phase III
MAJOR COMPONENT DEVELOPMENT

By L. L. Bryson and J. E. McCarty
Boeing Commercial Airplane Company

SUMMARY

This report covers the analytical and experimental investigations in phase III of a three-phase program performed to establish the feasibility of reinforcing metal aircraft structures with advanced filamentary composites.

Design concepts evaluated in phase I and phase II of the program (refs. 1 and 2) were incorporated in the design of large structural panels designed to meet realistic airframe structures criteria. Two reinforcing concepts were employed:

- Filamentary composites were applied as unidirectional reinforcement in the primary loading direction. The metal portion of the reinforced structure was designed to carry the transverse loads as well as its portion of the primary load.

- Multidirectional laminates of filamentary composites were used to reinforce metal structure for combined loading conditions.

Two material systems, aluminum-boron-epoxy and titanium-boron-epoxy, were used during this phase of the program. The material properties of these two material systems are tabulated in appendix A.

Three major components were selected for investigation:

- Fuselage damage containment panel—To demonstrate the application of filamentary composite reinforcement to pressurized, fuselage metal structure for weight-saving and damage containment capability.

- Multibay skin-stringer compression panels—To evaluate undirectional filamentary-composite-reinforced titanium fuselage compression structure for weight-saving potential.

- Window belt panel—To evaluate multidirectional filamentary-composite-reinforced, shear-critical titanium fuselage structure for weight-saving potential.

The results obtained from this investigation proved the feasibility of reinforcing large aircraft structural panels with filamentary composites. Structural weight savings for the three configurations studied were:

- Damage containment panel 19.6%
- Multibay skin-stringer compression panel 34.7%
- Window belt panel 36.9%

In addition to significant weight savings realized by the reinforced designs, improved structural performance was also demonstrated. Ultimate failure of the multibay compression panel occurred at a load equal to 111% of the ultimate load of a comparable all-metal design. Similarly, the composite-reinforced window belt panel exceeded the predicted design ultimate strength by 21%.

A successful repair of the pressurized panel was accomplished following the first blade penetration test. Planned, multiple damage containment tests were prematurely terminated due to a catastrophic failure of the panel during the second blade penetration test. As a result, damage containment capability of composite-reinforced panels was not conclusively demonstrated.

Three contract extensions have been made to further investigations in the following areas:

- Cyclic debonding of adhesive joints
- Residual-stress alleviation
- Stiffened-plate buckling analysis

The results of these investigations have been reported separately in references 3 through 7.

INTRODUCTION

The application of advanced filamentary composites for reinforcement of aircraft metal structures can result in significant weight savings. The selective reinforcement of aircraft metal structure minimizes the amount of the relatively high cost advanced composite materials used. The structural efficiency of the composite-metal-reinforced structural concept is very attractive when measured in dollars per pound of weight saved. In addition, economic advantages can be realized in manufacturing. The reinforced-metal structural concept is an extension of existing conventional structure, and most of the present fabrication and assembly techniques have direct application. Early application of composites to aircraft structures requiring low dollar per pound of weight saved is feasible by use of selective composite-metal-reinforced structural concepts.

As with any new material system, several problems must be solved before the materials are applied to primary aircraft structures. Of utmost importance was the establishment of a design philosophy which would fully recognize the unique characteristics of composite materials. This objective was achieved in the two preceding phases of the contract.

The purpose of phase I was to use existing material systems and investigate reinforcing metal aircraft structures with advanced filamentary composites. This included analytical studies of the feasibility of the reinforcing concepts, development of adhesive bonding and assembly techniques, and experimental verification of the predicted structural performance of the reinforced concepts (ref. 1).

The purpose of phase II was to continue the investigation of the reinforcing concepts developed in phase I, in the areas of fatigue cycling, crack growth, and residual strength. Emphasis was placed on fatigue and creep characteristics in the load transfer regions. The effects of thermal cycling were also investigated. These tests were conducted at temperatures representative of both subsonic and supersonic flight (ref. 2).

This program is the third phase of the three-phase investigation of aircraft metal structures reinforced with filamentary composites. This portion of the program accomplished a practical extension of the concepts developed during phases I and II. Three major components were selected that would simulate the complex design features of typical full-scale structure. These components were designed, analyzed, fabricated, and tested to meet aircraft structural requirements.

The three components evaluated in this program were:

- Fuselage damage containment panel—This panel was designed to meet the critical hoop tension loads associated with pressurized fuselage structure. The planned test program consisted of a series of blade penetration tests to evaluate the damage containment capabilities of the composite-reinforced structure. This panel also served to evaluate structural repair techniques.

- Multibay skin-stringer compression panels—This component was selected to validate, under realistic end-loading conditions, the application of unidirectional composite reinforcement concepts to large-scale aircraft compression structure. Design optimization and structural efficiency studies were conducted.

- Window belt panel—This component was selected to evaluate multidirectional composite-reinforcement concepts in shear critical aircraft structure. The selection was also influenced by the need to evaluate the use of composite reinforcement to attain load continuity around sizable cutouts in structural panels. The multidirectional nature of the loads in the window belt area provided a unique opportunity to evaluate the application of multidirectional composite laminates to reinforce structure for combined loading conditions.

SYMBOLS

Physical quantities defined in this paper are given in both the U.S. customary units and in the international system of units (SI) (ref. 8). Conversion factors pertinent to the present investigation are presented in appendix B.

A	area, square inches (square centimeters)
a	one-half crack length, inches (centimeters)
b	breadth, width of cross section, spacing, inches (centimeters)
c	distance from neutral axis to extreme fiber, inches (centimeters); fixity coefficient, nondimensional
d	rivet diameter, distance between centroids of sandwich faces, inches (centimeters)
E	modulus of elasticity, pounds per square inch (newtons per square meter)
F	allowable stress, pounds per square inch (newtons per square meter)
f	effective rivet offset, inches (centimeters)
I	moment of inertia, inches to the fourth power (centimeters to the fourth power)
K	buckling coefficient for isotropic plates, nondimensional
K_c	stress intensity factor, pounds per square inch times square root of inches (newtons per square meter times square root of meters)
L	column length, inches (centimeters)
L′	effective column length, inches (centimeters)
N	end load, pounds per inch (newtons per meter)
P	pressure, atmospheres
p	rivet pitch, inches (centimeters)
q	shear load intensity, pounds per inch (newtons per meter)
R	radius, inches (centimeters)
r	radius of gyration, inches (centimeters)
S_r	rivet strength, pounds per square inch (newtons per square meter)
T	temperature, degrees Fahrenheit (Kelvin)
T_o	stress-free temperature, degrees Fahrenheit (Kelvin)
ΔT	change in temperature, degrees Fahrenheit (Kelvin)
t	thickness, inches (centimeters)
w	panel width, inches (centimeters)
w_e	effective width, inches (centimeters)
x,y,z	orthogonal coordinate axis
γ	shear strain, inches per inch (centimeters per centimeter)
ϵ	axial strain, inches per inch (centimeters per centimeter)
ϵ_b	bending strain, inches per inch (centimeters per centimeter)
η,ξ	secondary coordinate axis

κ coefficient of thermal expansion, strain per degree temperature change, $\frac{\text{in./in. x } 10^{-6}}{°F}$ $\left(\frac{\text{cm/cm x } 10^{-6}}{°K}\right)$

ρ density, pounds per cubic inch (kilograms per cubic meter)

σ stress, pounds per square inch (newtons per square meter)

$\bar{\sigma}_{fr}$ strength of short riveted panel, pounds per square inch (newtons per square meter)

υ plasticity reduction factor for plates, nondimensional

$\bar{\upsilon}$ cladding reduction factor, nondimensional

Subscripts

Al aluminum

B boron

C composite

c compression

cc compression crippling

cy compression yield

e effective

f stiffener flange

L longitudinal direction

m metal

me metal equivalent

n element number

r rivet, rib, matrix, or adhesive

s skin, sheet, or shear

st stiffener

Ti titanium

t tension

ult ultimate

W transverse direction

w stiffener web

FUSELAGE DAMAGE CONTAINMENT PANEL

Objective

The objective of the fuselage damage containment portion of the program was to investigate the capability of fiber-reinforced metal structure to contain penetration damage under internal pressure loading. A secondary objective was to demonstrate the feasibility of structural repair of composite-reinforced metal structure.

Background and Approach

Aircraft pressure cabin structure typically consists of stiffened cyclinders closed with pressure bulkheads. As a consequence of accidents involving rapid decompression at high altitude resulting from fatigue cracks in the cabin skin, considerable research has been conducted to determine under what conditions explosive failures occur.

In the design of aircraft fuselages, emphasis is placed on the ability to prevent rapid crack growth resulting from large fatigue cracks or severe accidental damage. During the development of damage containment structure, the so-called blade penetration test was introduced. This test consists of the release of a sharpened steel blade against a pressurized fuselage panel in such a way that it penetrates the structure at a predetermined point. The test primarily simulates penetration of the fuselage by an engine turbine blade. In a successful test, the damage caused by the blade is contained in the area of penetration. The shell is still able to carry structural and pressure loads.

Analysis alone is not sufficent to determine damage containment. The typical analysis compares the stress intensity at the tip of the crack to values that have caused tears in the skin, and compares the stresses in the reinforcement in the presence of a crack to its ultimate strength. In most cases, however, the stress analysis involves assumptions that must be verified by tests on the specific configuration.

Blade penetration damage containment tests previously conducted in support of the Boeing commercial transport programs provided a data base for all metal structural concepts. The most current and directly applicable test data were obtained for the Boeing 747. Design requirements assume a relatively large area of the 747 fuselage (fig. 1) to be susceptible to turbine blade penetration. Body station 1530, contained within this penetration area, was selected as typical fuselage structure. Testing has been conducted on both conventional skin-stringer and aluminum honeycomb sandwich panels, which have been designed to meet the load criteria for this portion of the fuselage. The availability of these data was the reason for selection of the 747 fuselage as a baseline for the design of the composite-reinforced test panel.

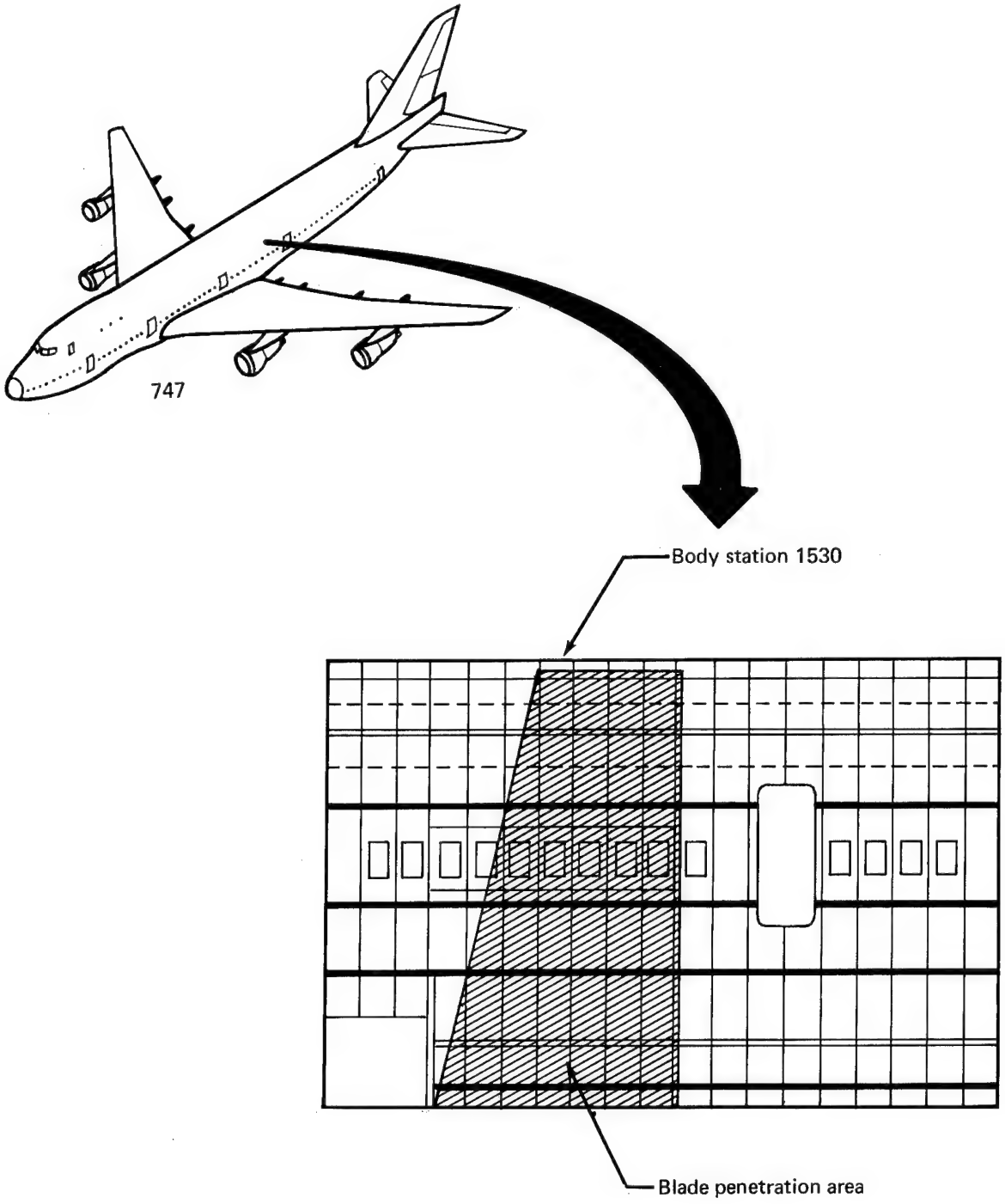

FIGURE 1.–747 FUSELAGE BLADE PENETRATION AREA

Design and Analysis

The Boeing 747 damage containment design criterion was used in the design of the composite-reinforced test panel. This criterion is as follows:

- For areas subject to possible penetration by rotating engine parts, the monocoque structure shall sustain a maximum pressure of 9.2 psi (63.5 kN/m^2) plus external aerodynamic pressure assuming loss of structure due to sudden penetration by a blade 12 in. (30.5 cm) wide by 0.5 in. (1.27 cm) thick.

In addition to the damage containment requirements, the following criterion was imposed on the panel design:

- The required blade penetration velocity of 77 ft/sec (23.5 m/sec) with an energy level of 970 ft-lb (1.315 kN-m) was established to simulate representative blade velocity/energy characteristics.

The 747 blade penetration test data indicated that for the sandwich structural concept, two face sheets of 0.053-in. (0.135-cm) 7075-T6 aluminum were required to meet the damage containment requirement. Correspondingly, the maximum axial load of 2.8 kip/in. (490 kN/m) due to side bending, required two faces of 0.032-in. (0.082-cm) 7075-T6 aluminum. The 0.032-in. (0.082-cm) faces also satisfied the vertical-bending-induced shear loads of 1520 lb/in. (266 kN/m).

The design adopted for the reinforced panel used the honeycomb sandwich concept to demonstrate weight saving by reinforcing with advanced composites.

The 0.032-in. (0.082-cm) 7075-T6 aluminum-faced sandwich, which was shown to be adequate to meet the maximum side and vertical bending load conditions, was selected as the basic panel design. The boron-epoxy reinforcement was applied to the panel faces with the fibers oriented in the circumferential direction to meet the hoop tension and penetration damage containment requirements.

A design approach was based on a comparison of the residual strength properties of composite-reinforced and unreinforced sandwich panels having equal static strengths. The reasoning behind this approach was that if equal or better residual strength properties could be demonstrated, a composite-reinforced sandwich panel could be designed on the basis of equivalent static strength to provide equal or better damage containment properties demonstrated by an unreinforced panel.

Residual strength data for boron-epoxy-reinforced aluminum sandwich were established during phase II of the program. Representative of these tests was a specimen designated as panel 1A. This specimen (fig. 2) was a honeycomb sandwich panel 16.0 in. (40.7 cm) wide, with 0.040-in. (0.102-cm) 7075-T6 faces reinforced with five layers of boron-epoxy. Following fatigue crack growth rate tests, when the crack in one face of the panel had grown to a 4-in. (10.2-cm) length, the panel was statically tested in tension to determine the residual strength. This test showed a residual strength of 97.8 kip (435 kN).

Boeing conducted a series of comparable residual strength tests on unreinforced 7075-T6 aluminum honeycomb sandwich panels of various face gages and core thicknesses (ref. 9.) The results of these tests were used to determine the stress intensity factor K_c for 7075-T6 aluminum sandwich. A typical value of $K_c = 75$ ksi $\sqrt{\text{in.}}$ (82.5 MN/m$^2\sqrt{\text{m}}$) was indicated for 0.032-in. (0.081 cm)-thick faces. The critical residual stress for damage containment for any given crack length (2a) can be calculated by substituting the K_c value in the equation

$$\sigma_{crit} = K_c/\sqrt{\pi a}$$

Solving this equation for a crack length of 4 in. (10.2 cm) to correspond with the panel 1A configuration, the indicated critical residual stress for 7075-T6 aluminum sandwich was $\sigma_{crit} = 29.8$ ksi (206 MN/m^2). Knowing the critical stress for damage containment, the residual strength of an aluminum sandwich panel having a static strength equivalent to a boron-epoxy-reinforced aluminum sandwich panel could be calculated.

Before the residual strength comparison can be made, an aluminum sandwich panel having an ultimate static strength equivalent to the static strength of the boron-epoxy-reinforced panel 1A must be determined. The reinforced sandwich panel is strength-limited by the ultimate strain capability of the boron fibers. For design purposes this value is considered to be $\epsilon = 6000$ μin./in. (μcm/cm). The aluminum at this strain level is operating in the elastic stress range. Having now established the residual strength of a boron-epoxy-reinforced 7075-T6 aluminum sandwich panel and the critical stress level for damage containment for an unreinforced 7075-T6 aluminum panel, the design proceeded on the following basis.

- Step 1: Calculate the face gage of an all-aluminum panel having static strength equal to that of the reinforced panel 1A.

  NOTE: Boron-epoxy-reinforced structure is design strength limited by a 6000-μin./in. (μcm/cm) critical fiber strain (ϵ_{crit})

$$(t_a)_{eq} = \frac{E_a \cdot \epsilon_{crit} \cdot t_a + n \cdot E_{be} \cdot \epsilon_{crit} \cdot t_{be}}{(F_{t_{ult}})_a}$$

  Converting the panel 1A configuration to equivalent aluminum

$$(t_{a_{eq}}) = \frac{(10.3 \times 10^6)(0.006)(0.040) + (5)(29.1 \times 10^6)(0.006)(0.0052)}{76{,}000}$$

$$= 0.093 \text{ in. } (0.234 \text{ cm})$$

- Step 2: Calculate the residual strength of this 0.093-in. (0.234-cm) face sandwich with a 4-in. (10.2-cm) crack

$$\text{Residual strength} = 2\,(t_{a_{eq}})(\text{panel width})(\sigma_{crit})$$

$$= (2)(0.093)(16)(29.8)$$

$$= 89.0 \text{ kip } (399 \text{ kN})$$

This residual strength compares to 97.8 kip (435 kN) for reinforced panel 1A. This is shown graphically in figure 2. These data reflect a 9.9% improvement in residual strength for the reinforced equivalent static strength panel. A weight comparison of the two designs shows a 33% weight advantage in favor of the reinforced design.

Thus, having demonstrated comparable residual strength for equivalent static strength designs, and assuming that the damage containment properties would be comparable, the sizing of the boron-epoxy reinforcement proceeds on the basis of designing for equivalent static strength, as shown in step 3.

- Step 3—sizing boron-epoxy reinforcement: Static strength of 0.053-in. (0.135-cm) 7075-T6 damage containment panel is calculated as end load per inch N_x.

$$N_x = 2\,t_a\,F_{t_{ult}}$$

$$= (2)(0.053)(76\,000)$$

$$= 8.05 \text{ kip/in. } (1410 \text{ kN/m})$$

Calculate the number of reinforcement plies n_{be} required for an 0.032-in. (0.081-cm) 7075-T6-faced sandwich to have a static strength of 8.05 kip/in. (1410 kN/m). Again applying the critical fiber strain critieria

$$N_x = 2t_aE_a\epsilon_{crit} + 2n_{be}t_{be}E_{be}\epsilon_{crit}$$

$$8050 = (2)(0.032)(10.3 \times 10^6)(0.006) + (2)n_{be}(0.0052)(29.1 \times 10^6)(0.006)$$

$$= 3960 + 1820n_{be}$$

$$n_{be} = \frac{8050 - 3960}{1820} = 2.2 \text{ plies per face}$$

On the basis of the 9.9% improvement in residual strength demonstrated by panel 1A, two plies were considered adequate to provide damage containment. Accordingly, the 0.032-in. (0.081-cm) 7075-T6 faces were reinforced with two circumferential layers of boron-epoxy.

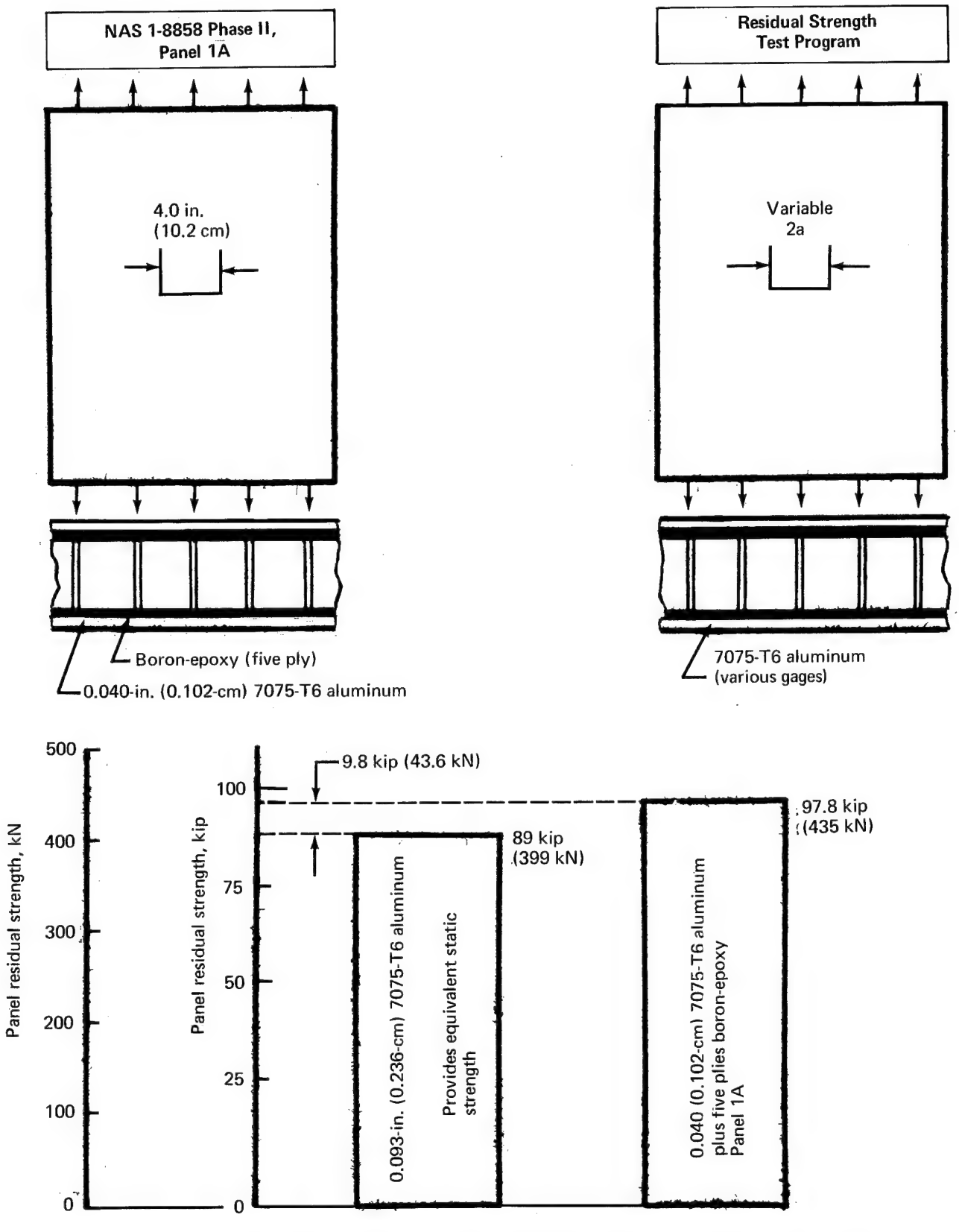

FIGURE 2.—FUSELAGE DAMAGE CONTAINMENT PANEL DESIGN CRITERIA

The design of the simulated 747 fuselage panel is shown in figure 3. The curved honeycomb panel size was 120 by 76 by 0.85 in. (304.5 by 193 by 2.2 cm), with six frames spaced at 20 in. (50.7 cm). Two tangs of 0.08 in. (0.203 cm) 2024-T3 aluminum are provided along the 120-in. (304.5-cm) length as a flexible attachment to the pressurizing test fixture. A dense core was used to shear the circumferential load from the tangs into the panel faces. Reinforcing pads are provided at the end of the frame members for the attachment of adjustable tension rods.

The boron-epoxy laminates are terminated by bonding to the 6Al-4V heat-treated titanium step fittings with the BP 907 matrix resin. The frame tees are bonded to the panel faces with extension J-sections being subsequently riveted into place.

A weight analysis was conducted to compare the weight of the reinforced damage containment panel design to that of the 747 riveted skin-stringer, fuselage structure. A detailed weight breakdown is presented in table 1 and indicates a 19.6% weight saving for the reinforced design.

Fabrication

The panel was bonded in two steps. The first, at 350° F (450° K), cured the laminates and attached them to the stepped end fittings. The second, at 250° F (394° K), included bonding the core to the laminates and to the loading tang and bonding the aluminum face sheets to the laminates and frame tees. The adhesive used was AF 126. The tooling and fabrication procedures are reviewed in appendix C. The completed panel is shown in figure 4.

Testing

Prior to installation in the test fixture, the panel was instrumented with 50 axial strain gages. The panel was installed in the test fixture, shown in figure 5, so that it would carry internal pressure. The hoop loads in the panel were reacted through the tangs, which were incorporated in the panel edges and through the threaded rods connected to the ends of the panel frames. The adjustable rods were strain gaged to allow regulation of the stress distribution in the panel. Details of the edge attachment are shown in figure 6. The fixture was designed to induce hoop loading only. Consequently, the panel was not fastened to the pressure bulkheads at the end of the fixture. These ends were sealed by a silicone rubber bladder.

Prior to testing, a strain survey was made of the panel in the following sequence:

- The panel was pressurized to 7 psi (48.3 kN/m^2).
- At 7 psi (48.3 kN/m^2) the tension in the frame rods were adjusted to attain a constant stress distribution in the panel.
- The panel was depressurized and the strain gages zeroed.
- The panel was repressurized to 4.6, 7.0, 7.9, 8.4, and 9.2 psi (31.7, 48.3, 54.5, 58.0, and 63.5 kN/m^2), and the strain readings recorded. These data were converted directly to engineering units and the stress-strain distribution throughout the panel graphically displayed.

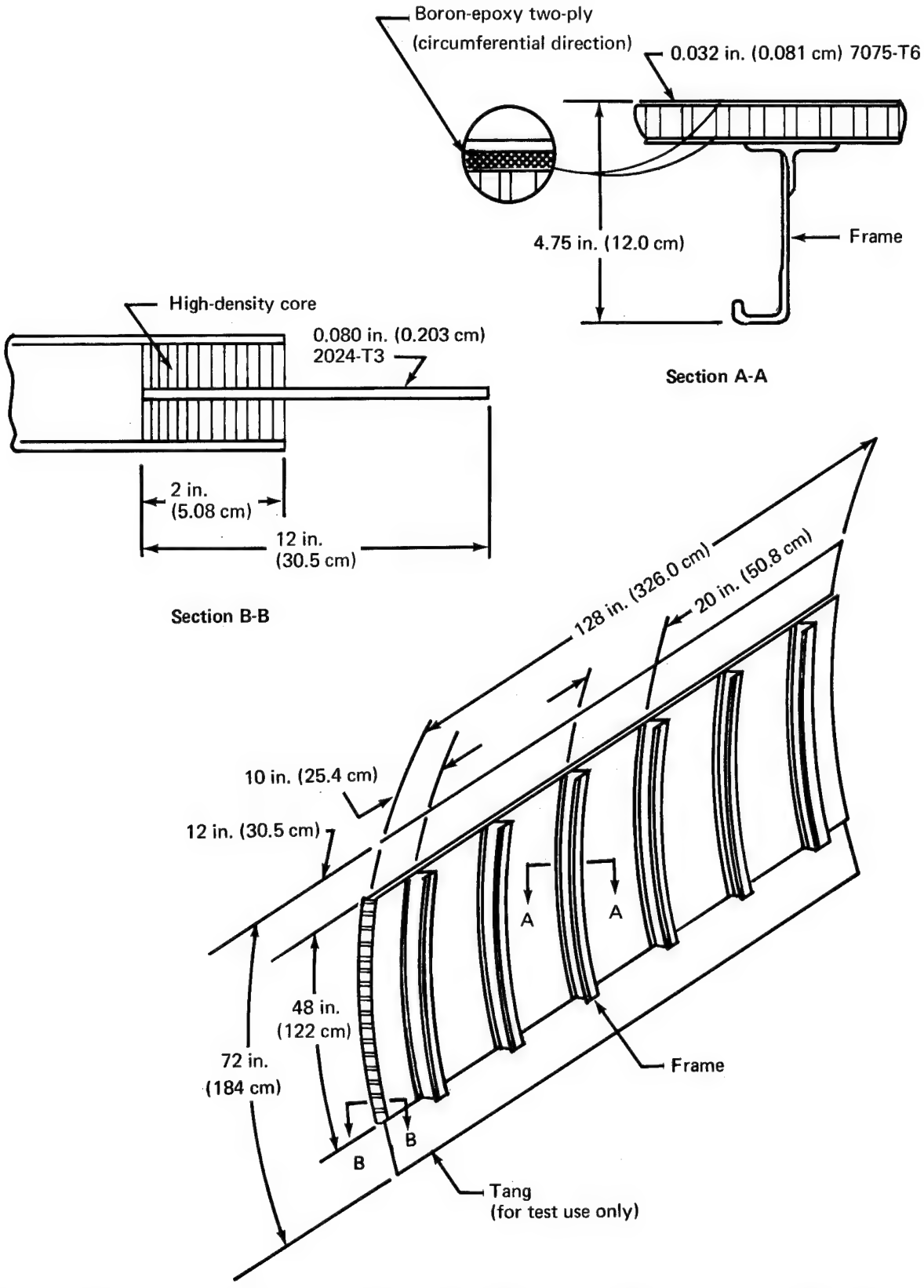

FIGURE 3.—GENERAL CONFIGURATION OF FUSELAGE DAMAGE CONTAINMENT PANEL

Table 1.—Weight Analysis of Damage Containment Panel

Component	Weight, lbm/ft^2(kg/m^2)	
	747 skin-stringer	Composite-reinforced honeycomb sandwich
Skins	1.120 (5.460)	0.924 (4.500)
Stringer	0.572 (2.780)	–
Tear strap	0.082 (0.400)	–
Adhesive	0.006 (0.029)	0.124 (0.604)
Boron-epoxy	–	0.229 (1.115)
Honeycomb core	–	0.194 (0.945)
Shear tie	0.075 (0.365)	0.085 (0.414)
Frame	0.294 (1.430)	0.171 (0.834)
Total	2.149(10.464)	1.727 (8.412)
Weight saved	–	0.422 (2.052)
Percent weight saved	–	19.6%

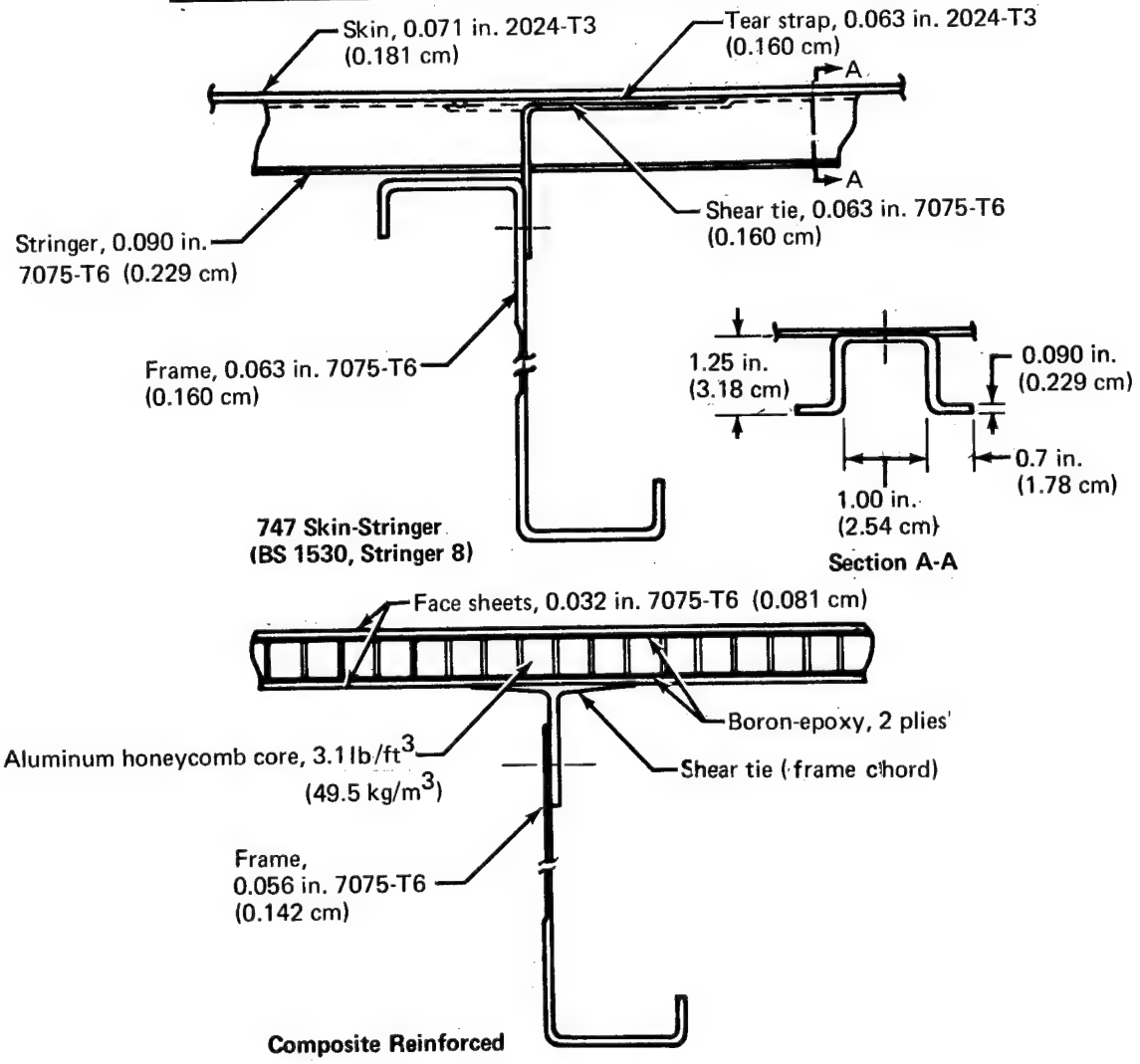

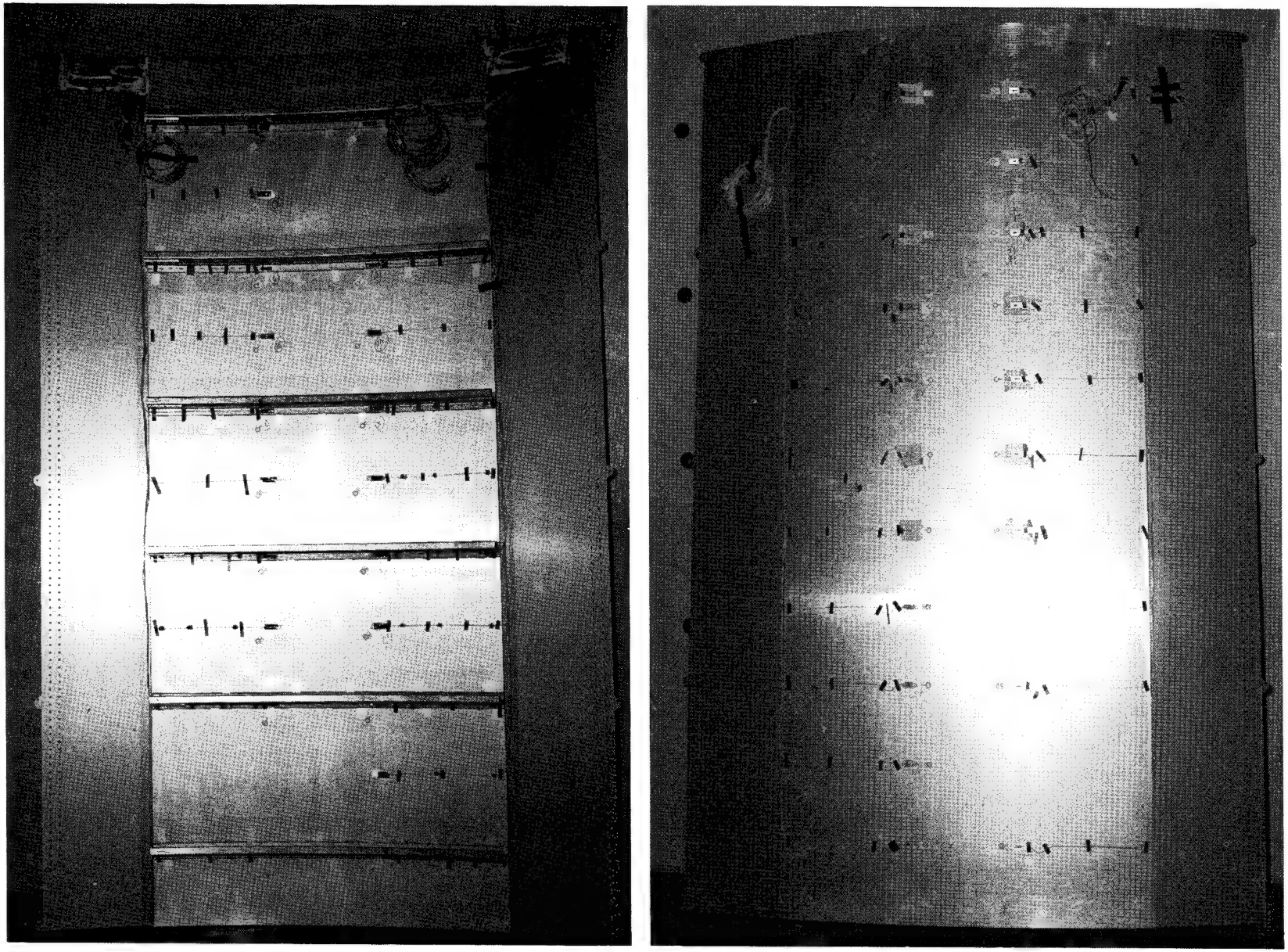

Internal Surface

External Surface

FIGURE 4.—FUSELAGE DAMAGE CONTAINMENT PANEL

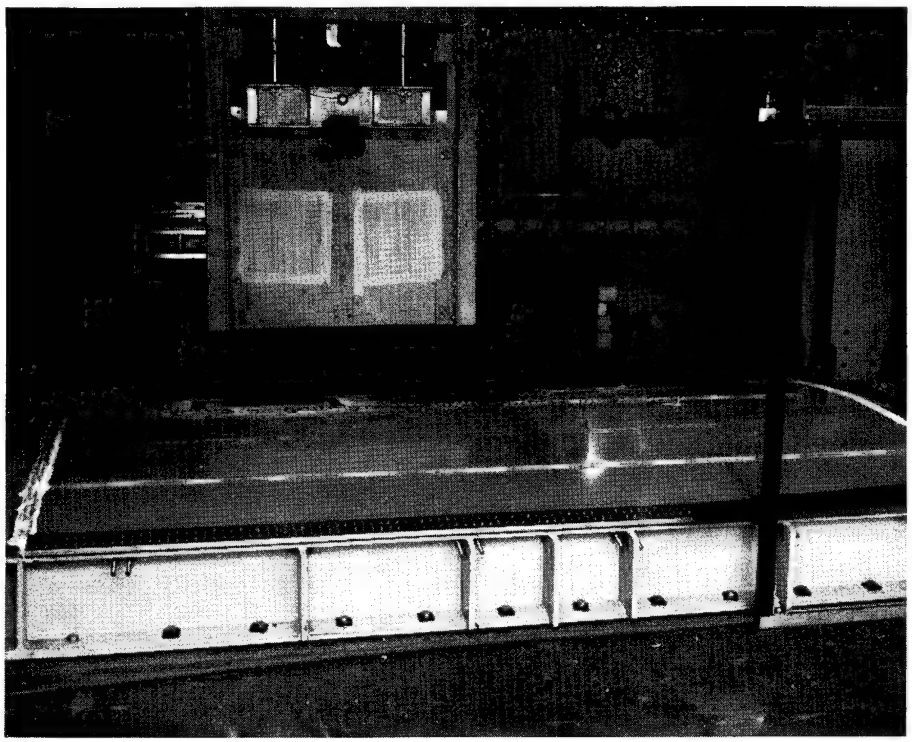

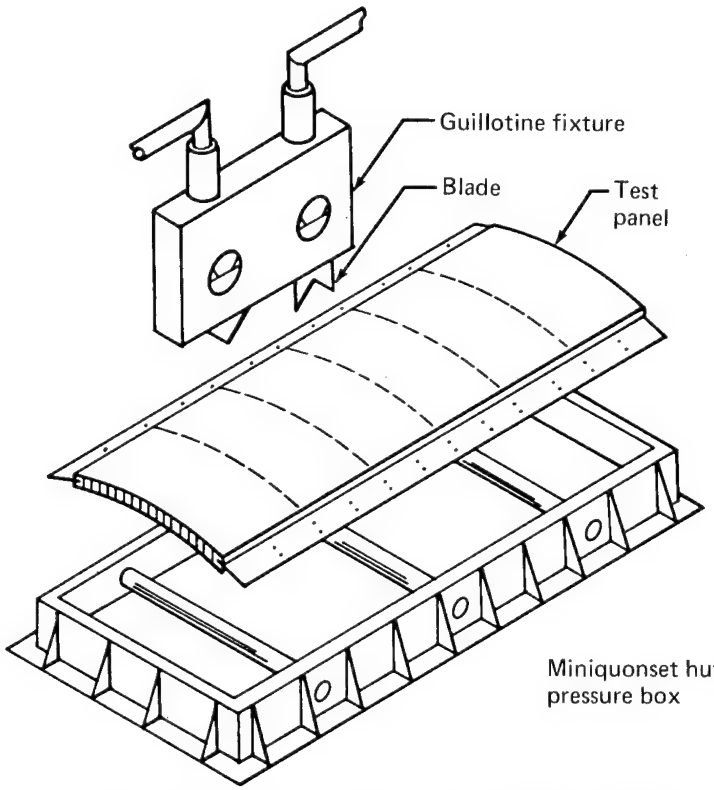

FIGURE 5.–TEST FIXTURE–FUSELAGE DAMAGE CONTAINMENT PANEL

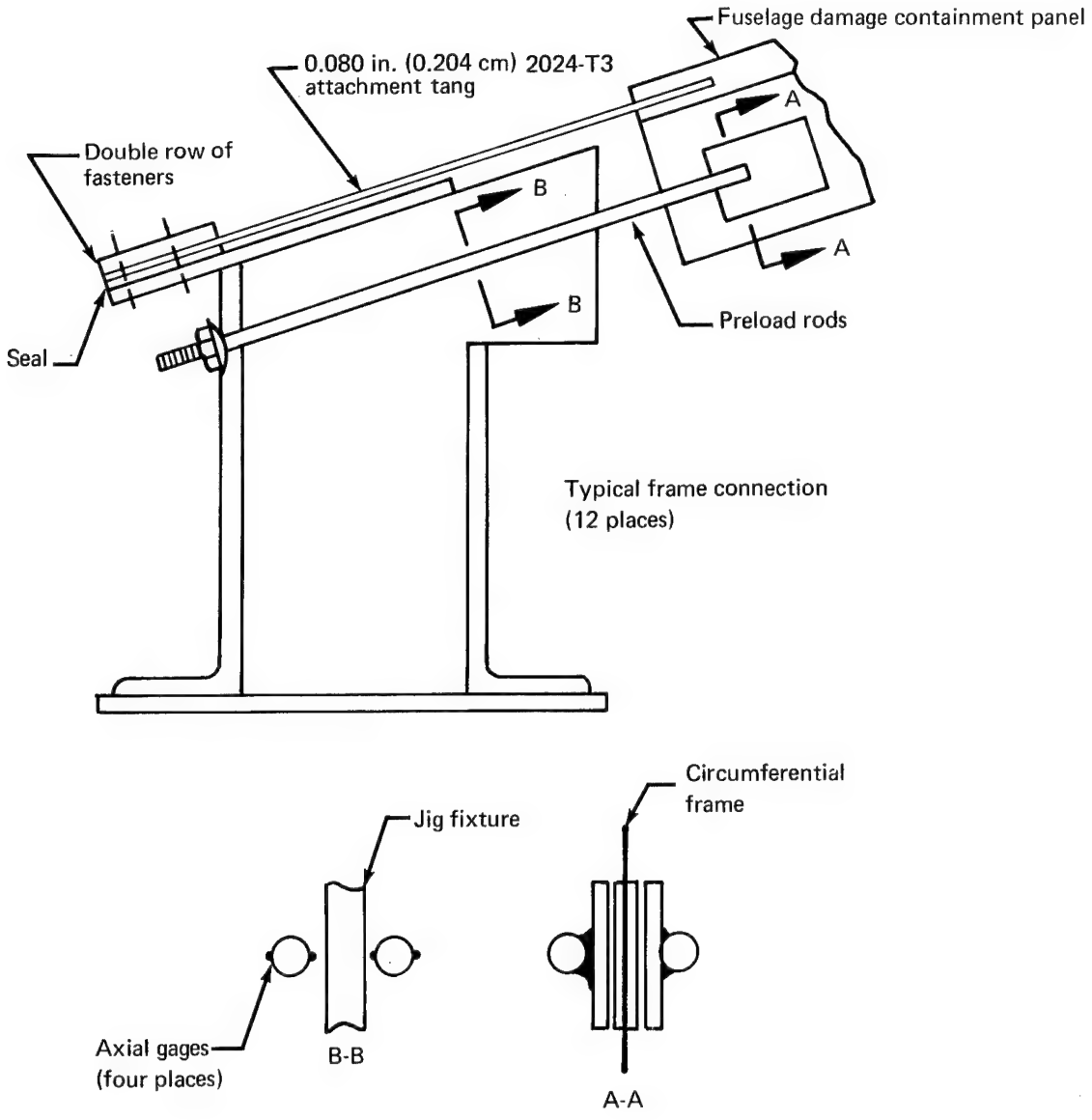

FIGURE 6.–PANEL AND FRAME ATTACHMENT TO THE PRESSURE BOX

The series of tests planned was first to test at a pressure lower than the design requirement, then repair, pressurize to a higher load, and retest. This procedure would be repeated until the panel failed catastrophically.

The panel pressure for the initial blade penetration was 7 psi (48.3 kN/m^2). A steel blade 12 in. (30.5 cm) wide and 0.5 in. (1.27 cm) thick, with a single point, was used. The blade and propelling fixture are shown mounted above the panel in figure 7.

The steel blade was shot at the panel at a location midway between the two center frames and 7 in. (17.8 cm) from the panel's longitudinal centerline. The blade did not completely penetrate the panel but was lodged in the skin, as shown in figure 8. The crack extended only a small distance from the edge of the entrance cut, as shown in figure 9. The extension of the crack was somewhat greater on the exit side, and is shown in figure 10. The repair of the damaged panel is described in appendix C.

The second shot was made at frame 5, again 7 in. (17.8 cm) from the panel centerline. The 12-in. (30.5-cm) blade used was double pointed to prevent it from being deflected by the frame (fig. 11). The pressure for the test was adjusted to 8.4 psi (58 kN/m^2). When the blade was fired, the panel split along the entire length. Figure 12 shows the outer surface of the panel after failure; figure 13 shows the inner surface.

Discussion

Complete failure of the panel at the 8.4-psi (58-kN/m^2) pressure level was unexpected. Additional tests at higher pressures had been planned.

Reinforcement for the panel was based on the results of previous static tests discussed earlier. These tests indicated that boron-epoxy-reinforced 7075-T6 aluminum skins had residual strength equivalent to that of unreinforced 7075-T6, which was thickness sized for equivalent strength.

Several factors may have accounted for the early failure. Among these are the following:

- Differential thermal contraction of the aluminum and boron-epoxy after curing results in residual tensile stresses in the metal which add to the pressure-induced stresses. The stress induced in the aluminum due to the differential contraction of the metal and composite from the 250° F (394° K) adhesive cure temperature to 70° F (294° K) is 8.94 ksi (61.5 MN/m^2). Disregarding the frames, the amount of pressure load carried by the aluminum skin is proportional to its stiffness, relative to the composite stiffness. At the panel failure pressure of 8.4 psi (58 kN/m^2) a residual stress of 8.5 ksi (58.6 MN/m^2) was developed in the aluminum faces. This gave a total stress in the aluminum of 17.44 ksi (120 MN/m^2). The total calculated stress in the reinforced aluminum for the initial 7-psi (48.3-kN/m^2) test was 16 ksi (110 MN/m^2). By contrast, the 0.053-in. (0.135-cm) unreinforced 7075-T6 aluminum faces had an operational stress of 11 ksi (75.8 MN/m^2) at 9.2 psi (63.5-kN/m^2) pressure.

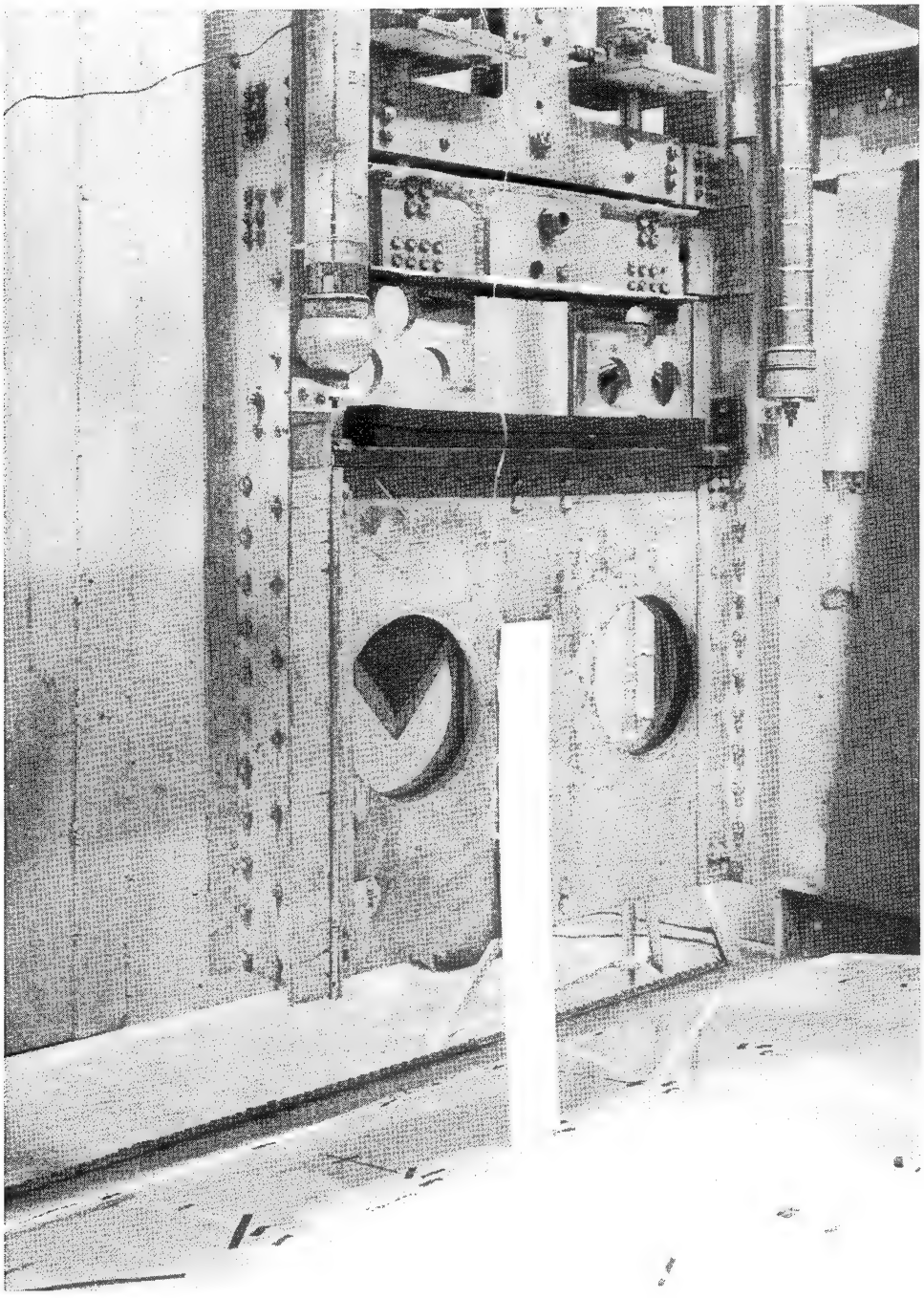

FIGURE 7.–GUILLOTINE ASSEMBLY

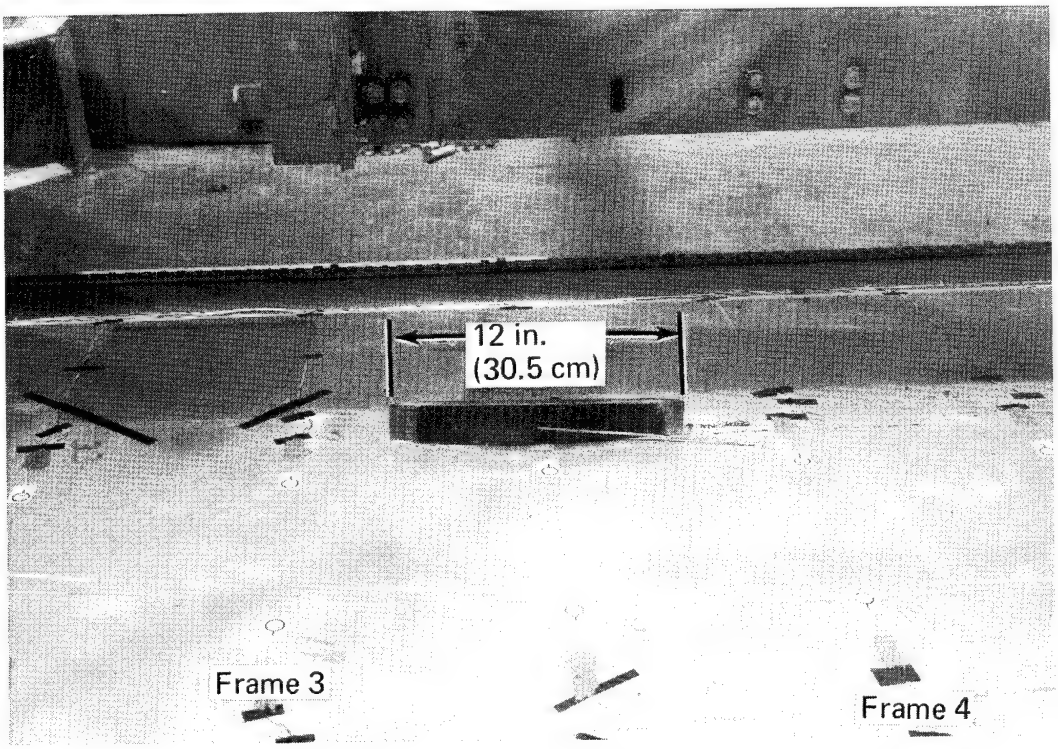

FIGURE 8.–FIRST BLADE PENETRATION–BETWEEN FRAMES

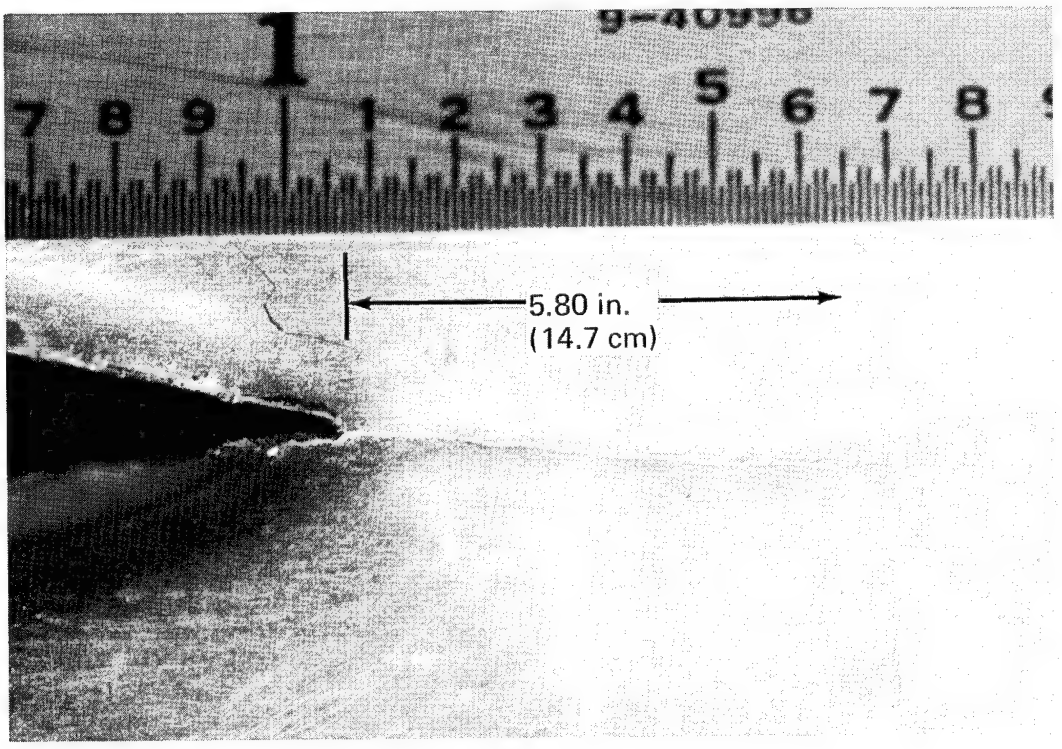

FIGURE 9.–CRACK GROWTH AT TIP OF GUILLOTINE BLADE

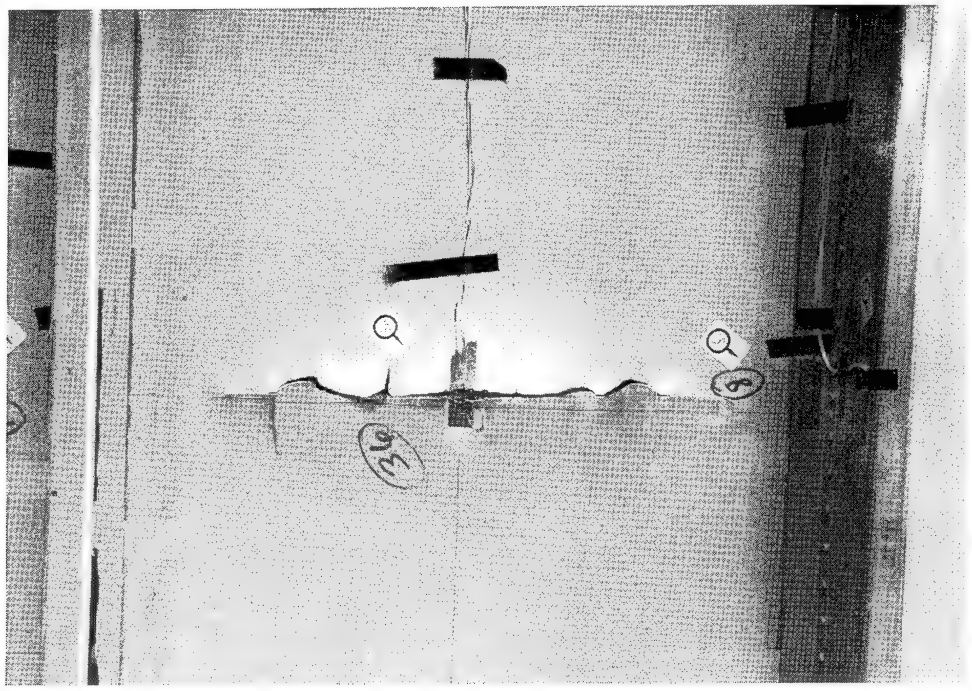

Internal Face

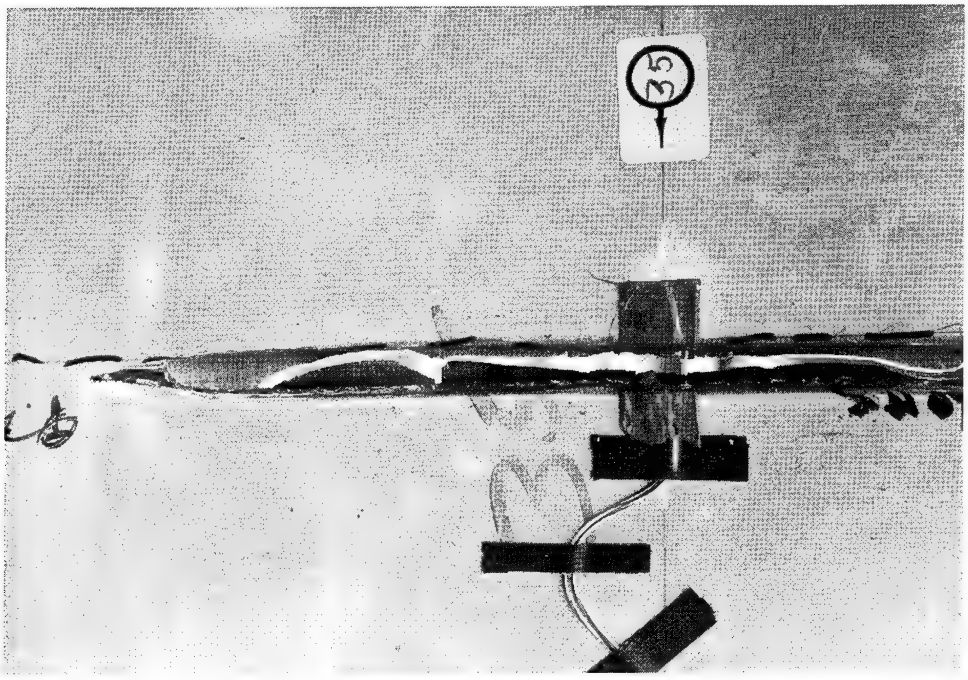

External Face

FIGURE 10.—DAMAGE SUSTAINED BY PANEL FACES DURING FIRST BLADE PENETRATION TEST

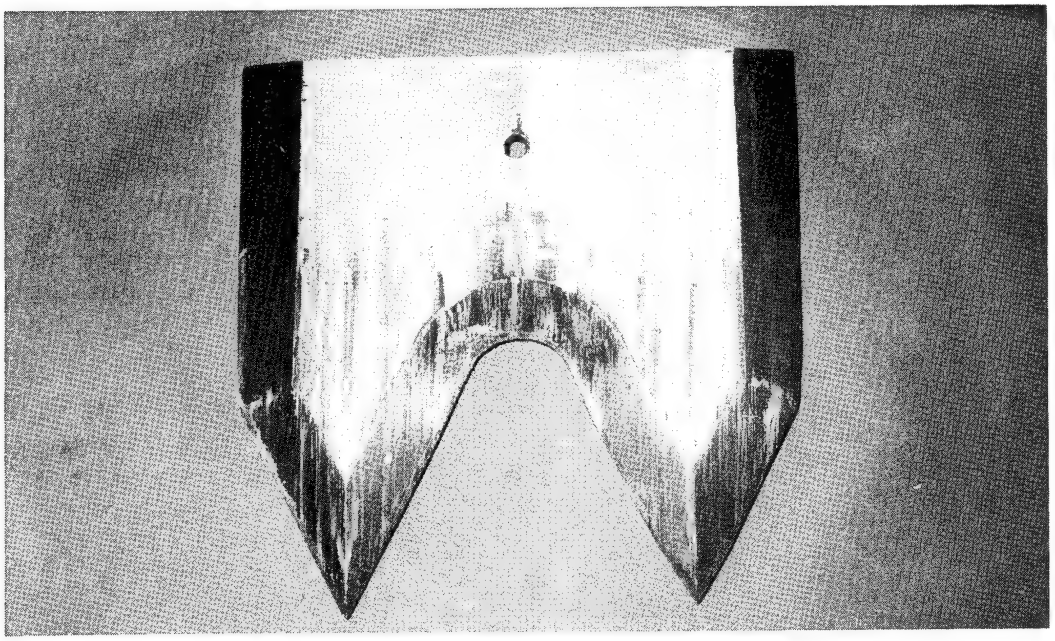

FIGURE 11.–DOUBLE-POINTED BLADE FOR FRAME PENETRATION

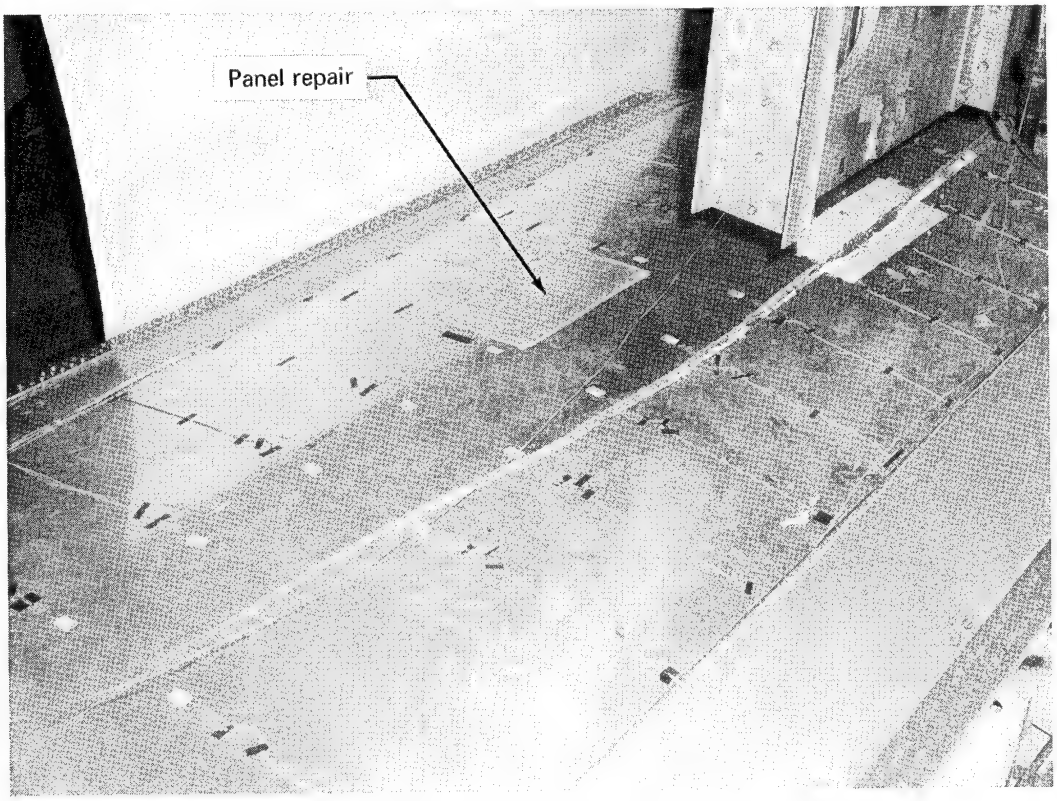

FIGURE 12.–CATASTROPHIC FAILURE OF PANEL DURING SECOND BLADE PENETRATION TEST

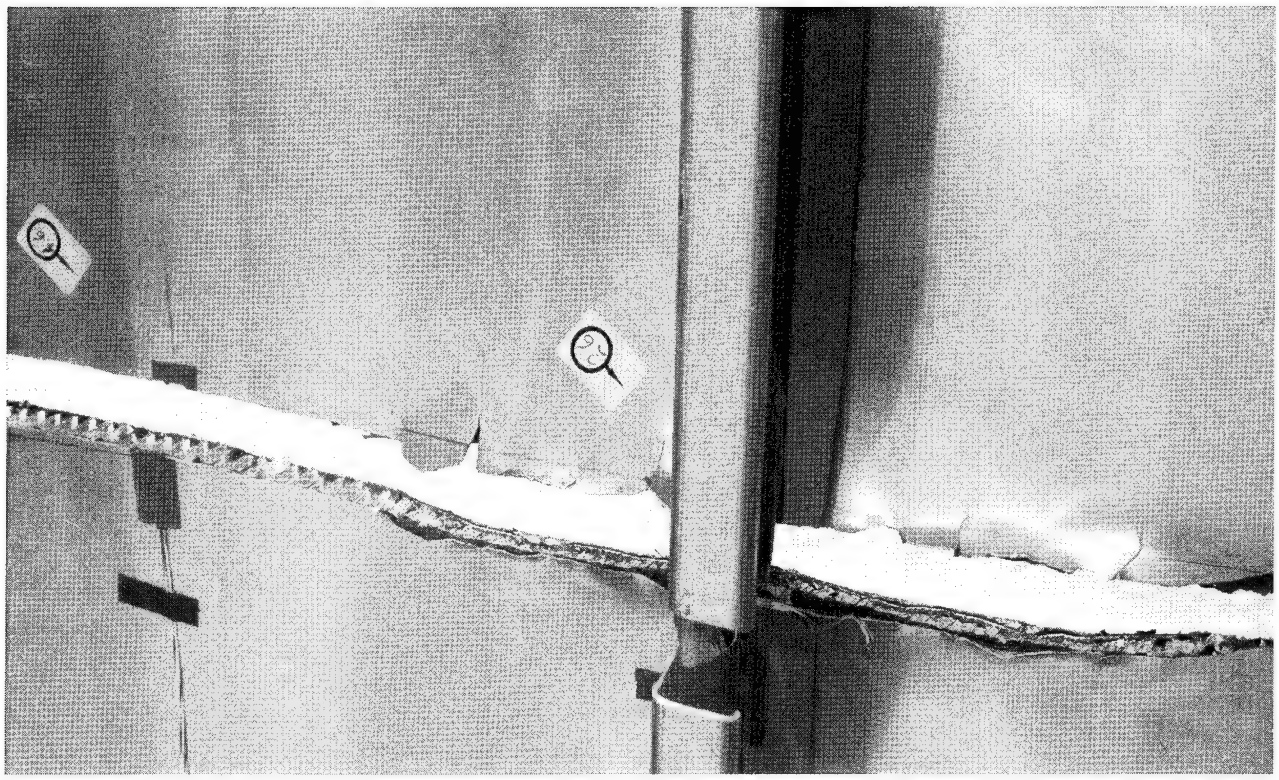

FIGURE 13.—FRAME AND PANEL DAMAGE SUSTAINED DURING SECOND BLADE PENETRATION TEST

- Blade penetration resistance is another point of consideration. The established test criteria required that the blade be fired at a specific energy level. Reexamination of the unreinforced panel test indicated that the blade had penetrated the basic sandwich and had severed the bonded flanges of the frame tee. It had not, however, cut into the outstanding leg of the tee or the attached J-section. This left approximately 60% of frame material remaining to resist the circumferential load. In observing the high-speed film of the reinforced panel test, it was noted that the panel did not fail until the blade penetrated deep enough into the panel to completely sever the bonded tee and cut into the riveted J. This additional load from the frames being dumped into the sandwich was sufficient to cause failure. This variation in sustained frame damage is attributed to lower resistance to penetration offered by the 0.032-in. (0.081-cm) reinforced face sheets.

Additional factors having direct bearing on damage containment capabilities, which are not fully understood for composite-reinforced metal structure, are:

- Residual strength properties of reinforced metal structure
- Load transfer mechanism from the damaged portion of the panel into the boron fibers
- The dynamic effects of the blade penetration and the dumping of the frame loads into the reinforced skin

Further study of these areas is necessary to ensure fail-safe design of composite-reinforced structure.

MULTIBAY SKIN-STRINGER COMPRESSION PANEL

Objective

This portion of the program evaluated the application of unidirectional filamentary composite reinforcement to the USA Supersonic Transport (SST) titanium fuselage compression structure.

Background and Approach

The reinforcing concepts developed and the test data established during phase I of the program were used in detailed design studies to develop a structurally efficient composite-metal-reinforced SST skin-stringer fuselage panel. A section of the SST pressurized, lower aft fuselage, as shown in figure 14, was selected to:

- Establish a realistic set of design conditions
- Provide a comparative conventional design base

All-metal skin-stringer compression panels were designed and tested as a part of the SST program. Data for these panels were readily available and provided a convenient base with which to compare the reinforced design. These panels were designed to meet the criteria established for the lower aft SST fuselage at body station 2827. The structure in this area of the fuselage is compression critical. In addition to a 7.0-kip/in. (1.225-MN/m) compression end load, the structure is required to carry 670 lb/in. (117.5 kN/m) in shear. Additional structural requirements including pressure containment, fatigue life, fail-safety, and panel flutter stability were imposed on the panel design. The resulting design was directly comparable to the SST panels tested and consisted of a multibay, composite-metal-reinforced, stiffened skin-stringer panel.

Test Panel Design

The test panel design was selected to represent a typical section of the SST structure, to which unidirectional reinforcement could be applicable. To provide a direct comparative base, a specific location of the SST fuselage was selected for which current, conventional skin-stringer design, analysis, and test data were available. Body station 2827 of the Boeing SST fuselage, located just forward of the aft pressure bulkhead, was selected for the comparative study. The lower fuselage structure in this section is compression critical, making the structure attractive for unidirectional reinforcement. In addition, several compression-allowable test programs were conducted for structural application in this section. These programs also provided a direct comparison for the reinforced design.

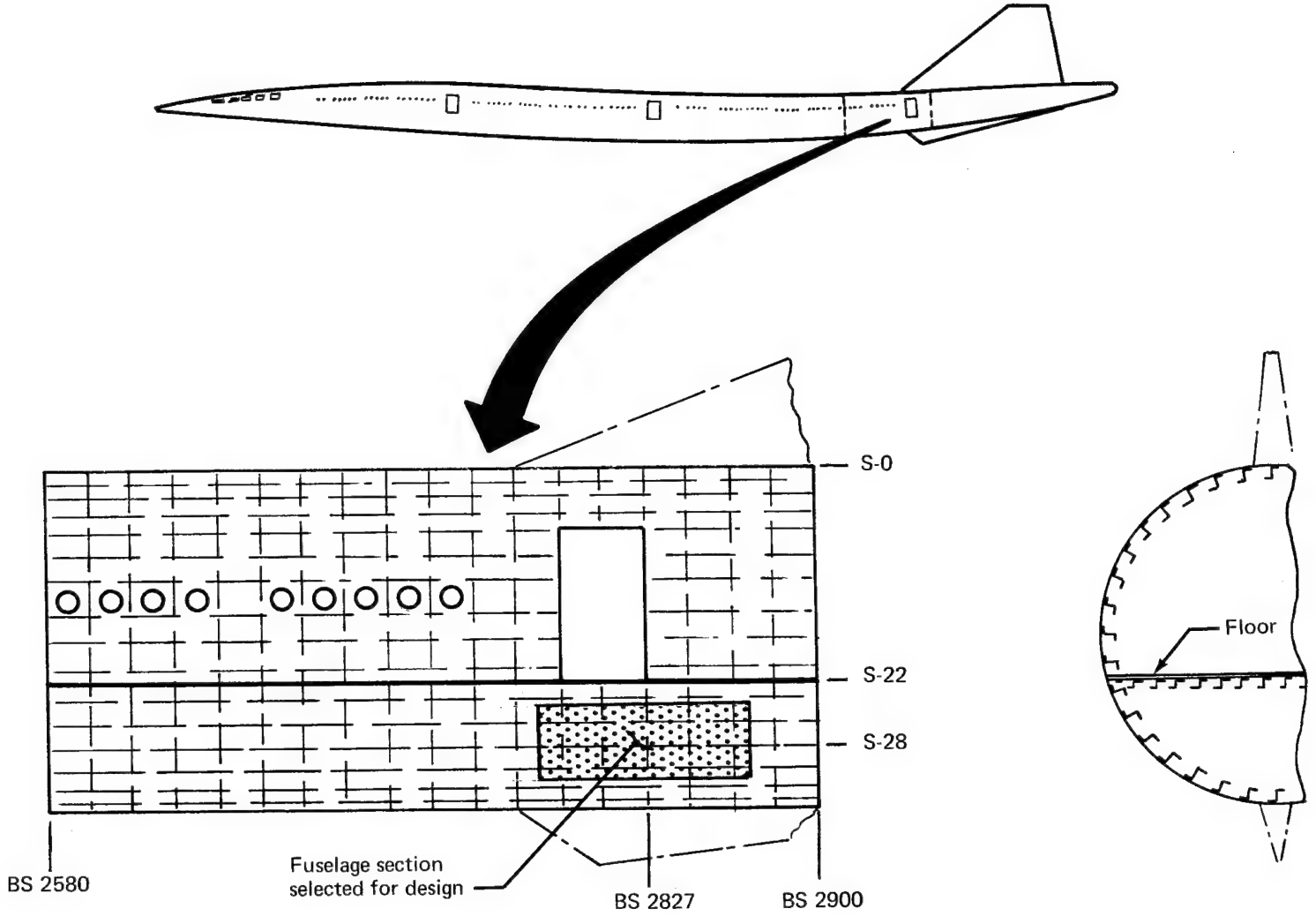

FIGURE 14.– SST AFT FUSELAGE–BASELINE FOR COMPRESSION PANEL DESIGN

Design loads and structural requirements.—The design loads and requirements were selected directly from the SST design load criteria established for the aft pressurized fuselage. The criteria for the lower fuselage are listed below.

- The critical design condition was compression. The structure was required to carry a compression end load of 7 kip/in. (1.225 MN/m).

- In addition to the compression load, the structure must withstand a shear load of 670 lb/in. (117.5 kN/m).

- The principal source of fatigue loading encountered by the aft fuselage structure is sonic fatigue. The frame spacing and stringer configuration were controlled so that the panel first-mode vibration frequency met the minimum SST sonic fatigue requirements.

- A maximum hoop tension stress level of 37 000 psi (255 MN/m^2) was maintained in order to meet the crack growth requirements for a 50 000-hr life.

Panel design and analysis.—The panel design configuration was controlled to some degree by the requirement to provide a one-to-one comparison with the SST test panel. The panel length, width, number of frames, and design load conditions were fixed. Design variables considered included face gage, stiffener section properties, stiffener spacing, and the composite reinforcement concepts.

Structural efficiency curves for reinforced, stiffened panel concepts were developed from concept verification panel and column crippling tests conducted during phase I. These data were used to optimize the reinforced stiffener configuration for the design end load.

The preliminary design analysis studies were based on conventional compression, column, and crippling analysis methods. The design equations used in the analysis are summarized in table 2. The composite-reinforced panel cross section was transformed into an equivalent all-metal configuration on the basis of elastic moduli and area ratios. The structural slenderness ratio (L'/r) was then determined from the transformed section properties and frame spacing. A Johnson parabola curve (fig. 15) developed from phase I crippling data was used to determine the critical panel strain and ultimate load intensity capability. The stringer spacing was determined by sonic fatigue requirements, and the panel design was analyzed for flutter. The face sheet was sized to meet fatigue crack growth requirements.

Initial skin buckling characteristics of the panel were analyzed with the aid of the computer program BUCLASP (ref. 10). This program, developed under this contract, is an exact linear buckling analysis capable of determining the minimum skin buckling loads and their corresponding eigenvector, from which the buckling mode shape is determined.

A weight analysis was performed comparing the weight of the reinforced panel design to that of the SST all-titanium panel designed to the same criteria. This analysis, the results of which are summarized in table 3, shows a 34.7% weight saving for the reinforced design.

Table 2.—Compression Panel Analysis Methods

Condition		Equation or requirement	Reference
1.	Frame stiffness	$EI = 4(w/\pi)^4 \cdot N/L$	NACA TN 3785
2.	Flange width	As required for next size rivet	Boeing Design Manual
3.	Rivet clearance	Minimum for installation	Boeing Design Manual
4.	Rivet strength	$S_r > \left(\frac{0.7}{E_{st}}\right)\left(\frac{b_s}{d}\right)\left(\frac{p}{d}\right)\left(\frac{\bar{\sigma}_w}{\eta}\right)^2$	NACA TN 3785
5.	Interrivet buckling	$F_{ir} = K E \frac{t^2}{L^2}$	Boeing Design Manual
6.	Wrinkling	$\frac{\bar{\sigma}_{fr}}{\bar{\sigma}_{cy}} = 17.9 \left(\frac{t_w}{f}\right)^{4/3} \left(\frac{t_w}{b_w}\right)^{1/6} \left[\frac{t_s}{b_s}\left(\frac{\bar{\eta}E}{\sigma_{cy}}\right)\right]^{1/2}$	NACA TN 3785
7.	Effective skin width	$w_e = 0.85\ t\sqrt{\frac{E}{F_c}}$	Boeing Design Manual
8.	Formed section crippling	$F_{cc} = \frac{\Sigma F_{cc_n} b_n t_n}{\Sigma b_n t_n}$	Boeing Design Manual
9.	Overall panel buckling	Johnson parabola	NASA CR-1859

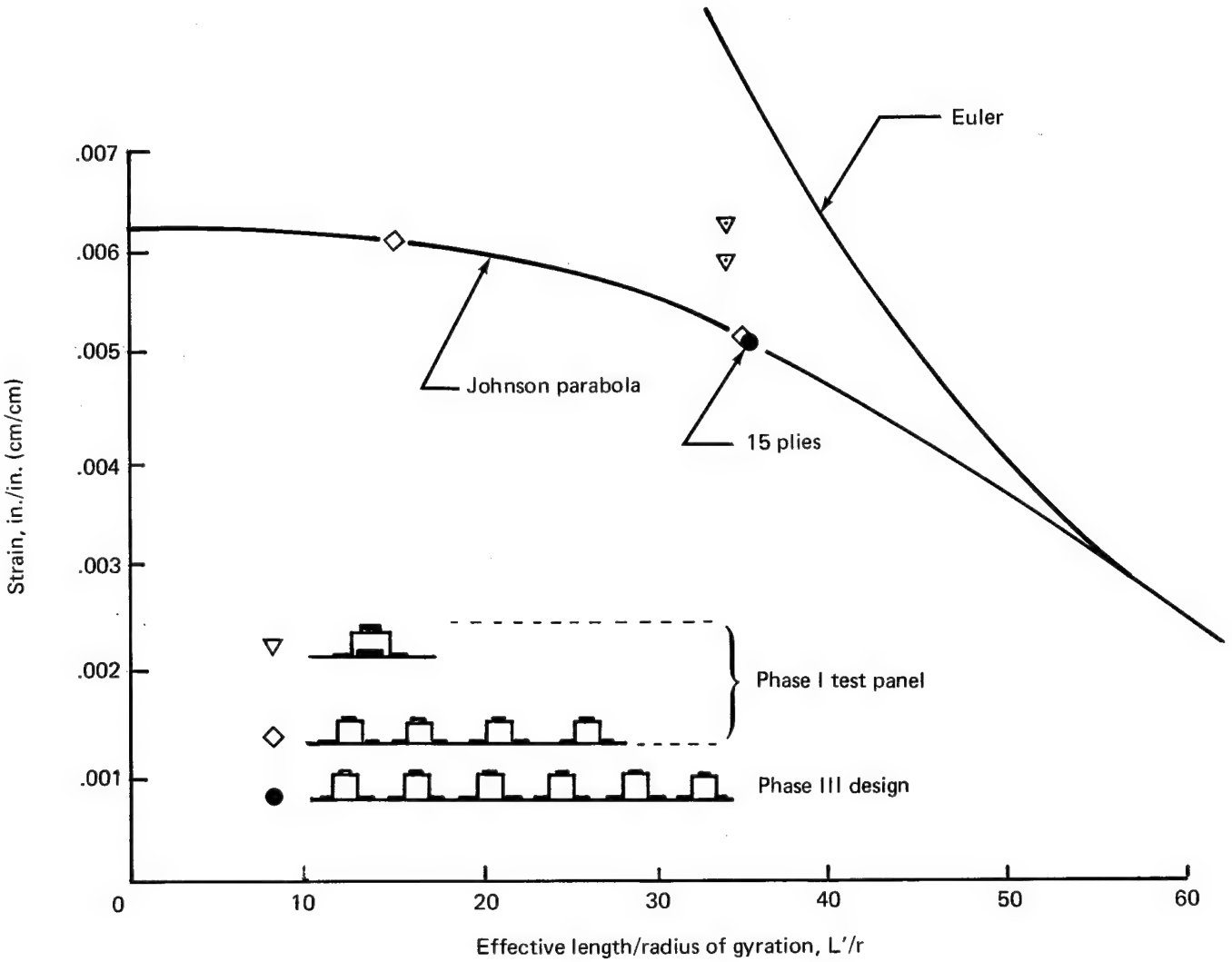

FIGURE 15.—DESIGN BASIS FOR PANEL COMPRESSION BUCKLING STABILITY

Table 3.—Weight Analysis and Comparison of All-Metal and Reinforced Design Concepts

Component	Weight,[a] lbm/ft^2 (kg/m^2)			
	SST all-metal design		Hat-stiffened composite-reinforced design	
Skin	1.15	(5.64)	1.15	(5.64)
Stringer	1.79	(8.76)	0.95	(4.60)
Strap	0.46	(2.27)	—	—
Boron-epoxy	—	—	0.13	(0.63)
Total	3.40	(16.67)	2.23	(10.87)
Weight saved	—	—	1.17	(5.80)
Percent weight saved	—	—	34.7%	
Configuration	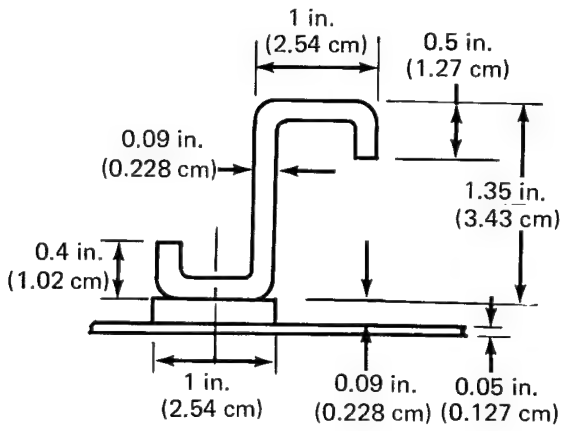		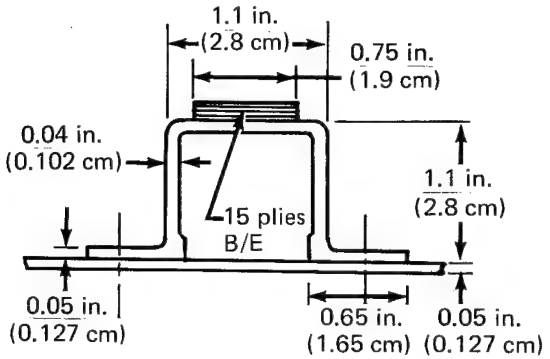	
Stringer spacing	4.5 in. (11.4 cm)		5 in. (12.7 cm)	
Material	(6Al-4V titanium)		(Boron-epoxy/6Al-4V titanium)	

[a]Weight of basic skin-stringer panel; does not include the weight of the frames.

Test panel configuration.—The final test panel design configuration, shown in figure 16, consisted of a flat, boron-epoxy-reinforced skin-stringer panel, 96 in. (243.8 cm) long by 36 in. (91.5 cm) wide. The titanium alloy (Ti-6Al-4V condition I) face sheet was 0.050 in. (0.127 cm) thick and was stiffened by six titanium hat section stiffeners reinforced with 15-ply, laminated boron-epoxy straps. The stiffeners were located symmetrically about the panel longitudinal centerline on 5-in. (12.7-cm) spacings. Four titanium U-channel frames were attached symmetrically about the transverse centerline of the panel forming three central 18-in. (45.7-cm) bays and two 21-in. (53.4-cm) end bays. The two longitudinal panel edges were slotted to reduce the effective width of the panel to 30 in. (76.3 cm). The slotted portion of the face sheet was a structural test requirement to provide simple support to the unloaded edges of the panel without picking up axial load. The design ultimate compression load for this 30-in. (76.3-cm) effective width panel was calculated to be 210 kip (934 kN).

Test Panel Fabrication

Two reinforced multibay skin-stringer panels were fabricated for structural testing. The face sheets, stiffeners, and frames were fabricated from annealed titanium alloy (Ti-6Al-4V condition I) sheet. The hat section stiffeners were hot-roll-formed and chemically milled to produce the required section properties. The U-channel frames were also hot-roll-formed. The boron-epoxy reinforcement was prepared in the form of multilayered straps complete with stepped titanium load transfer end fittings.

Final panel assembly was by structural adhesive bonding and mechanical fastening. The reinforcing straps were bonded to the crown of the hat stiffeners in a subassembly bond operation. Two rivets attached each load transfer fitting to the stiffener to provide additional load transfer capability. The stiffener flanges were then bonded to the face sheet in a second-stage cure cycle. Additional fastening was provided by a single row of rivets through each flange. The U-channel frames were attached to the panel by means of riveted clips and shear ties. The final fabrication consisted of slotting the unloaded edges of the panel and machining the loaded edges flat and parallel to facilitate structural testing of the panels in compression.

A more detailed description of the panel fabrication processes and procedures is provided in appendix C.

Structural Test

The test program for the multibay reinforced compression panels was conducted in two parts. The first panel was tested to failure in compression at room temperature. Strain surveys and data recording were carried out at predetermined load increments. The second panel was cyclically loaded for 100 compression cycles prior to compression loading to failure at room temperature. Strain surveys were recorded for selected cyclic loadings and at regular intervals during the ultimate failure test.

Panel configuration:

Dimensions

Length: 96 in. (243.8 cm)
Width (effective): 30 in. (76.3 cm)
Equivalent area: 1.84 in.^{2} (11.87 cm^2)

Face sheet

0.050-in. (0.127-cm) titanium (6Al-4V condition I)

Stiffeners

Six hat section stringers
5-in. (12.7-cm) stringer spacing

Frames

Four U-channel frames
18-in. (45.72-cm) spacing

Reinforcement

0.75-in. (1.9-cm), 15-ply boron-epoxy
strap-on stiffener crown

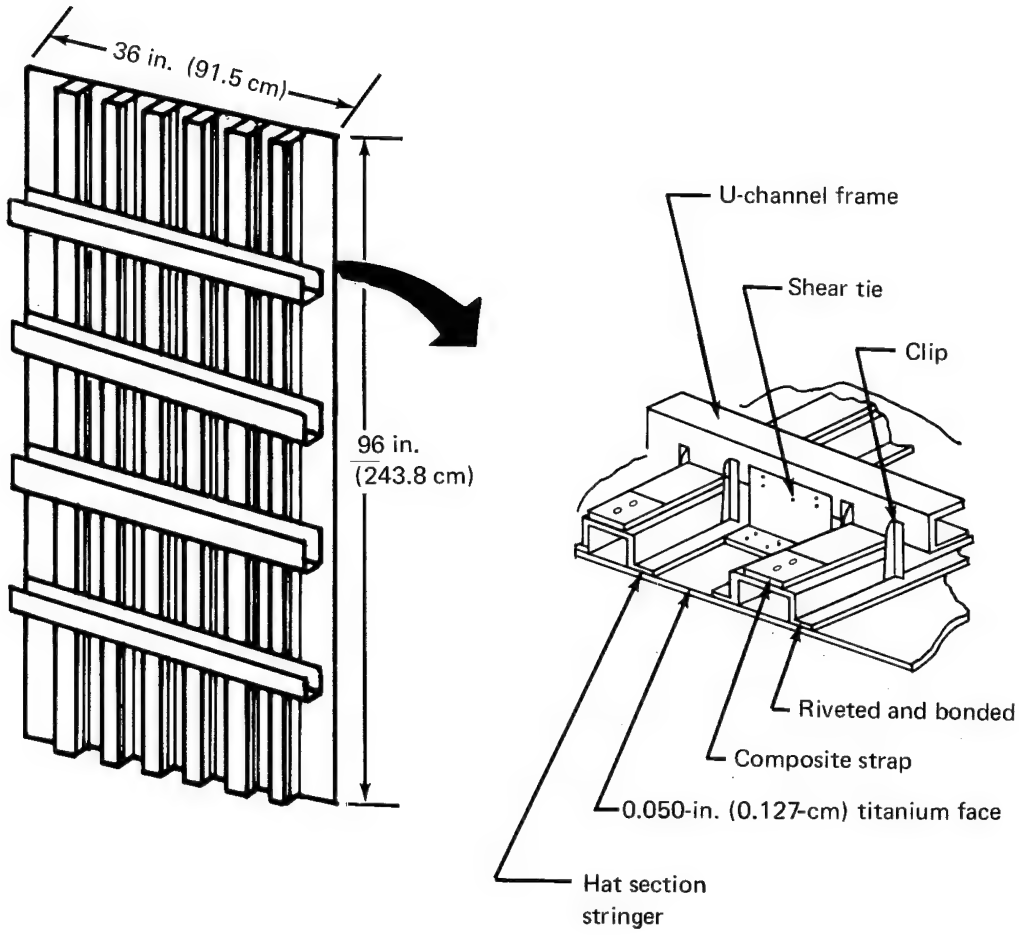

FIGURE 16.—MULTIBAY SKIN-STRINGER COMPRESSION PANEL CONFIGURATION

Panel instrumentation.—Instrumentation of both compression panels was identical. Thirty-two uniaxial strain gages were placed back-to-back in pairs to monitor load distribution across the width of the panel and to monitor panel bending modes along the length of the panel. Eleven electrical deflection indicators (EDIs) were attached at equal intervals along the panel centerline to record lateral deflections, from which the panel buckling modes were determined. Additional EDIs were used to monitor deflections in the test fixture. Figure 17 shows the instrumentation location.

Panel buckling modes were monitored by the Moiré grid shadow technique. Photographs of the Moiré fringe patterns established during the test were used to correlate the buckling pattern predicted by the BUCLASP analysis method.

Test fixture.—The compression panel test fixture consisted of a flat, machined steel base plate and three vertical uprights. Two of the uprights were equipped with knife edges to provide simple support to the unloaded panel edges. The third upright was positioned to the rear of the panel. V-shaped support members between this upright and the panel frames provided a pinned connection permitting frame rotation in the vertical plane but restricting lateral deflection. The panel is shown installed in the test fixture in figure 18. The test setup was identical for both panels. The panel flatness was recorded and the strain gages connected and electrically balanced. The panels were then positioned and clamped to an alignment fixture to remove any deformations. A preload of 1200 lb (5.35 kN) was applied and the panel ends shimmed as required to mate the panel with the load bearing plates. The knife-edge side restraints and lateral frame supports were installed and the alignment fixture removed. Strain gage readings were taken before and after the alignment to record the induced strains due to the straightening procedure.

Test procedure.—Test panel 1.—Two preloads of 90 kip (400 kN) were applied to obtain Moiré fringe and skin buckling data, followed by compression loading to ultimate failure. Repeatability of these data was demonstrated by comparing the two preload excursions. The load was applied in 15-kip (66.8-kN) increments, with strain gage and EDI data recorded for each increment of load. The Moiré grid shadow fringe patterns were photographed at 5-kip (22.2-kN) load increments to determine the load level at which the half-wave skin buckle pattern was established.

Test panel 2.—A cyclic compression load segment was conducted prior to ultimate compression loading of the panel. This procedure was introduced to simulate space shuttle fuselage compression panel requirements. A cyclic load amplitude of 96 kip (427 kN) was based on 80% of limit load. Limit load was set at 67% of the ultimate failure load of the first test panel. The first cyclic load applied to the panel was extended to 120 kip (534 kN). The remaining 99 load cycles were applied between 5 and 96 kip (22.2 and 427 kN). The 5-kip (22.2-kN) preload was retained to ensure that the panel did not shift in the jig. A load rate of 50 kip/min (222 kN/min) was maintained for the first 20 cycles and then increased to 75 kip/min (333 kN/min) for the remaining 80 cycles. Strain gage and EDI data were recorded at 15-kip (66.8-kN) load increments and at the maximum load during cycles 1, 10, 40, 70, and 100. Load deflection curves were generated for each cycle.

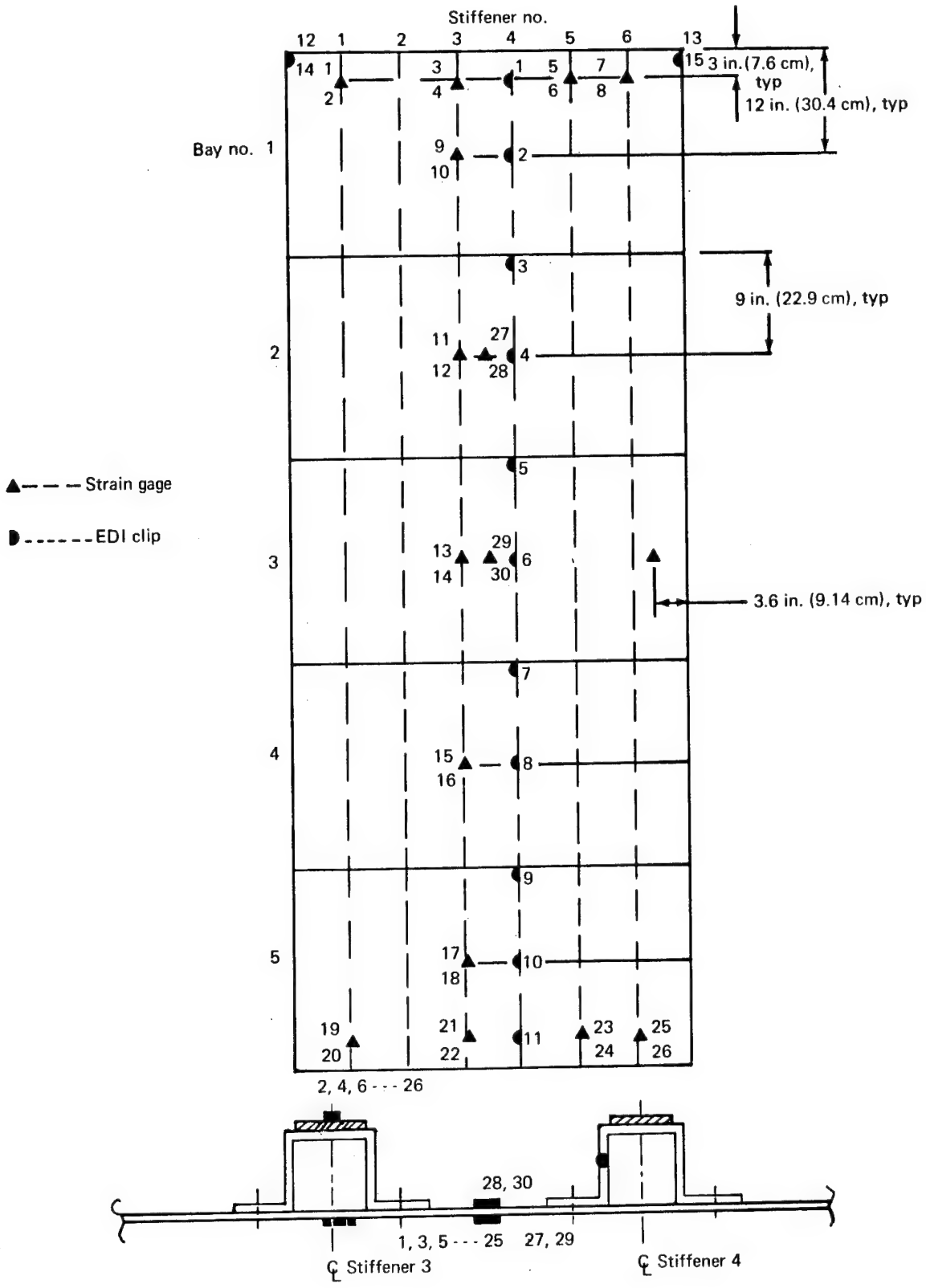

FIGURE 17.—COMPRESSION PANEL INSTRUMENTATION

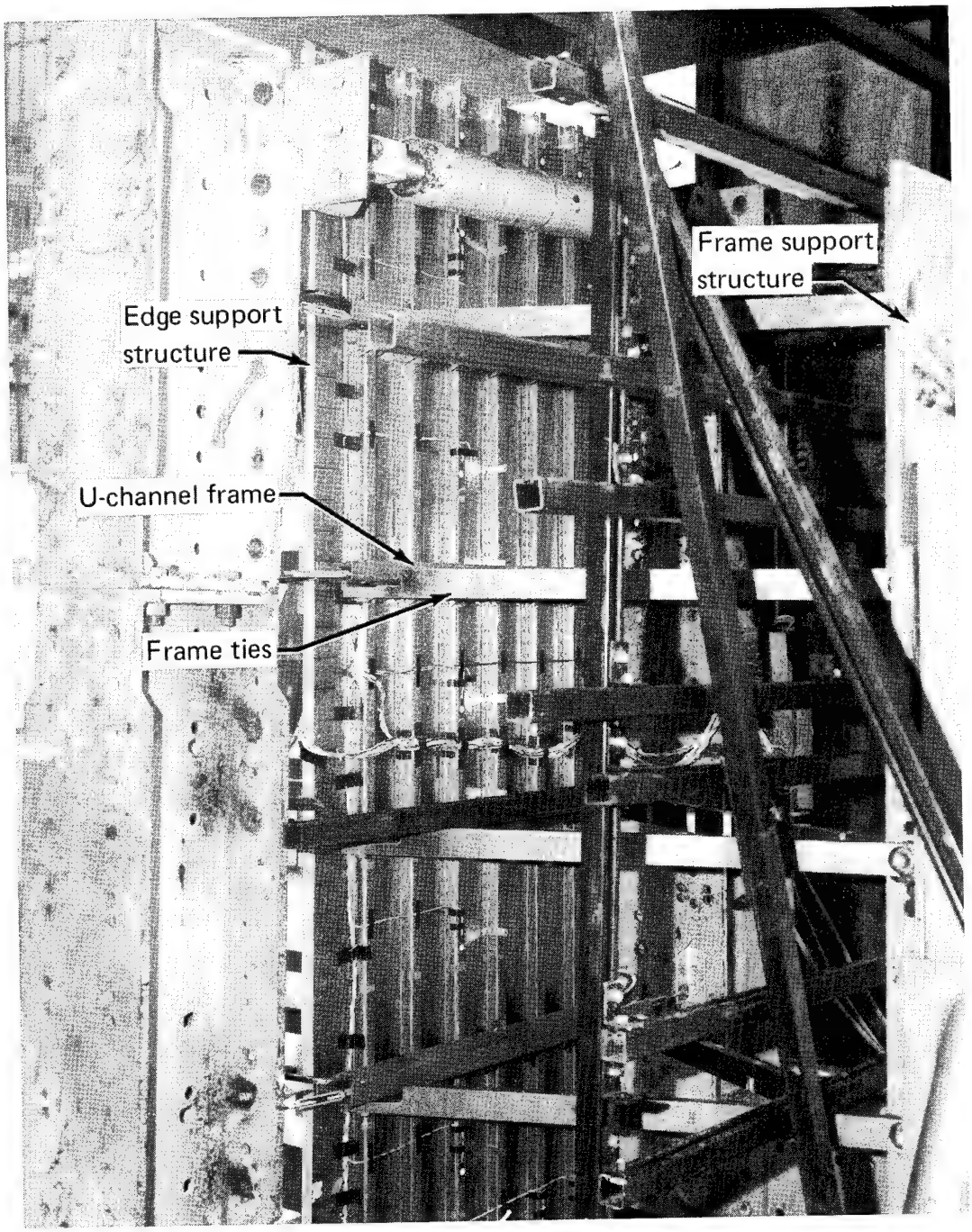

FIGURE 18.–COMPRESSION PANEL TEST FIXTURE

On the 101st cycle, the load was continued to ultimate failure of the panel. Data were recorded at 15-kip (66.8-kN) intervals to a load of 165 kip (735 kN) at 5-sec intervals from 165 to 200 kip (735 to 890 kN), and then continuously to failure. Loading was continuous with no stops for data recording.

Test results.—Both panels were designed to meet the 7 kip/in. (1.226 MN/m) design compression ultimate load and were expected to carry an applied load of 210 kip (934 kN). The panel test results are compared to this design ultimate load.

Test panel 1.—Loaded to failure in compression, the panel failed at an applied load of 180 kip (800 kN). This was a premature failure, occurring at 14.3% below the design ultimate load of 210 kip (934 kN). At the time of failure the load was being held to record data for the 180-kip (800-kN) load increment. The panel failed before the data were recorded.

The failure mode consisted of a general instability buckle in the fourth bay between frames 3 and 4. The failure is shown in figure 19. The crown of the hat section stiffeners crippled inward. The composite reinforcement straps fractured at the crippling line and separated from the stiffeners by peeling back to the frames, as illustrated by figure 20. A close examination of the failed bonds between the straps and stiffeners revealed a consistent failure pattern. A 0.125- to 0.25-in. (0.318- to 0.636-cm)-wide band in the center of the bond line showed a cohesive failure, while the remaining area on each side of this narrow band showed an adhesive failure indicative of a substandard bond (fig. 20).

The premature failure of this panel, precipitated by the poor bond between the composite strap and hat stiffener, prompted a reexamination of the bond lines on the second panel. Nondestructive testing indicated the presence of low-quality bonds in this panel as well. A rework program, described in appendix C, was developed to remove and rebond the reinforcing straps.

The Moiré grid shadow fringe pattern (fig. 21a) visually portrays the axial skin buckling half-wave pattern established in the panel face sheet during the test. This photograph was taken at an applied load of 79 kip (351 kN) and shows the seven half-wave pattern established in selective areas of the panel. At the 180-kip (800-kN) failure load the pattern was uniform and highly defined (fig. 21b).

Bending strains in the panel face sheet were recorded by the back-to-back strain gages (Nos. 29 and 30) at the center of the panel. The bending strains $\Delta\epsilon$ defined as one-half the difference between the two back-to-back gage readings, were used in a modified Southwell plot to experimentally determine the critical skin buckling load. The plots presented in figure 22 for the two 90-kip (400-kN) compression preloads indicate a critical buckling load of 89 kip (396 kN). This compares to the BUCLASP predictions of 79.8 kip (355 kN).

The last set of data obtained before failure of the panel was at an applied load of 165 kip (735 kN); these data are summarized in figure 23. The axial strains recorded from the back-to-back gages located on the panel face sheet and composite reinforcement straps are plotted as a function of the gage position along the panel length. The magnitudes of the measured strains were found to fall between the theoretical values predicted by assuming fully effective skin and conservatively assuming an effective skin width $W_e = 0.85t\sqrt{E/F_c}$.

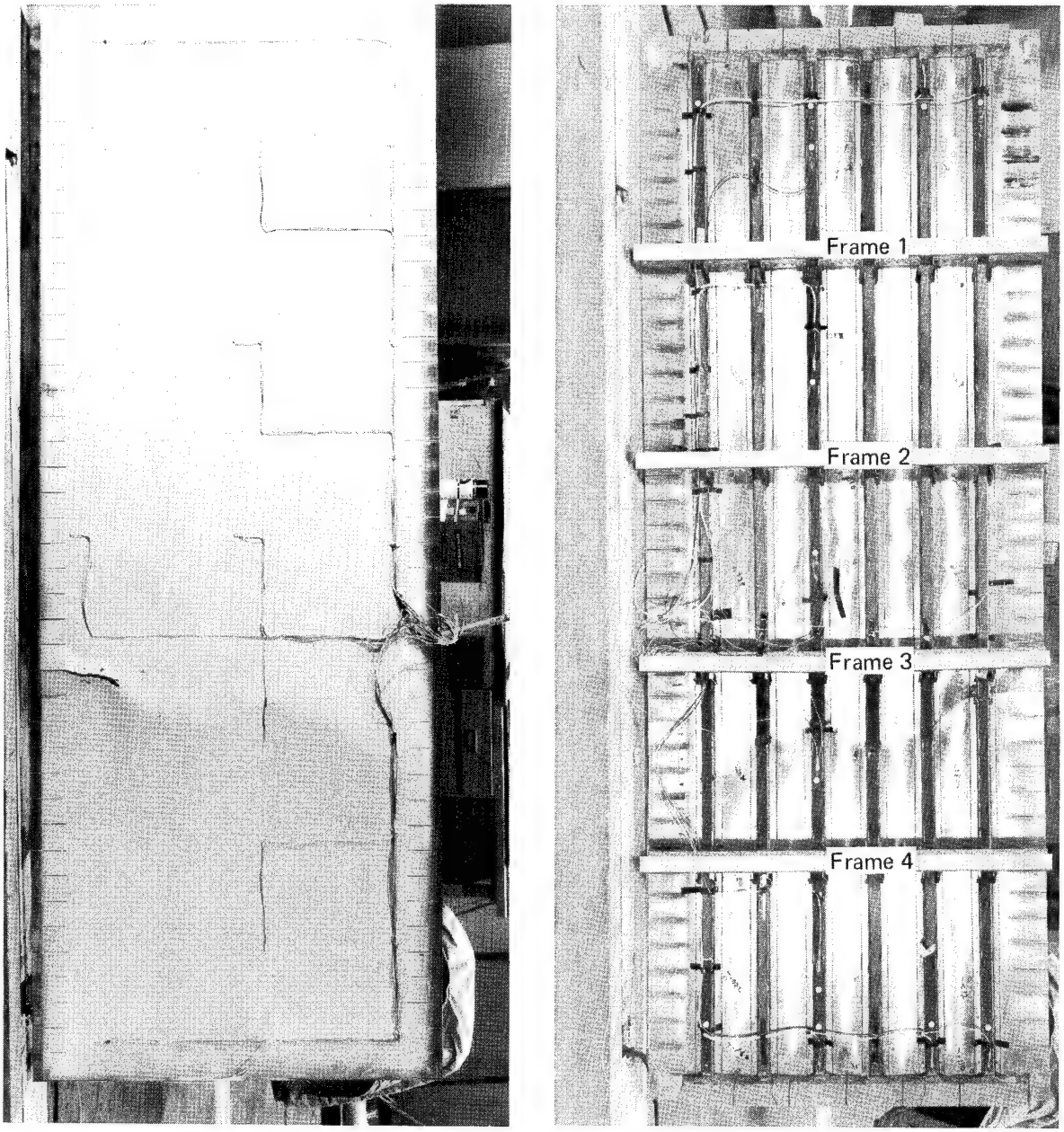

Front View **Rear View**

FIGURE 19.–FAILURE OF COMPRESSION PANEL 1

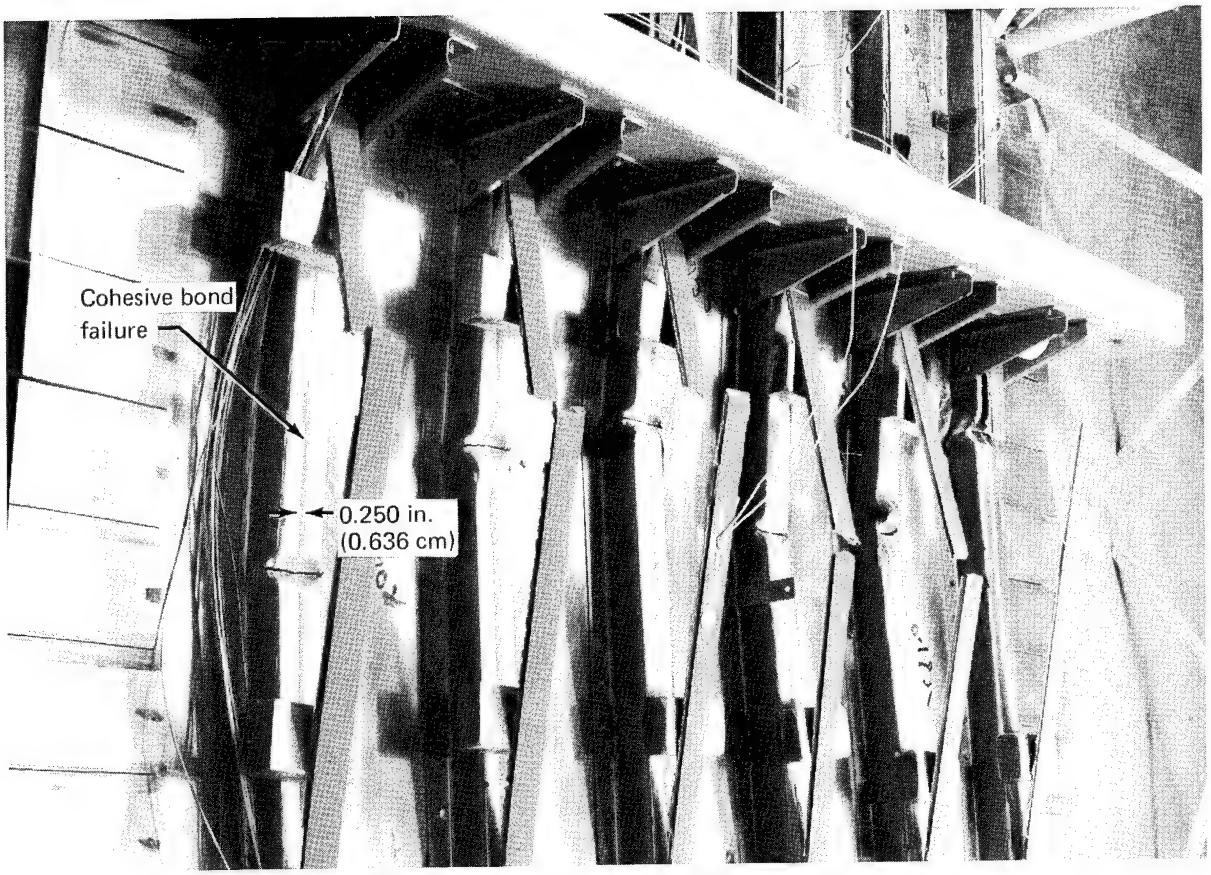

FIGURE 20.–CLOSEUP VIEW OF FAILED AREA–PANEL 1

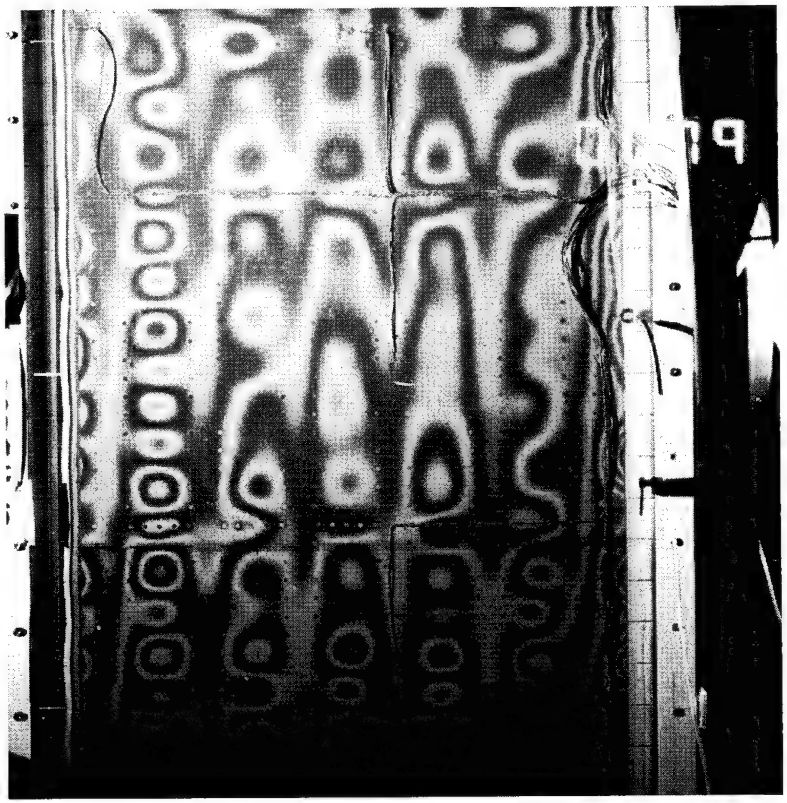

(a) **Seven Half-Wave Skin Buckling Pattern**

Established in selective areas of the panel for an applied load of 79 kip (351 kN)

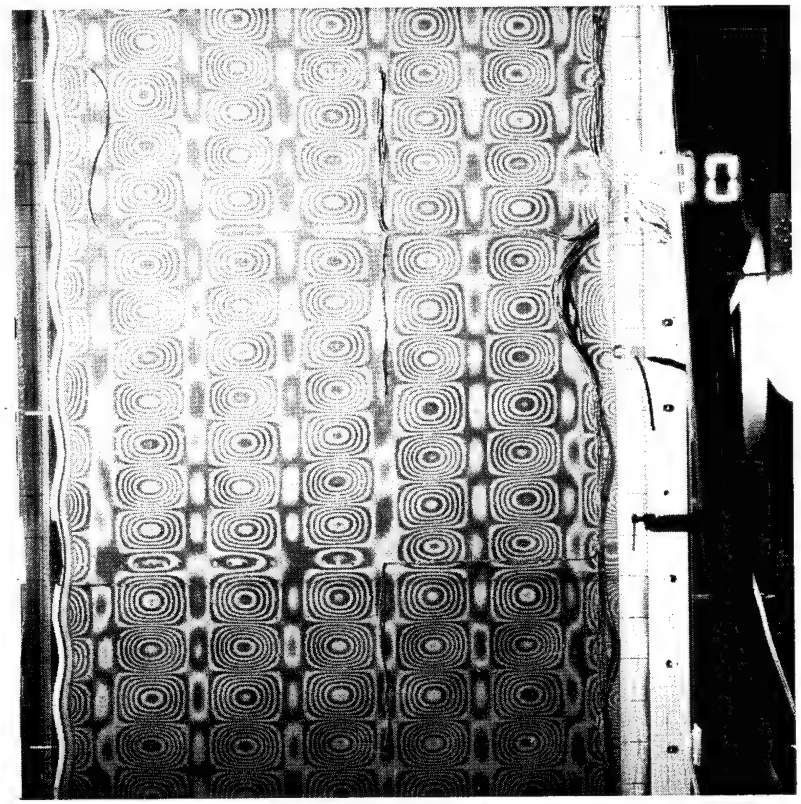

(b) **Fully Defined, Uniform Seven Half-Wave Skin Buckling Pattern**

Established at an applied load of 180 kip (800 kN)

FIGURE 21.–MOIRE´ GRID SHADOW FRINGE PATTERN INDICATING LOCAL SKIN BUCKLING

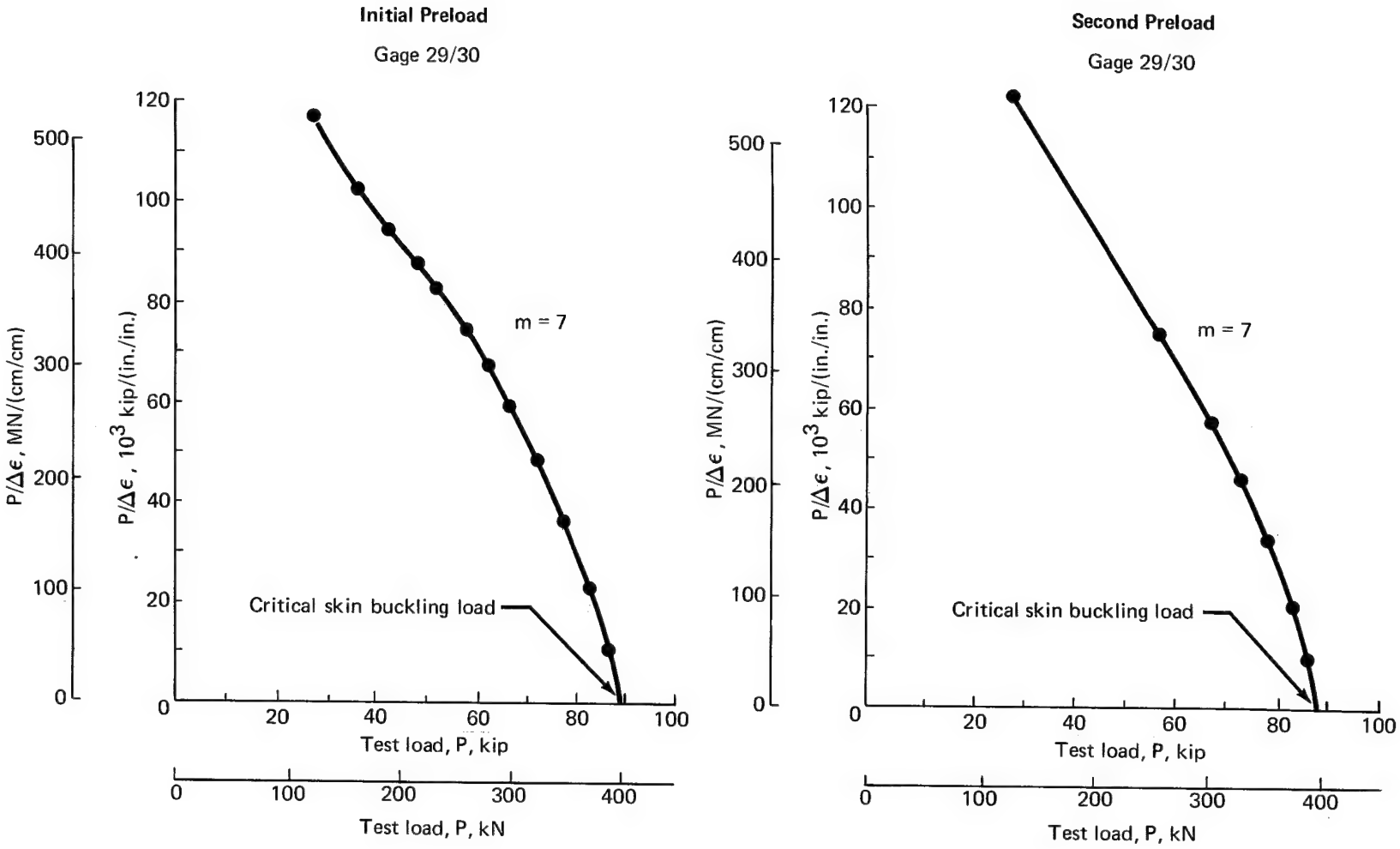

FIGURE 22.– EMPIRICAL DETERMINATION OF CRITICAL SKIN BUCKLING LOAD–MODIFIED SOUTHWELL PLOT

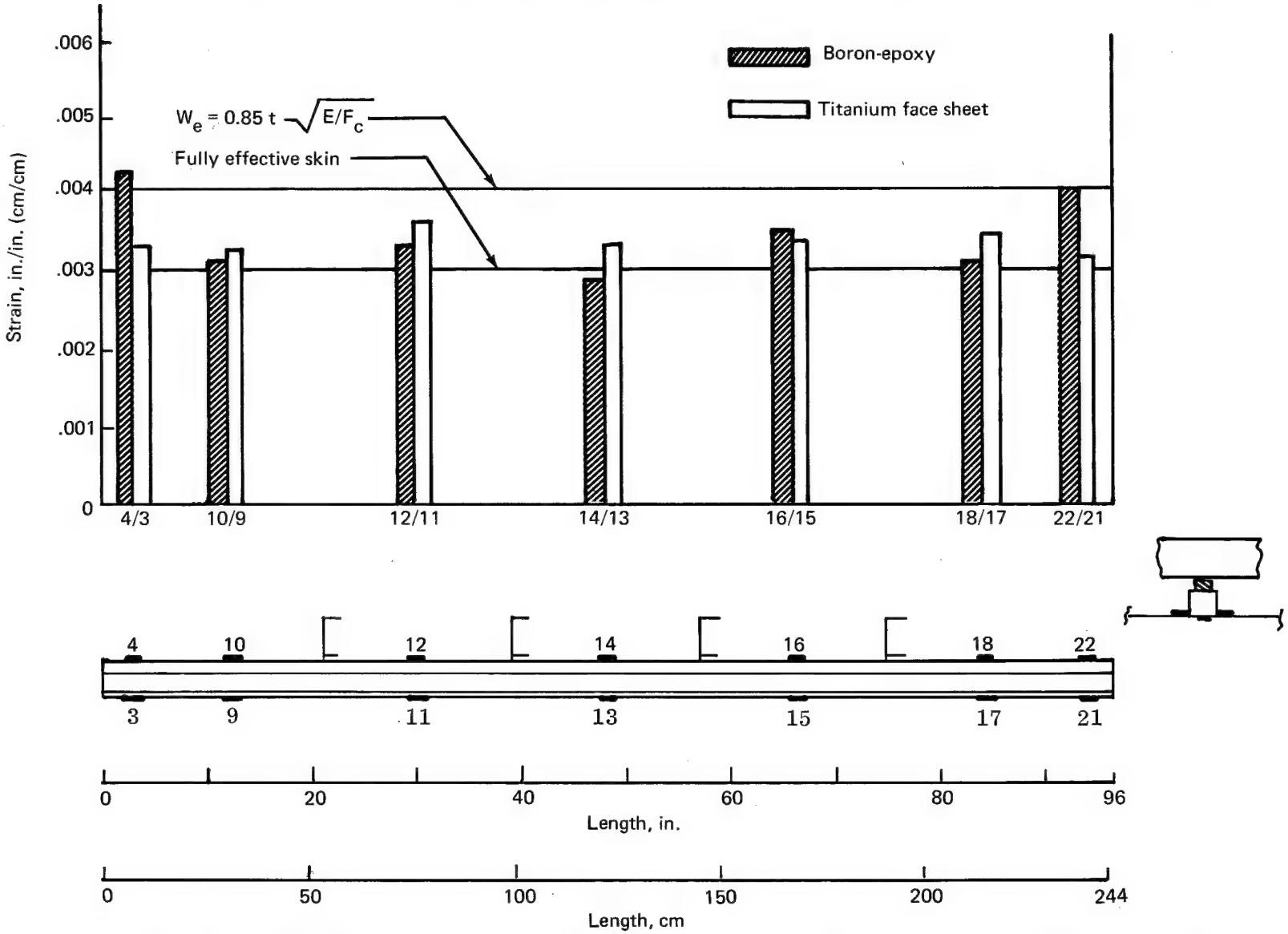

FIGURE 23.–TEST PANEL 1–AXIAL STRAINS MEASURED IN TITANIUM FACE SHEET AND COMPOSITE REINFORCEMENT–APPLIED LOAD = 165 KIP (733 kN)

The electrical deflection indicators (EDIs) showed that all except the number 3 frame remained reasonably fixed during the test. The panel in the area of frame 3 deflected laterally at a relatively low load and remained in this position until the panel failed.

Test panel 2.—No degradation in strength was incurred due to the cyclic loading of the second test panel. Load deflection curves recorded for each cyclic load application were identically repetitive.

The compression load to failure portion of the test was equally successful. The panel failed at an applied load of 228.25 kip (1015.3 kN), an 11% increase over the design ultimate failure load of 210 kip (934 kN).

The ultimate failure, a general instability compression buckle, occurred in the second bay adjacent to the second frame, as illustrated in figure 24. The face sheet buckled outward, away from the stiffeners, causing a sharp crimping failure in the stiffener crown. The boron-epoxy reinforcement straps fractured at the failure line but remained bonded to the stiffeners.

The back-to-back strain gage data recorded at a load level of 227.6 kip (1012.4 kN), just prior to the ultimate panel failure, indicated the presence of local bending modes which introduced increased compression loads in the face sheets and decreased loads in the reinforcing straps. This form of loading was consistent with the resulting failure mode. The strain data are presented in graphic form in figure 25.

In addition to the 34.7% weight savings achieved by the reinforced panel design, an 11% increase in ultimate strength was demonstrated by the second panel, in comparison to the all-titanium design. The ultimate strengths of the three panels are compared in bar chart form in figure 26. This figure also demonstrates the panel performance with respect to design requirements.

Discussion

The composite-reinforced design achieved a higher test load intensity and lighter structural weight than the all-titanium panel designed to the same criteria. A 34.7% lighter weight was realized for the reinforced design.

The premature failure of the first test panel may be directly attributed to the adhesive bond line failure between the reinforcing straps and hat stiffener. Although the anticipated ultimate failure load was not achieved during this test, data relating to local skin buckling phenomena were obtained. Strain gage data and Moiré fringe patterns confirmed close correlation between actual skin buckling and theoretical predictions based on the BUCLASP program. The measured critical skin buckling load was within 11% of the predicted values, while the critical strains were within 6% of predicted values. The number of half-wave buckles agreed with predictions.

The 100 compression load cycles prior to ultimate failure loading of the second panel caused no apparent structural damage to the specimen.

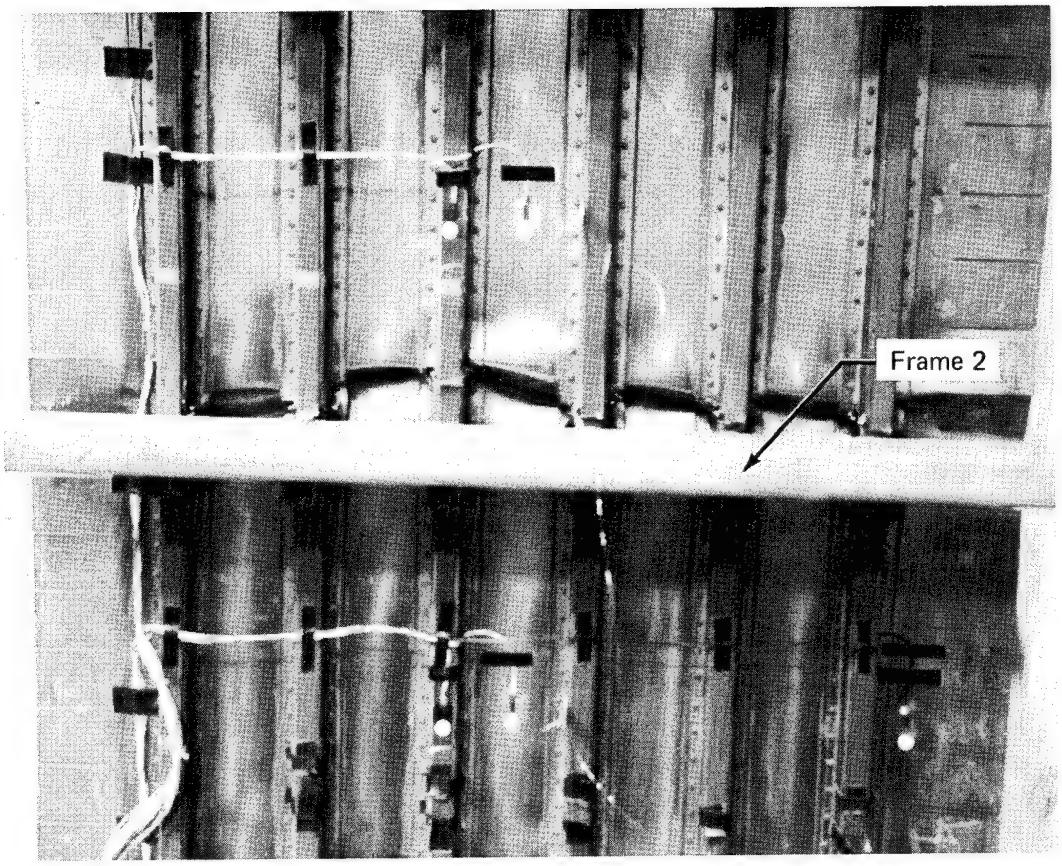

FIGURE 24.—FAILURE OF COMPRESSION PANEL 2

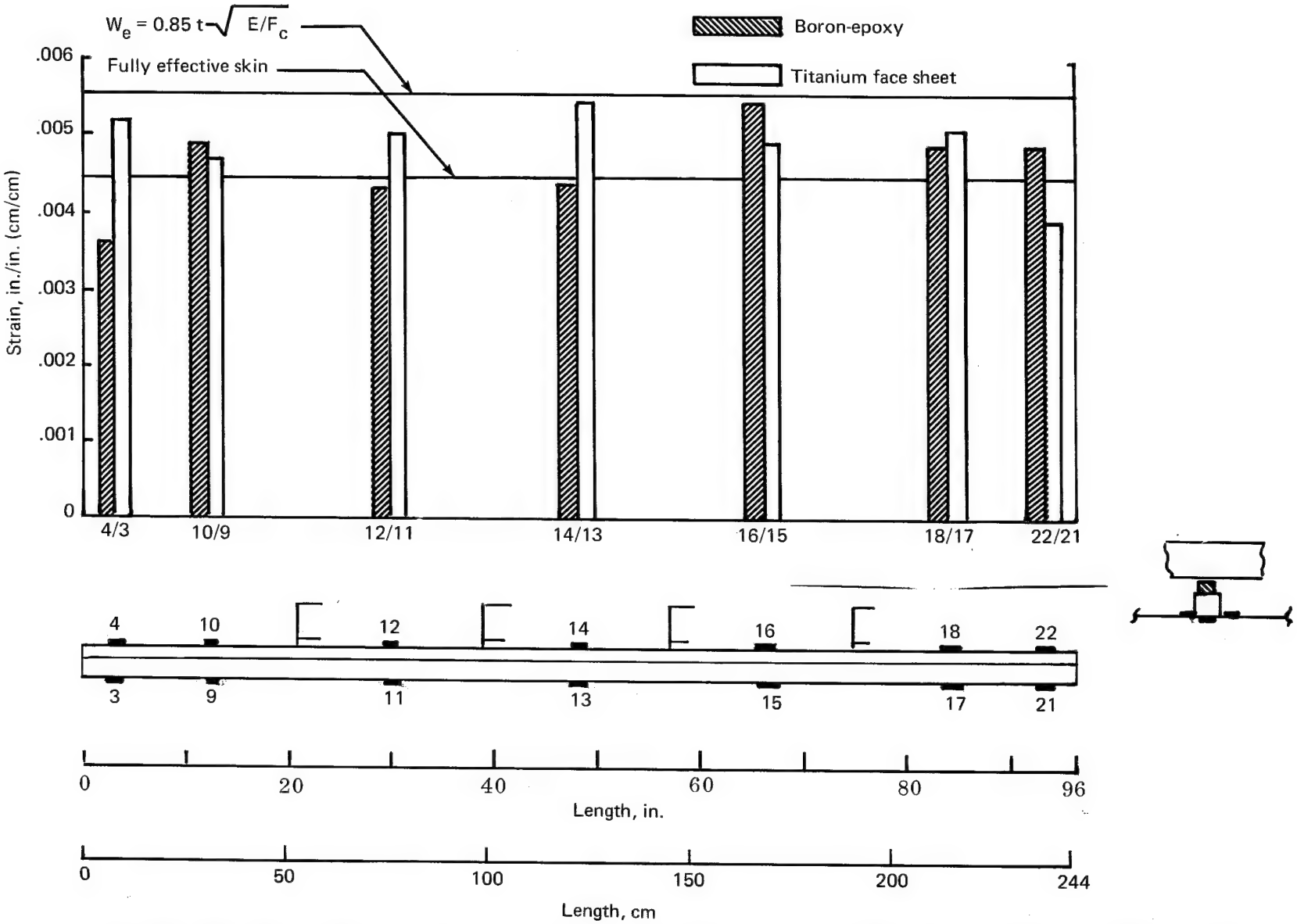

FIGURE 25.—TEST PANEL 2—AXIAL STRAINS MEASURED IN TITANIUM FACE SHEET AND COMPOSITE REINFORCEMENT—APPLIED LOAD = 227 KIP (1010 kN)

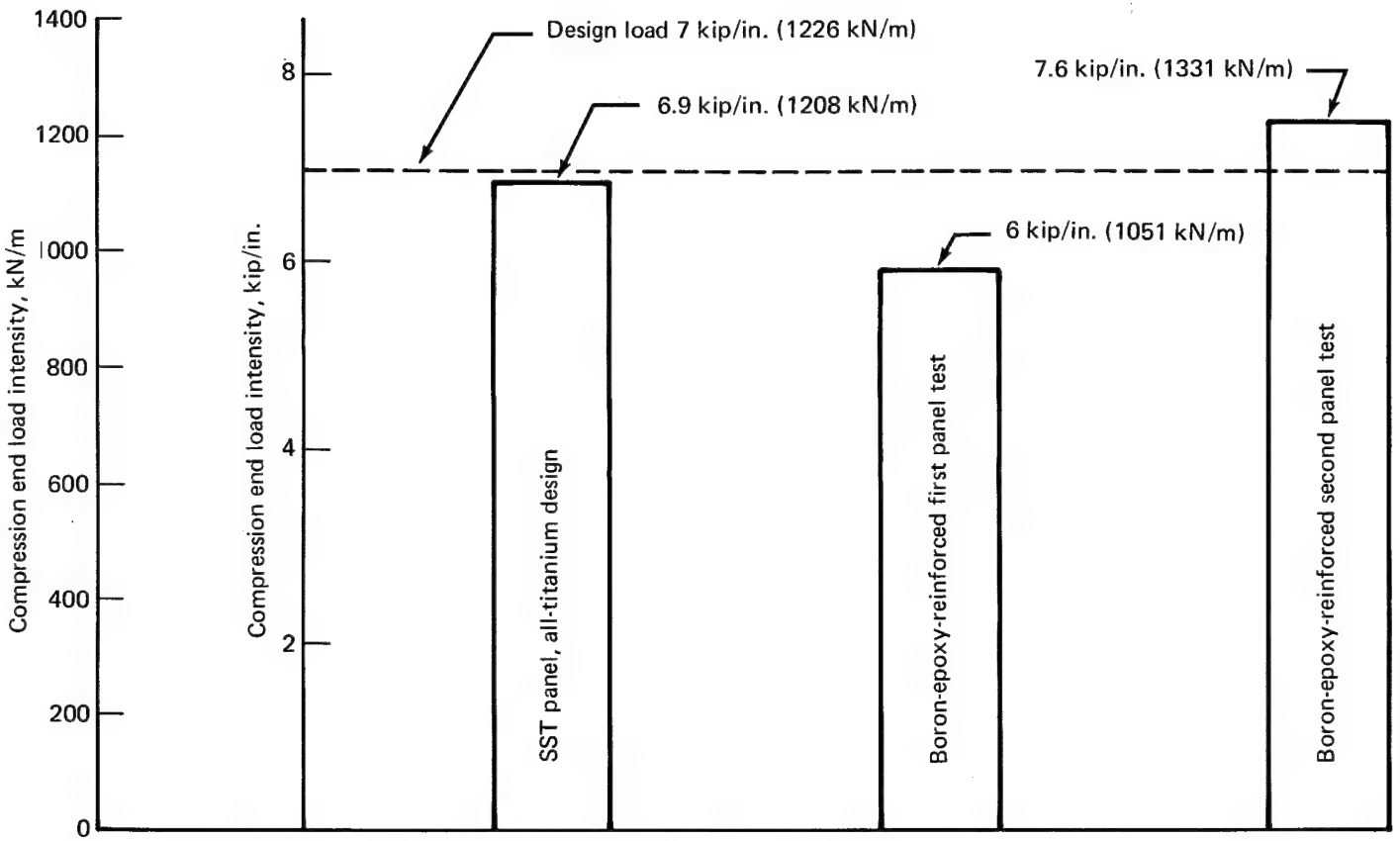

FIGURE 26.—COMPARISON OF ULTIMATE COMPRESSION STRENGTH OF ALL-TITANIUM AND BORON-EPOXY-REINFORCED MULTIBAY COMPRESSION PANELS

WINDOW BELT PANEL

Objective and Background

This portion of the program was to evaluate the effectiveness of multidirectional boron-epoxy reinforcement applied to cutouts in shear-critical aircraft structure. To perform this investigation the following steps were considered.

- Design and fabricate a boron-epoxy-reinforced metal panel capable of meeting the multidirectional load requirements of a typical aircraft fuselage.
- Demonstrate the amount of potential weight savings which might be realized by using a boron-epoxy-reinforced design in lieu of the conventional all-metal design.
- Structurally test the component under realistic load conditions to verify the design concept and analysis predictions.

The window belt section of the 747 aircraft was chosen in order to investigate the reinforcement capabilities of filamentary composites for multidirectional loading and for load transfer around structural cutouts. The fuselage structure in the window belt area is required to carry a combined loading consisting of shear, hoop tension, and side-bending components. The shear loads, accompanied by the large ratio of hole-out to remaining area in the immediate window belt area, creates a requirement for local reinforcement.

The selection of the 747 window belt area in particular had several attractions. First, the present 747 design represents the current state of the art of conventional skin stringer fuselage design. Secondly, extensive analysis of this structure was available as a base for comparison.

A three-window panel, designed to meet the static design requirements of the 747 side body, was fabricated and tested. Body station 1530, shown in figure 27, was selected. The panel was designed using boron-reinforced metal and tested to evaluate fabrication and analysis procedures.

Panel Design

Design loads.—Four ultimate load cases were selected as critical for design purposes:

- Hoop Tension—Internal Pressurization—2P, where 2P = two factors ultimate on the maximum pressure differential.
- Hoop Tension Combined with Vertical Bending—1.5P + VB

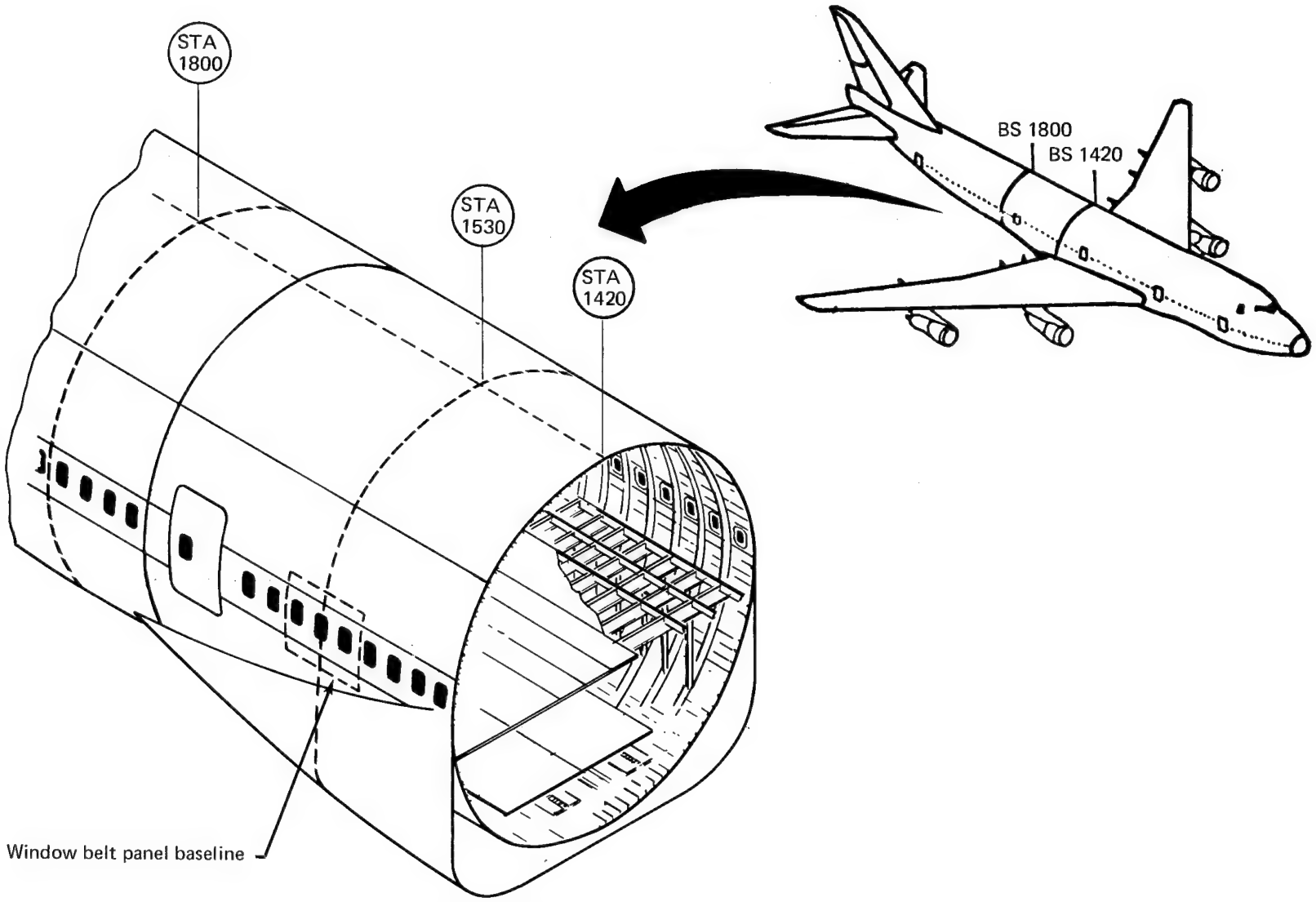

FIGURE 27.–747 WINDOW BELT–BASELINE FOR DESIGN

- Hoop Tension Combined with Side Bending–1.5P + SB
- Vertical Bending–VB

The principal loads associated with each of the four load cases are summarized in table 4.

Material selection.–Boron-epoxy-reinforced titanium sheet was selected as the primary material system for the window belt panel. This material system offered a high strength-to-density ratio and improved residual thermal stress characteristics over those of a composite-aluminum material system.

The titanium face sheets were 6Al-4V condition I titanium alloy. Aluminum honeycomb core (5052 alloy) was selected for the sandwich core material. Various core densities were used, depending on the panel detail requirements.

A moderate-temperature curing epoxy adhesive, AF-126, was used. BP-907 resin was used for preparation of the boron-epoxy tapes.

Test panel concepts.–Two panel design concepts were considered in some depth before the test panel design was finalized. Both concepts incorporated honeycomb sandwich construction, which in itself represented a major deviation from conventional primary aircraft structure design practices. This approach was taken to benefit from the increased stability, improved fatigue performance, and reduced weight provided by this type design.

In the initial design concept, the reinforcement was concentrated in precured, multilayered, unidirectional straps. These straps were positioned to form a composite truss and interconnected through titanium load transfer fittings. The unidirectional boron filaments in each strap were used to carry the body shear loads around the window cutouts. The metal sandwich faces provide the stiffness required to prevent lateral buckling, contain the fuselage pressure, and carry loads away from the window frames to be redistributed in the basic structure. The general concept is illustrated in figure 28.

This design concept underwent several iterations considering aluminum faces, titanium faces, and configurations incorporating a low-modulus, fiberglass plug in the low-stress regions immediately above and below the window openings. A lightweight panel design using the composite-truss titanium face sandwich configuration was produced.

The second design concept consisted of selectively reinforcing the panel face sheets by bonding precured composite laminates to the inside surface of the faces. The individual, unidirectional laminates were selectively located and oriented to form a multidirectional composite doubler which, when bonded to the panel face sheet, formed a true orthotropic sandwich panel. The number of reinforcement laminates and their filament orientations were determined by the magnitude and principal direction of the anticipated loads. In this concept, the metal face sheets and the boron-epoxy reinforcement jointly share the primary applied loads and pressure containment requirements. This concept is illustrated in figure 29.

Table 4.–747 Fuselage Body Station 1530 Design Load Requirements

Load case	N_c lb/in. (kN/m)	N_L lb/in. (kN/m)	q_o lb/in. (kN/m)
2P	2400 (420)	1200 (210)	0
1.5P + VB	1800 (315)	900 (157)	1520 (266)
1.5P + SB(T)	1800 (315)	3360 (588)	1035 (181)
VB*	0	0	1520 (266)

P–maximum relief valve setting
VP–vertical bending
SB(T)–side bending (tension)
*Test load case

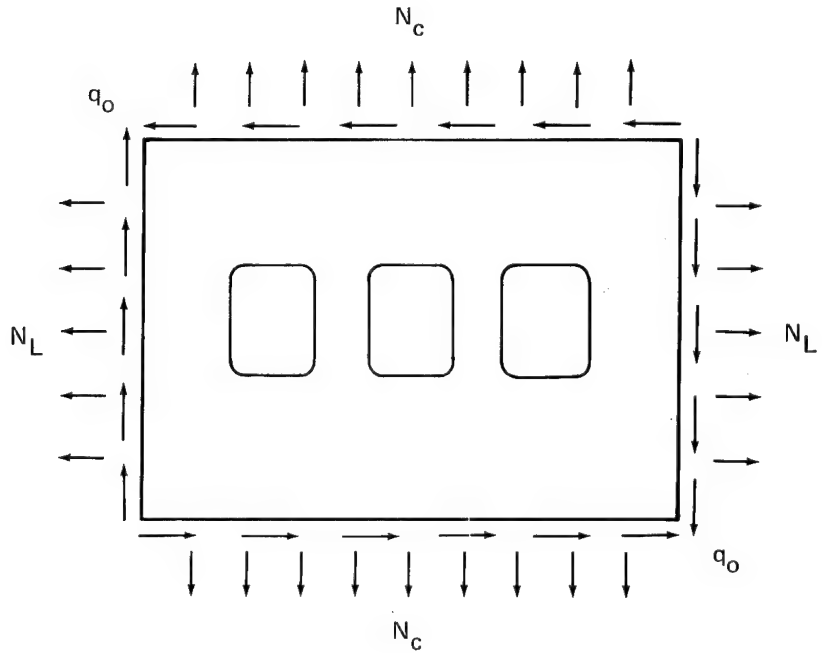

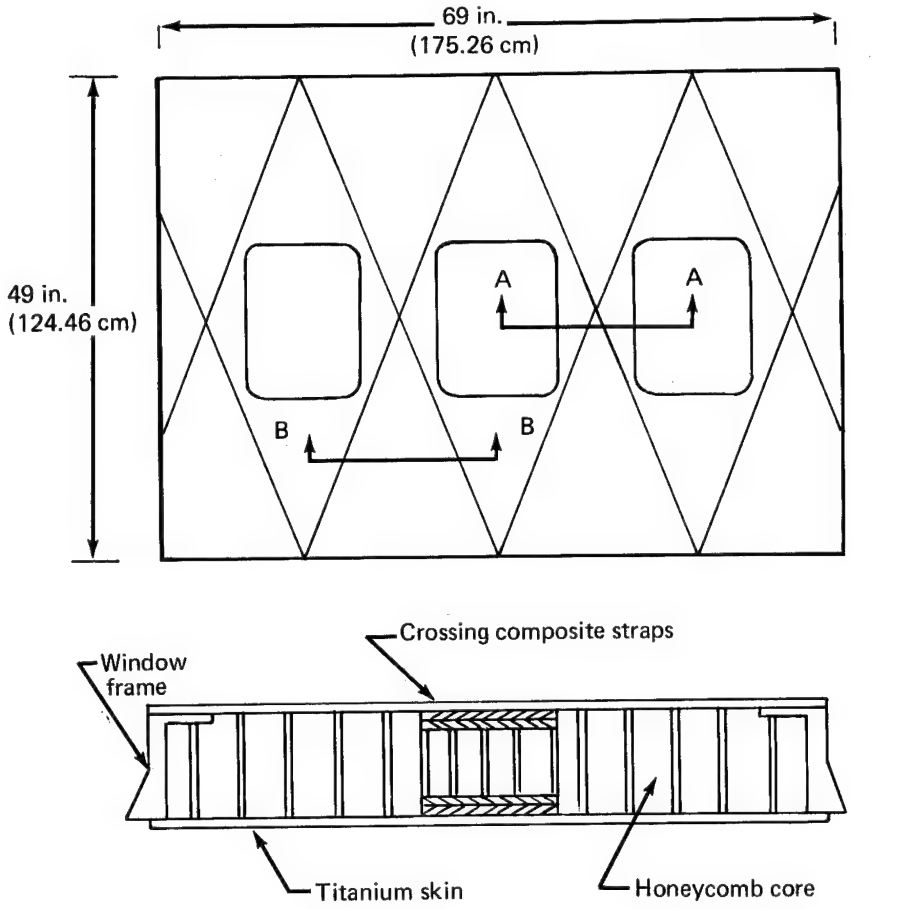

FIGURE 28.—REINFORCED WINDOW BELT PANEL—COMPOSITE TRUSS DESIGN CONCEPT

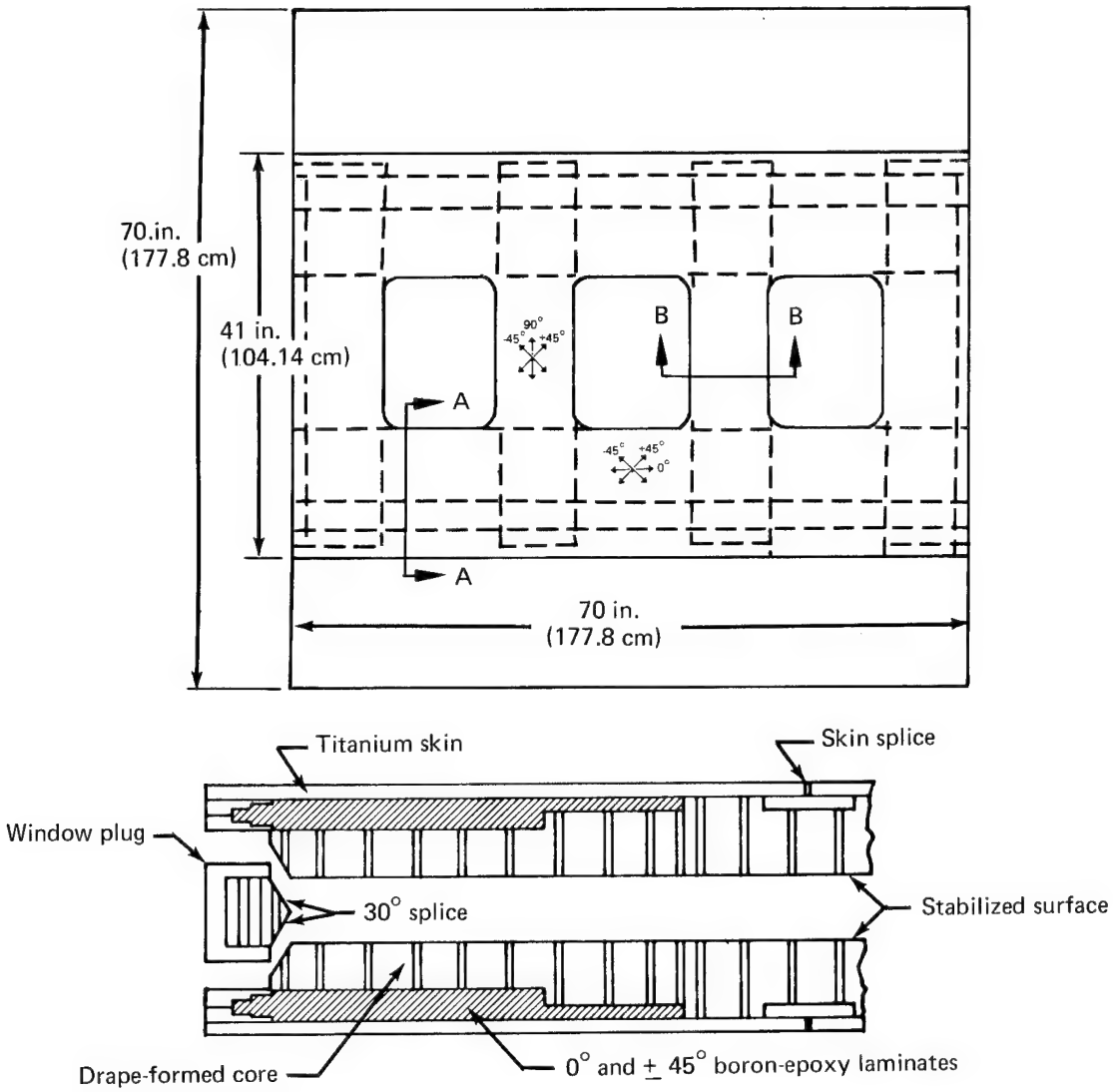

FIGURE 29.—REINFORCED WINDOW BELT PANEL—MULTIDIRECTIONAL LAMINATE CONFIGURATION

As in the truss concept, several configurations using aluminum and titanium face sheets of various gages and varying degrees of composite reinforcement were considered. A lightweight panel design was also achieved with this concept.

Design concept selection.—The composite-truss and laminated-doubler reinforcing concepts were attractive from both structural and weight-saving considerations. The truss concept demonstrated slightly greater weight savings, but this advantage was offset by a fabrication tolerance problem. The criss-cross pattern of the truss straps necessitated that the straps be located in different planes within the sandwich thickness, to prevent interference at the strap intersection points between the windows. This requirement gave rise to numerous core details of varying thickness and of irregular shapes. This fact, combined with the difficulty anticipated in dealing with the tolerance buildup, made the laminated-doubler design appear more attractive from practical producibility considerations.

The cross-ply laminated-doubler concept required comparable quantities of boron-epoxy reinforcement, and the estimated fabrication costs were considerably less than those estimated for the truss concept. In addition, the doubler concept lent itself to innovative fabrication procedures which effectively eliminated the tolerance buildup problem. The cross-ply laminate concept was therefore selected for the test panel design.

Design analysis.—The panel design was based on an ultimate load analysis and was performed in two parts. A hand analysis employing conventional stress methods with simplifying assumptions was applied initially for preliminary sizing of face sheet and boron reinforcement requirements. The window frames and other metal details were sized in the same manner. A honeycomb sandwich, shear buckling stability analysis determined the core requirements. The panel design determined by this procedure was used as a design input for a finite-element analysis. This, based on a forced-displacement, plane stress solution, provided a detailed analysis of the panel under the combined loading conditions established for the four design load cases. Results of this analysis were used to refine the design by redistributing the boron reinforcement to indicated high-stress areas. The refined design was then reanalyzed in an iterative process before the final design was achieved. The 0°, ±45°, and 90° cross-ply orientations were considered as fixed design parameters.

Hand analysis procedure.—The maximum predicted longitudinal, circumferential, and shear loads associated with the four design load cases were considered to be applied independently and the face sheets and boron reinforcement sized to carry the individual loads. The applied loads were assumed to be evenly distributed along the 70-in. (177.8-cm) panel edges and equally shared by the two sandwich faces. The basic metal faces, in areas remote from the window cutouts, were sized so that they would sustain the three components of the applied loads. This face gage was then continued through the window belt area and reinforced as required with the boron-epoxy laminates.

Sufficient reinforcement was added in both the longitudinal and circumferential directions to replace the material lost in the window cutouts. Longitudinal reinforcement straps were placed both above and below the windows, primarily to carry the side-bending loads. Since the reinforcement was continuous along the window belt length, there was little tendency for stress concentration to occur. This reinforcing material, added strictly as a replacement, was more than adequate.

Circumferential reinforcement was required between the windows to carry the hoop tension loads due to internal pressure. The straps were extended for some distance above and below the window line to allow gradual distribution of the loads to or from the basic face sheet.

Additional shear material in the form of ±45° cross-ply laminates was provided over the whole window belt area. Load transfer fittings were used around the window openings to ensure positive load transfer in the high-shear regions. The titanium window frames were thickened at the corners to withstand the load concentrations at these locations.

Results from a previous finite-element program were valuable in determining the amount of required shear reinforcement. Allowances were made for the increased shear buildup around the window openings. The maximum shear between the windows was approximately 2.5 times the required calculated average.

The quantity of reinforcement required was determined by first calculating the load capability of the titanium face sheet. The strength of the titanium in the reinforced area is limited by the strain capability of the boron filaments. The design criteria established by phase I testing indicated that the boron fiber extensional strain should not exceed 6000 μin./in. (μcm/cm). This limits the titanium strength to 96 ksi (662 MN/m^2) in tension, based on an E of 16 x 10^6 psi (110 GN/m^2). The difference between the applied load and that carried by the face sheets represented the load to be carried by the reinforcement. The load capacity of a single boron-epoxy laminate was based on a 50% fiber volume and a ply thickness of 0.0055 in. (0.014 cm). Using a filament E of 58 x 10^6 psi (400 GN/m^2), the limiting ply tensile strength is 906 lb/in. (159 kN/m). The number of reinforcing plies required was then determined by the simple ratio of the load to be carried versus the load capability per ply (906 lb/in. (159 kN/m)). This amount of reinforcement was applied to the metal face sheet material to obtain a positive margin of safety.

The number of ±45° cross-ply laminates for shear reinforcement was determined in a similar manner. The effective shear strength of the basic face sheet was calculated using strain compatibility and the critical extensional strain of the boron filaments as design criteria. This shear strength was then converted to shear load capability per inch of face sheet. The difference between the applied shear load and that carried by the face sheet represented the load to be carried by the cross-ply reinforcing laminates. The ultimate shear strength of a single ±45° cross-ply laminate was converted to a load-per-inch capability of 670 lb/in. (118 kN/m). The number of cross-ply laminates required was then determined by the simple ratio of load to be carried versus load capability. The 2.5 factor was applied to the total shear load to account for the load buildup around the window openings.

A stepped, laminated layup was selected on the basis of previous experience of load buildup patterns around cutouts. A symmetrical layup was also selected to reduce residual stress distortions.

Computer analysis–finite-element program.–A finite-element program, based on a forced displacement, plane stress analysis concept, was used to analyze the window belt panel. The analysis was conducted in two stages. The first stage consisted of solving for three basic distortion modes of unit amplitude–circumferential extension, longitudinal

extension, and shear deformation—for an infinitely long panel. A typical three-window region was extracted from the infinitely long panel for detailed analysis. The resultant external forces required to produce the unitary deformation states were then calculated.

In the second stage of the analysis, the design loads were applied to the three-window panel, and the plane stress solution for each case was obtained by proper scaling and superposition of the unitary distortion cases. A more definitive analysis was then conducted on a quarter window section.

The basic plane stress finite element used in the analysis was the arbitrary quadrilateral with five nodal points. A two-node rod element was used to model the fuselage frames. The finite-element grid used for the quarter window analysis was composed of 893 plate elements, 49 rod elements, and 800 nodal points.

The output from the plane stress finite-element analysis program consists of the following:

- Nodal displacements and nodal forces, including reactions
- A panel equilibrium check
- Strain values at nodal points and at the center of each grid element: the x-y strain components (ϵ_{xx}, ϵ_{yy}, γ_{xy}), the principal strains in the x-y plane (ϵ_{11}, ϵ_{22}), the maximum principal shear strain γ_{max}, and the transverse strain ϵ_3 in the z-direction
- The corresponding x-y stress components, principal stresses in the x-y plane, and maximum principal shear stresses
- Strain and stress envelopes for each material
- Contour plots of the above computed solutions

A contour plot of the predicted principal strains (ϵ_{11}) for the test load case is reproduced in figure 30. The predicted strains have been further resolved in the principal fiber directions (0°, ±45°, and 90°) and contour plots sketched for these orientations (fig. 31). Maximum strains for the four critical design conditions are presented in table 5.

Test panel description.—The resulting design consisted of a three-window panel, 70 in. (177.8 cm) square and 0.75 in. (1.90 cm) thick. The panel was of bonded sandwich construction with 0.020-in. (0.051-cm) titanium alloy (Ti-6Al-4V) face sheets and varying-density aluminum alloy (5052) honeycomb core. The boron-epoxy reinforcement was applied at the interface of the titanium face sheets and the honeycomb core. The reinforcement was confined, circumferentially, to a central 36-in. (91.4-cm) wide section of the panel encompassing the window cutouts. Chemically milled titanium step fittings were incorporated in the design for efficient load transfer in load concentration areas such as around the window openings. The window frames were machined from titanium plate to form a

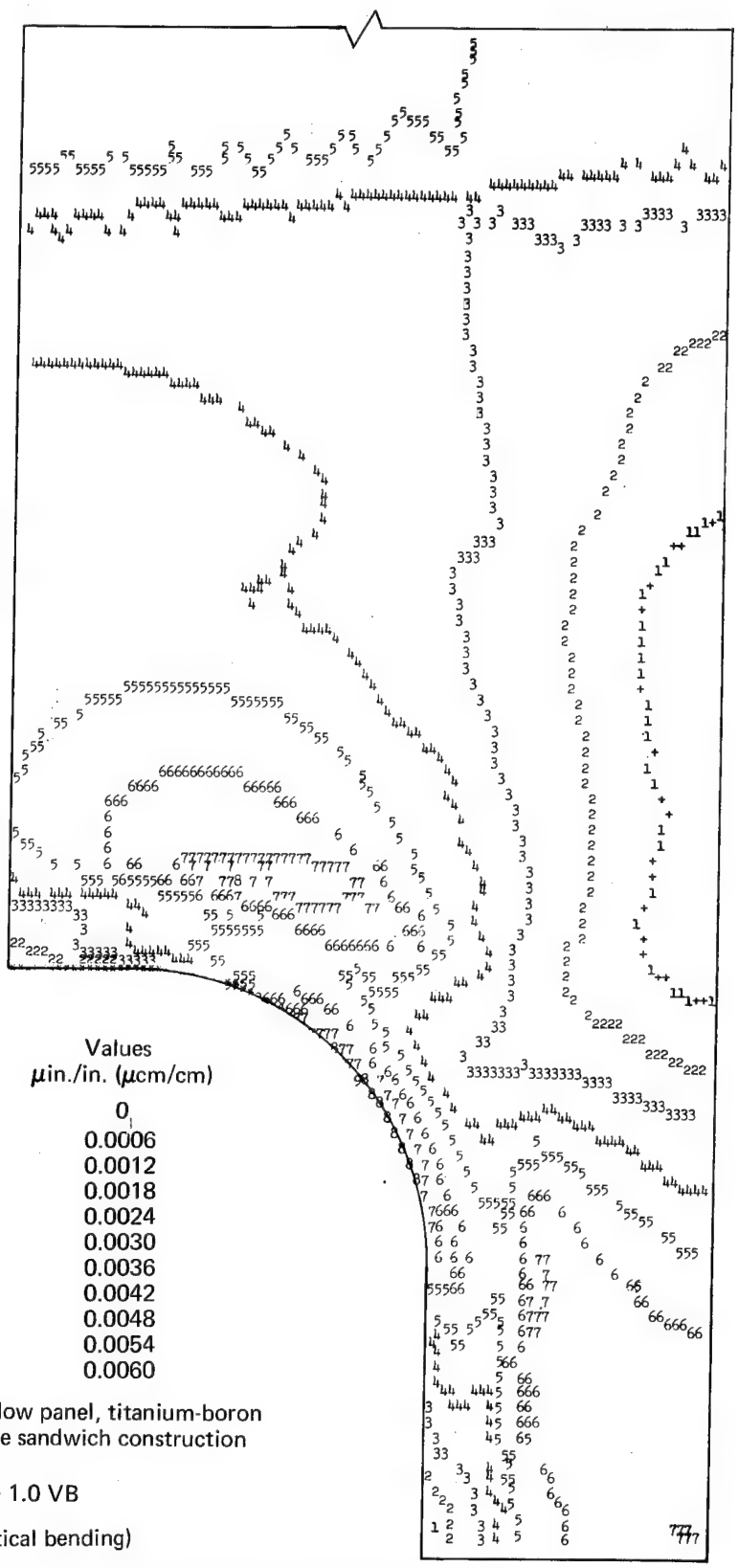

Character	Values μin./in. (μcm/cm)
0	0
1	0.0006
2	0.0012
3	0.0018
4	0.0024
5	0.0030
6	0.0036
7	0.0042
8	0.0048
9	0.0054
10	0.0060

747 window panel, titanium-boron composite sandwich construction

Loadcase 1.0 VB

(VB=vertical bending)

FIGURE 30.—PRINCIPAL STRAINS FOR VERTICAL BENDING LOAD CASE

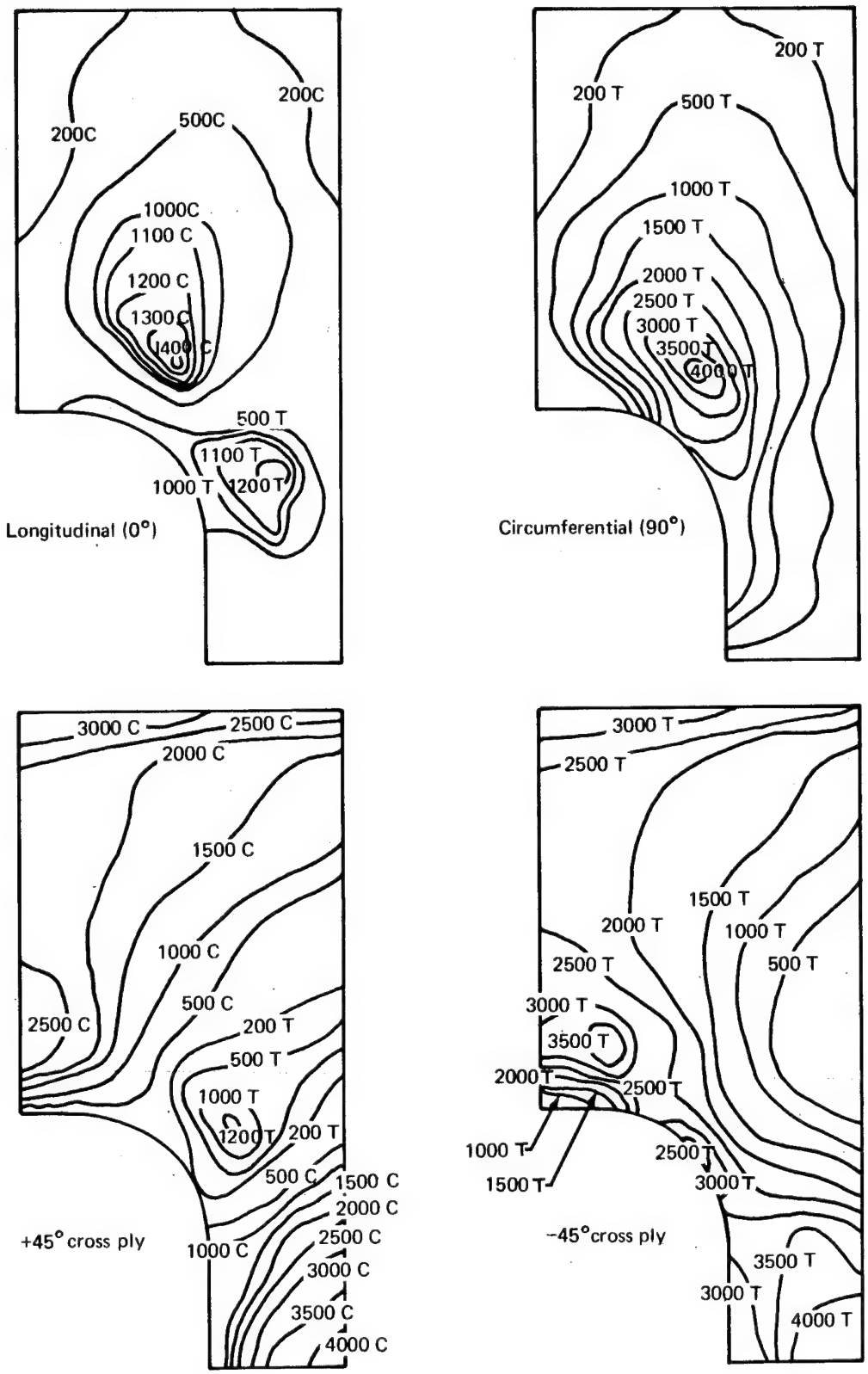

FIGURE 31.–PREDICTED STRAIN DISTRIBUTIONS IN PRINCIPAL FIBER DIRECTION

Table 5.—Critical Element Strains Predicted by Finite-Element Analysis

Load case	Critical strain ϵ_{11}, μin./in. (μcm/cm)[a]			
	Titanium	Boron-epoxy reinforcement		
	ϵ_{11}	ϵ_{fiber}[b]	Direction	MS[c]
2P	3230	2975	90°	1.02
1.5P + VB	7283	5654	135°	0.06
1.5P + SB(T)	6350	4975	135°	0.21
VB	5500	4215	135°	0.42

[a]Critical strains based on maximum principal strain at element centers for the design loads associated with each load case (ref. table 4)

[b]Maximum principal strain resolved into fiber direction

[c]Margin of safety based on an ultimate fiber strain of 6000μin./in. (μcm/cm)

one-piece frame of U-channel cross section. The web thickness was increased at the window corners to accommodate the load concentration in these areas. Pertinent panel detail design features are illustrated in figure 32. The layup sequence for the precured boron-epoxy laminates is shown in figure 33.

Structural weight comparisons between composite-reinforced and conventional window belt structure were based on a typical 44 - by 20-in. (112 - by 51-cm.) window section. The results of this weight analysis are presented in table 6. Potential weight savings of 36.9% of the 747 baseline window belt panel were indicated for the composite reinforced design. Actual weight saving for the as-manufactured panel was 33.2%.

Test Specimen Fabrication

The window belt panel was assembled by structural adhesive bonding to form a flat, composite-reinforced sandwich panel. Several fabrication and assembly techniques, including chemical milling, numerical control machining, drape form bonding, and core stabilization were required to complete the window belt panel. A discussion of these techniques and a complete review of the panel fabrication is presented in appendix C.

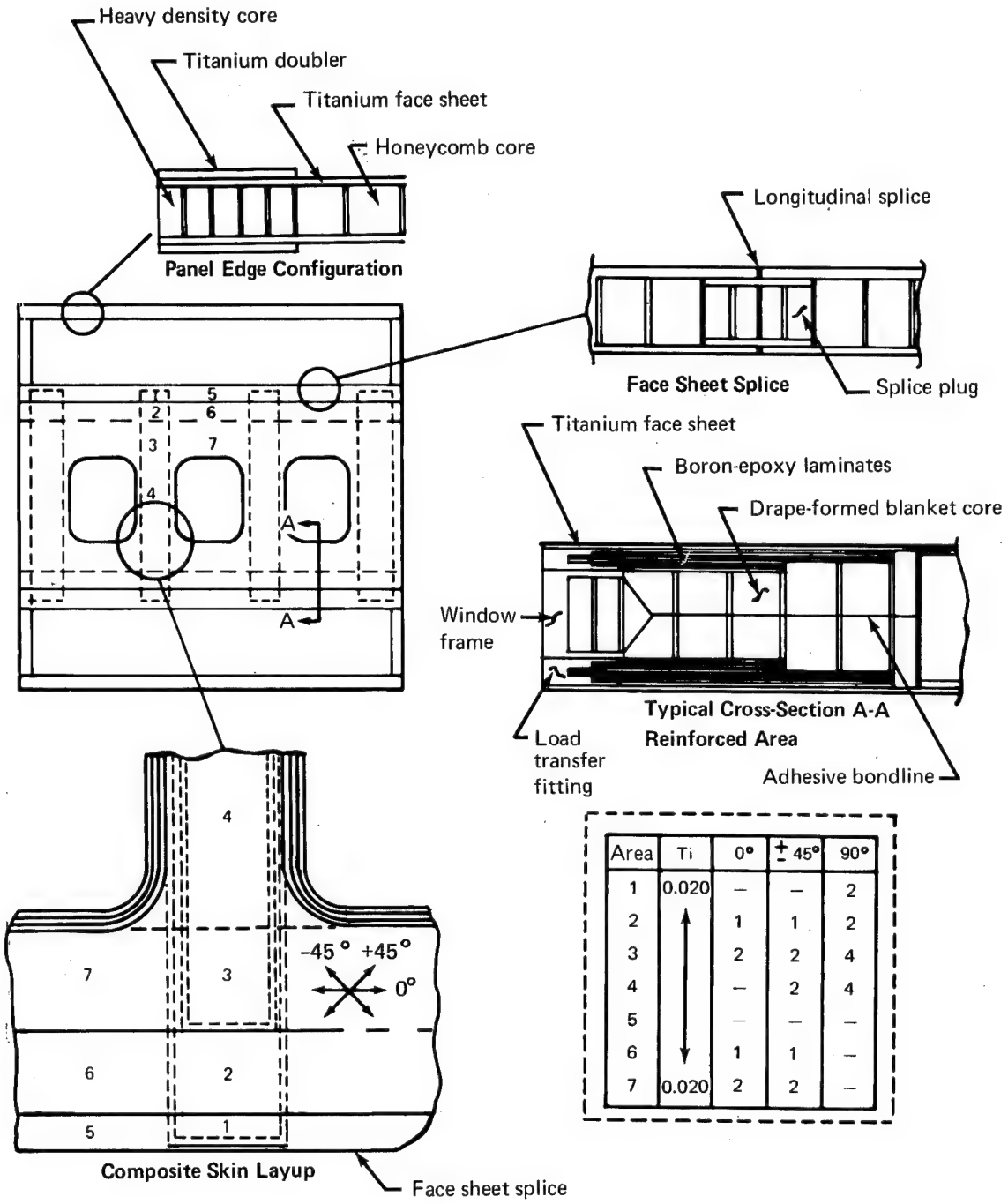

Area	Ti	0°	± 45°	90°
1	0.020	–	–	2
2		1	1	2
3		2	2	4
4		–	2	4
5		–	–	–
6		1	1	–
7	0.020	2	2	–

FIGURE 32.—PERTINENT DETAIL DESIGN FEATURES OF REINFORCED WINDOW BELT PANEL

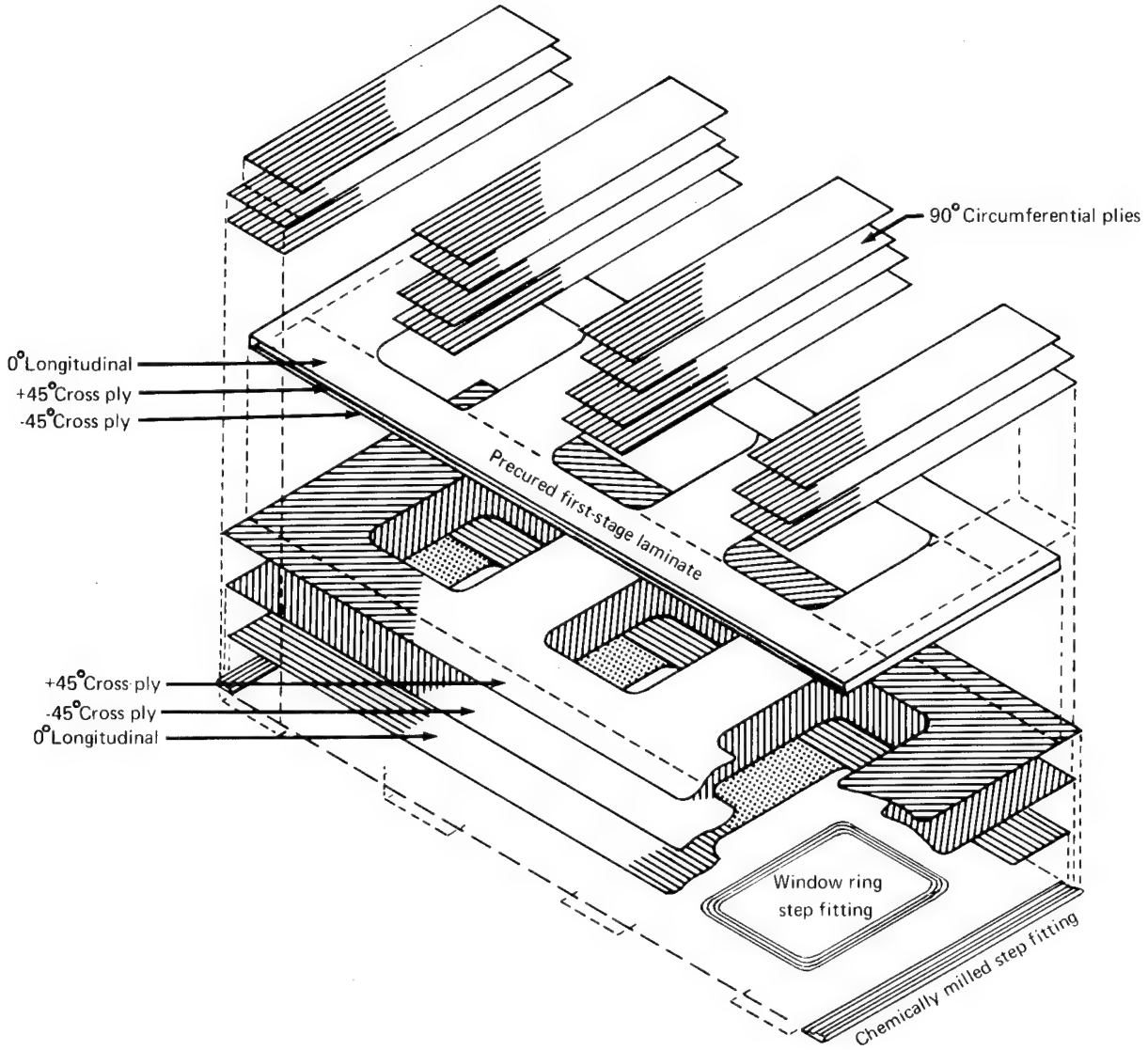

FIGURE 33.—LAYUP SEQUENCE OF MULTIDIRECTIONAL REINFORCEMENT LAMINATES

Table 6.—Weight Analysis of Window Belt Panel

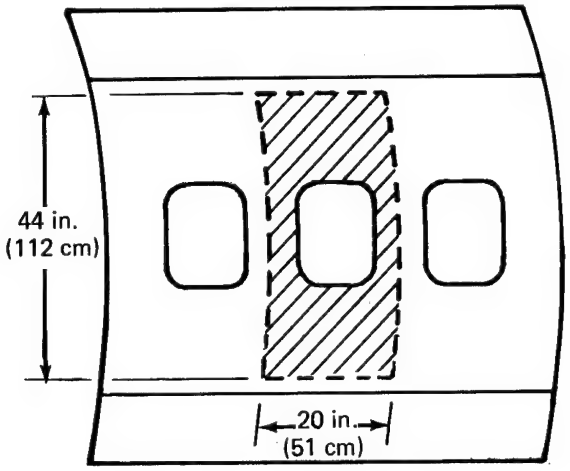

Component	Structural weight, lb (kg)			
	747 conventional skin-stringer		Boron-epoxy-reinforced titanium sandwich	
Skin	5.70	(2.58)	4.46	(2.03)
Stringers	4.80	(2.17)	—	—
Doubler	4.40	(1.99)	—	—
Window frame	6.60	(2.99)	1.46	(0.66)
Load transfer fitting	—	—	0.50	(0.23)
Honeycomb core	—	—	1.62	(0.73)
Boron-epoxy	—	—	2.50	(1.13)
Adhesive	0.20	(0.09)	2.84	(1.29)
Fuselage frame	1.60	(0.73)	1.32	(0.60)
Total	23.30	(10.55)	14.70	(6.67)
Weight saved			8.60	(3.88)
Percent weight saved			36.9%	

Testing

The test plan involved simulation of the vertical bending load by testing the window belt panel in pure shear. A brief description of the test fixture, panel instrumentation, data recording system, test procedure, and a summary of test results are presented.

Test fixture.—The test fixture consisted of a modified picture frame, shear loading fixture shown in figure 34. Each of the four sides of the picture frame consisted of two steel bars, 1.5 in. (3.81 cm) thick and 5 in. (12.7 cm) wide running the full length of the panel and interconnected at the ends with pinned joints.

The shear load was transferred from the picture frame to the panel by means of high-strength Z-section flexure members. The flexures were designed to provide sufficient inline shear stiffness to transfer the shear load and at the same time present very little transverse bending stiffness to permit in-plane panel deflection.

The panel and test fixture was installed in the 1200-kip (5337-kN) Baldwin Universal test machine. The test load was introduced through clevis assemblies pinned to two diagonal corners of the picture frame (fig. 35). The pinned connection ensured essentially pure shear loading of the panel. Lateral deflection of the two free corners of the panel was prevented by two restraining fixtures mounted on the test machine.

Instrumentation.—The primary panel instrumentation consisted of 11 axial and 39 rectangular rosette, electrical-resistance-wire strain gages. These gages were the principal source of quantitative numerical data. A small portion of the panel was instrumented with a birefringent photoelastic coating. The principal purpose of the photoelastic data was to provide a visual record of the strain distribution around the window cutout.

The axial gages were used to measure the strain in the titanium window frame web. The majority of gages were installed on the center window frame, with a corresponding gage location on the two outboard window frames to check for symmetry of loading.

The rosette gages were installed on the panel faces. Ten gages were located around the periphery, approximately 6 in. from the panel edge, to monitor the symmetry of load application. The remaining gages were concentrated around the center window portion of the panel in the high-strain areas indicated by the computer analysis. Gages located in the composite-reinforced skin areas were oriented so that each leg of the gage was parallel to the principal fiber directions. In this way, the strain recorded for each leg closely represents the true strain in the fibers. These data could then be compared directly with predicted fiber strains for the particular panel location. Six gage locations were selected for back-to-back gage installation. By strain gaging each face of the panel, a comparison of the strains in corresponding legs would indicate the presence and magnitude of any out-of-plane bending of the panel.

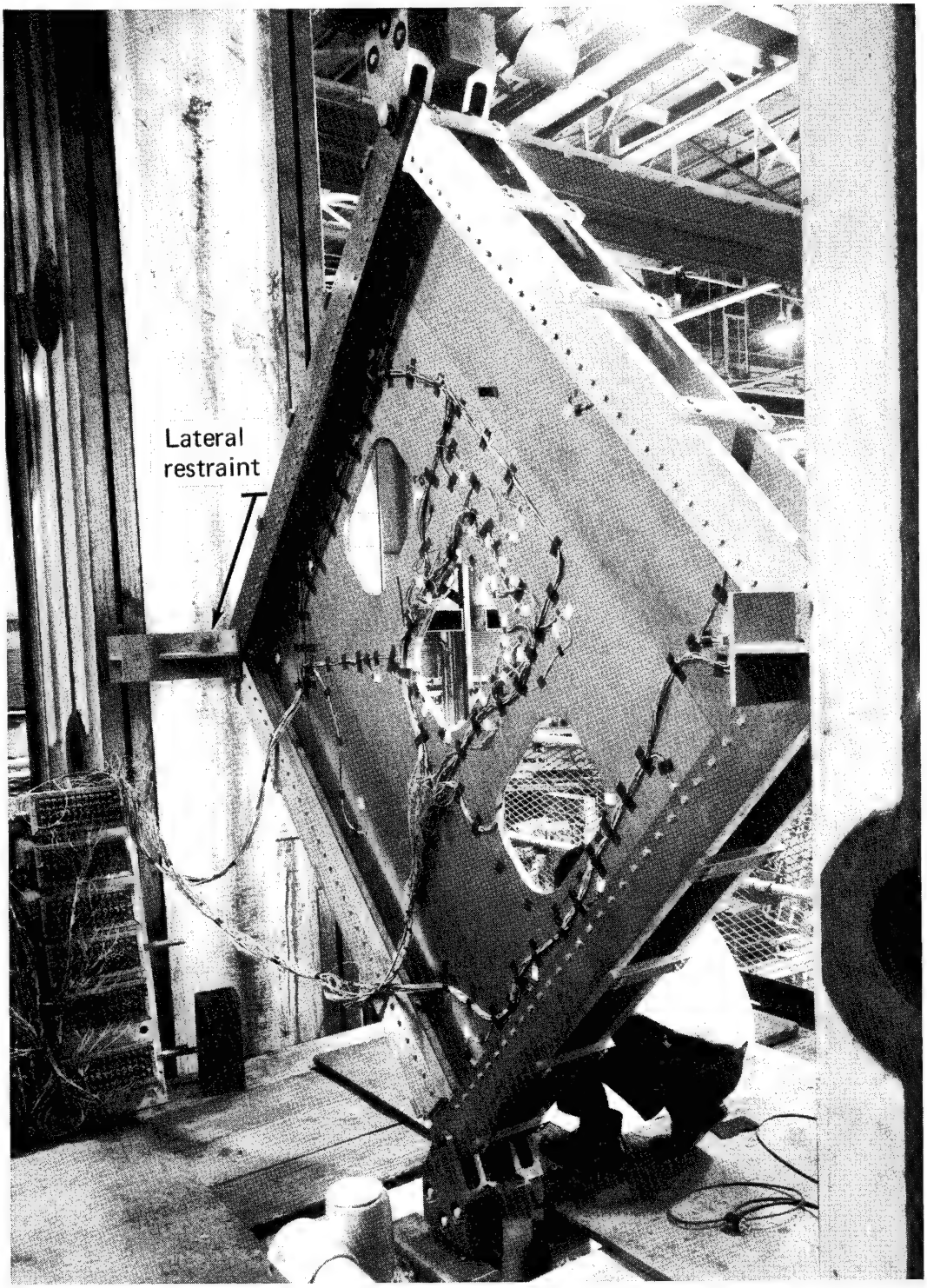

FIGURE 34.—PICTURE FRAME SHEAR TEST FIXTURE

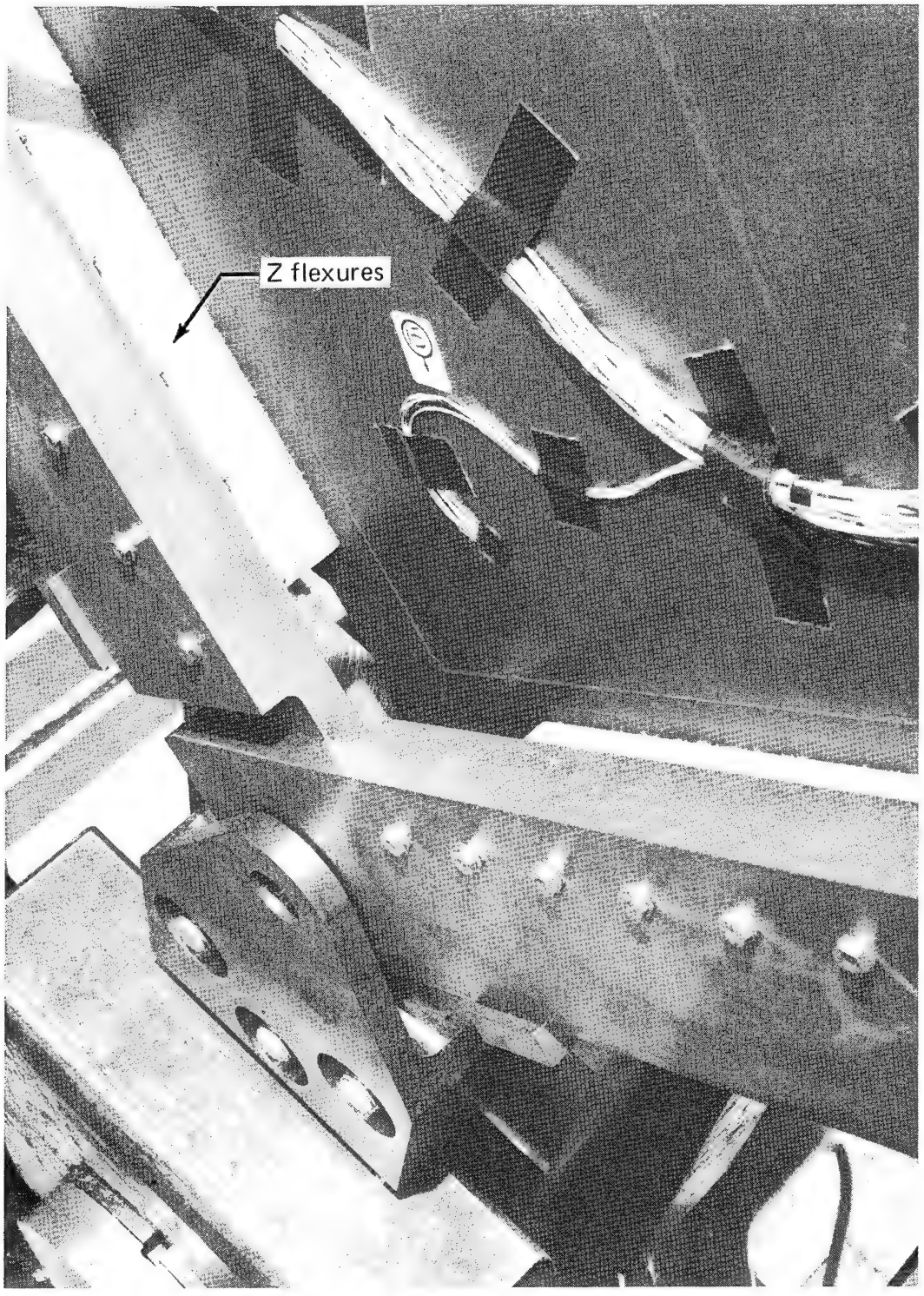

FIGURE 35.–PINNED CLEVIS LOADING MECHANISM

The birefringent photoelastic coating was applied to a quarter section of the center window, diagonally opposite to the highly instrumented window corner. This section also corresponded to the portion of the panel analyzed by the finite-element analysis program. The strain distribution patterns and the fringe order magnitudes would serve as a comparative base for the predicted and measured strains and distributions. Figure 36 illustrates the strain gage locations and positioning of the birefringent photoelastic material. High-speed motion picture coverage was included in the instrumentation in an attempt to photograph the panel failure sequence.

Test procedures.—The test procedure established for the panel shear test consisted of the following steps:

- Record a zero load scan of the strain gages and read the photostress.
- Establish a loading rate of 20 000 lb/min (88.960 kN/min) and commence loading to the first programmed "hold" at 15 kip (66.72 kN). Record strain gage and photoelastic readings. Review computer online strain data output and progress to next load increment.
- Repeat step 2 above for 30, 45, 60, 75, and 90 kip (133.4, 200.16, 266.8, 333.6, and 400.3 kN). Take isochromatic photographs of photostress area at each increment of load. Review strain gage data, and monitor critical stress areas prior to progressing to next load increment.
- Progress at 15-kip (66.72-kN) increments to 120 kip (533.76 kN). Record strain gage data and take isochromatic photographs at each increment. Hold at 120 kip (533.76 kN) and review data. Establish a recommended load rate to failure and initiation of high-speed motion picture cameras.
- Continue loading at determined load rate to failure. Record strain gage data at 5-kip (22.24-kN) intervals to 140 kip (622.72 kN), then continuously to failure. Photograph area at 10-kip (44.48-kN) intervals to failure.
- Initiate high-speed motion picture cameras at predetermined load and continue through to failure.

Test results.—A successful shear test of the window belt panel was achieved for the vertical bending load case. The panel failed at a total load of 261.07 kip (1161 kN) corresponding to an ultimate shear load of 2635 lb/in. (461.4 kN/m). In evaluating the test results it must be noted that the pure shear or vertical bending load case was not the critical loading condition for which the panel was designed. The most critical load case was a combined loading of 1.5 pressure plus vertical bending. As a result, at the vertical bending design shear load of 1520 lb/in. (266 kN/m) the maximum calculated fiber strain was 4200 μin./in. (μcm/cm), compared to a fiber ultimate strain of 6000 μin./in. (μcm/cm). Because of this, the ultimate load was adjusted by the ratio 6000/4200. This gave an adjusted design ultimate load of 2170 lb/in. (380 kN/m), which corresponds to a test jig tension load of 213 kip (950 kN).

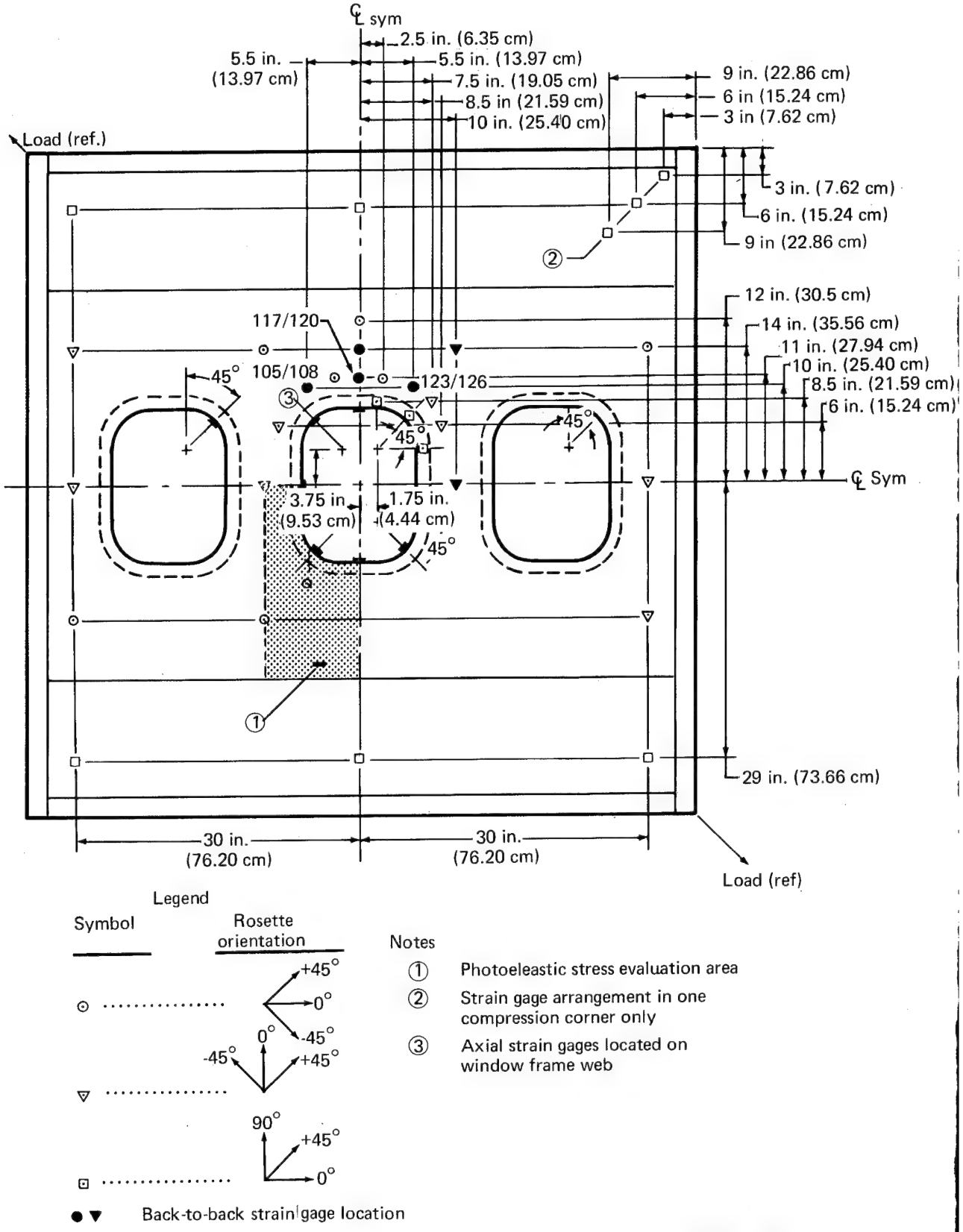

FIGURE 36.—INSTRUMENTATION LAYOUT—REINFORCED WINDOW BELT PANEL

The average shear load applied to the panel edges at failure was 2635 lb/in. (461.4 kN/m), which represents a 21.4% increase over the adjusted ultimate design load. Examination of the failed panel (fig. 37) indicated two predominant failure modes. A pronounced panel buckle extended diagonally across one corner of the panel, while a complete fracture of the panel extended diagonally across the panel in the opposite direction and then ran parallel and adjacent to the boron-epoxy-reinforcement laminate. Dimensions pertinent to these two failure modes are superimposed on a photograph of the failed panel in figure 37. Unfortunately, the failure sequence was not recorded due to a film breakage in a high-speed motion picture camera included in the instrumentation for this purpose.

A review of the peripheral strain gage data indicated that relatively uniform shear loading was achieved along the panel edges. Termination of the shear flexure, load transfer members short of the panel ends was a successful means of relieving the panel corners of high stress concentrations, normally a problem in shear testing. The uniformity of loading was well demonstrated by test instrumentation incorporated for this purpose. Back-to-back strain gages installed to detect panel bending indicated a virtual absence of bending strains until well after the design ultimate load of 213 kip (950N) had been reached. Bending strains due to out-of-plane effects are plotted (fig. 38) against axial strain for increasing load conditions. These strains were measured in the +45° direction and represent the compression component of strain due to the applied shear loading.

The structural symmetry of the panel, as well as the uniformity of loading, is demonstrated by a plot of strain readings recorded for corresponding points on the three window frames (fig. 39). Only slight variations, well within an expected scatter band, were encountered through the elastic portion of the load-strain curves. Some divergence was encountered beyond this point, which may be attributed to local yielding and shear deformation.

A direct comparison between predicted and measured strain magnitudes and distributions has been made for selected points around the center window. The comparison has been made for a panel loading of 150 kip (667 kN) corresponding to the vertical bending shear load of 1520 lb/in. (266 kN/m) used in the finite-element analysis. The predicted and measured strains in the four fiber directions are tabulated in table 7. The plot of actual versus predicted strains in the 45° and 135° fiber directions (fig. 40) illustrates the close correlation obtained between the analysis predictions and test results.

Variations between the actual and predicted readings may be reasonably attributed to minor changes in the reinforcement layup, incorporated after the analysis to facilitate fabrication. Some error is also encountered in interpretation of the higher order, photoelastic fringe patterns.

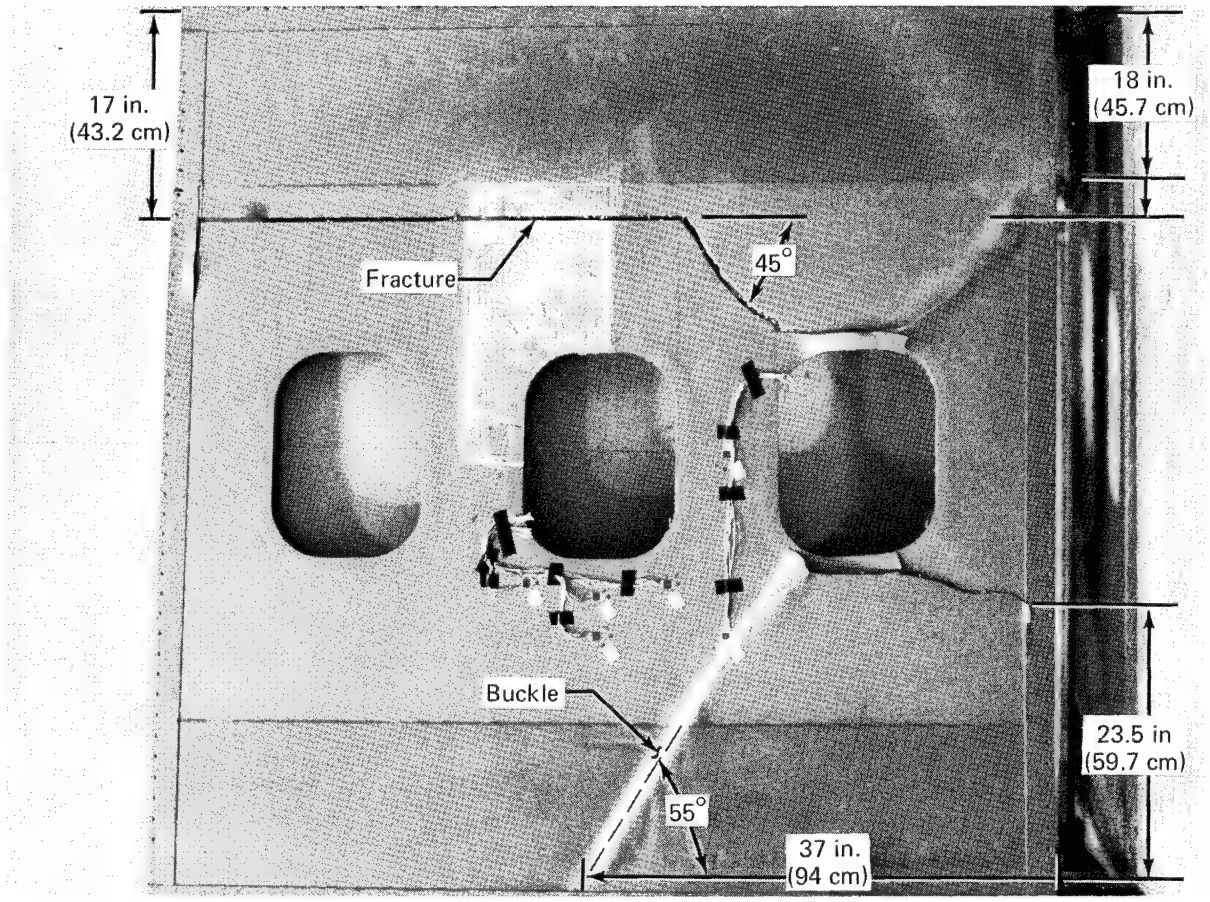

FIGURE 37.—WINDOW BELT PANEL FAILURE

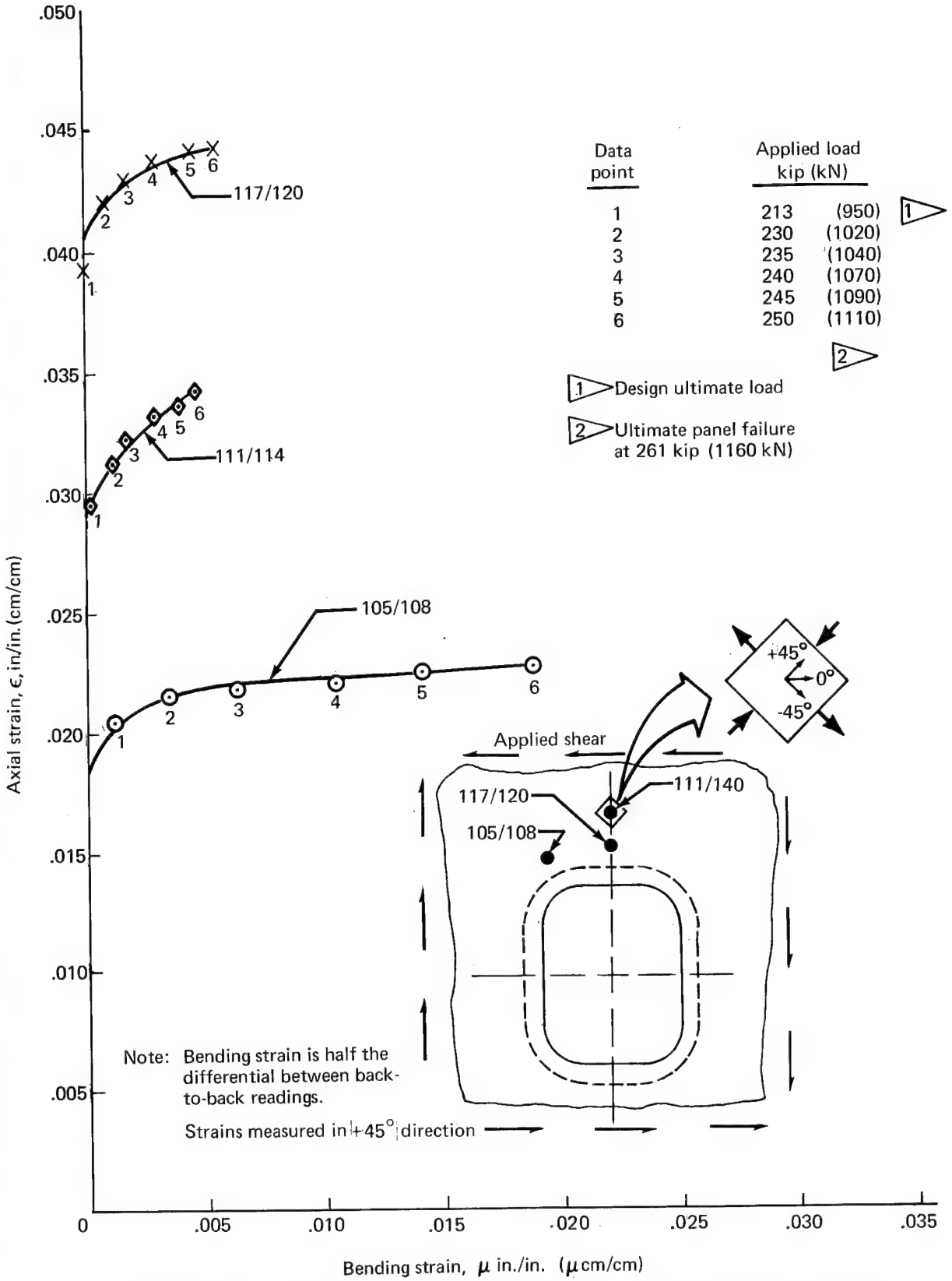

FIGURE 38.— BENDING STRAINS FOR PANEL LOCATIONS INDICATED

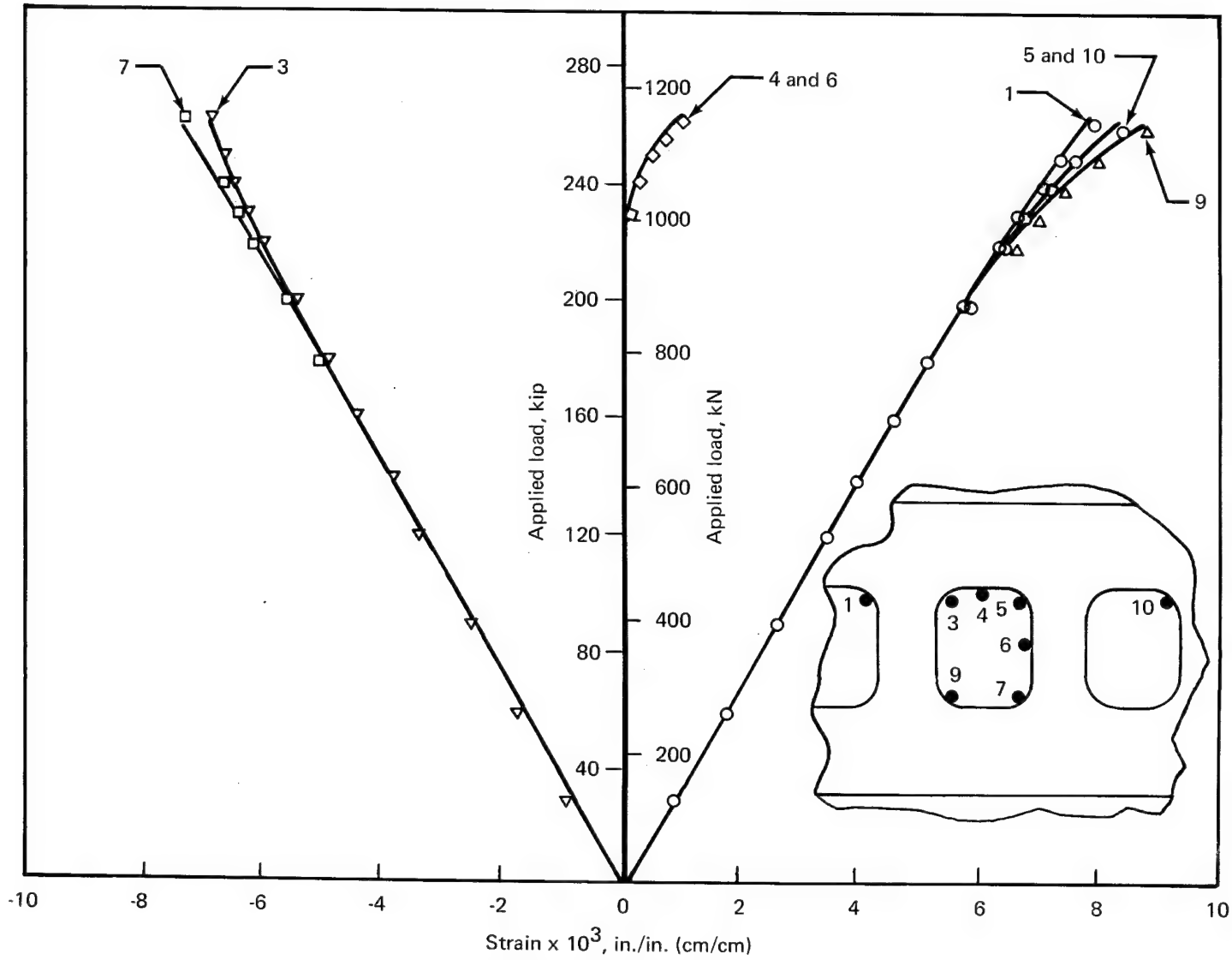

FIGURE 39.—LOAD STRAIN CURVES FOR INDICATED POINTS ON WINDOW FRAMES

Table 7.—Predicted and Measured Strains in the Four Principal Fiber Directions

Gage no.	0°		45°		90°		135°	
	Pred	Actual	Pred	Actual	Pred	Actual	Pred	Actual
63	- 42	120	-2301	-2250	44	—	2303	2380
69	- 946	- 870	-1917	-1920	2161	—	3133	2930
78	115	—	685	770	1256	1470	687	850
81	791	—	- 710	- 730	346	230	1848	1930
84	688	680	-1323	-1050	177	190	2189	—
87	558	600	344	10	2534	1960	2748	—
90	309	- 130	-1201	-1030	1803	1800	3313	—
93	- 108	—	- 674	- 355	144	-10	714	515
102	4	—	-4190	-3650	18	-45	4212	3780
111	- 82	50	-2849	-2010	104	—	2871	2190
117	- 90	50	-2971	-2780	232	—	3113	2880
123	-1204	-1110	200	90	3002	—	1598	1570

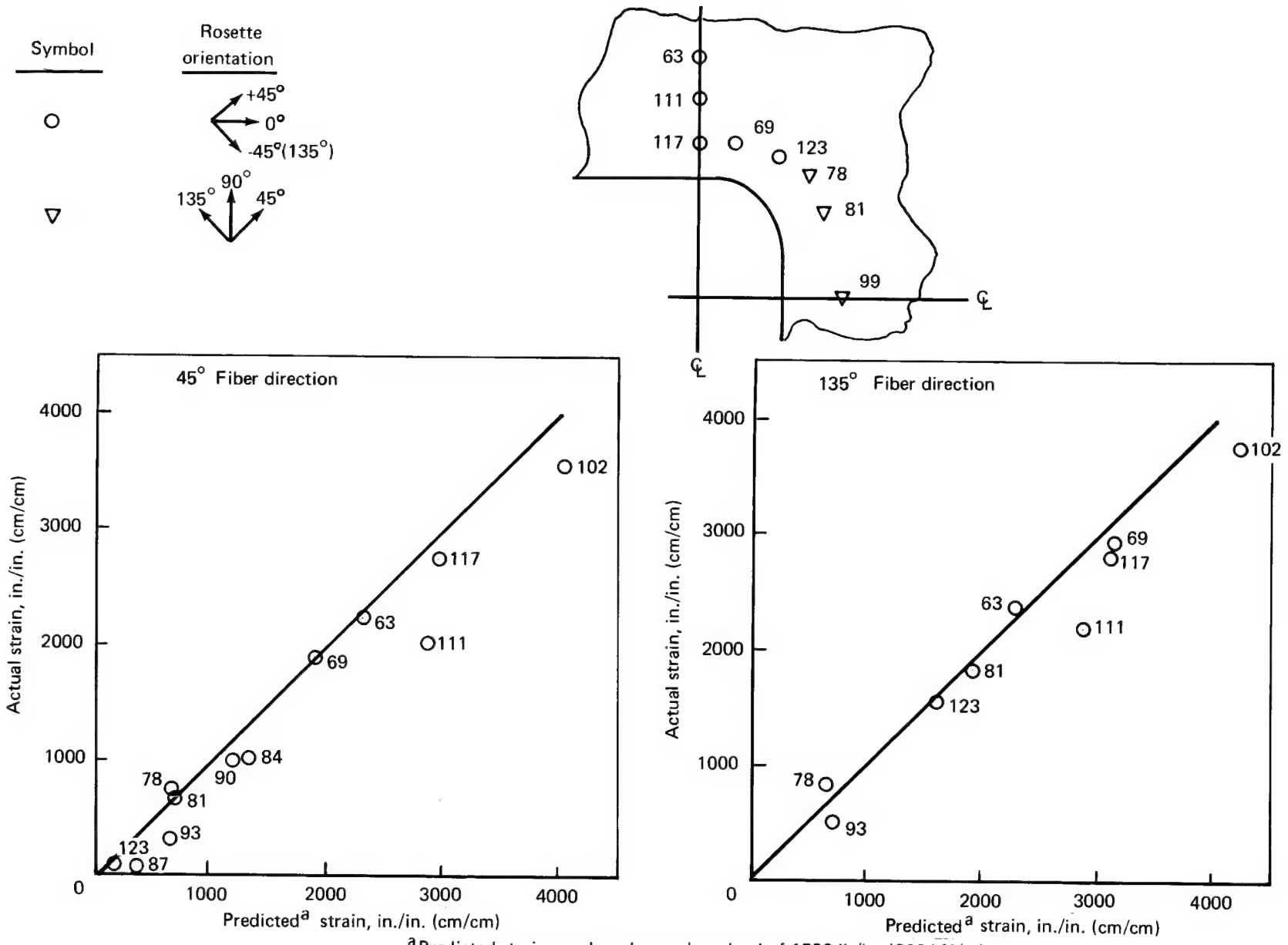

FIGURE 40.–COMPARISON OF ACTUAL AND PREDICTED FIBER STRAINS

Discussion

The objectives established for the reinforced window belt panel were successfully accomplished. The application of filamentary composites as an effective method for reinforcing around structural cutouts in shear-critical aircraft metal structure was adequately demonstrated. The 45° cross-ply composite laminates provided effective load transfer from the highly stressed window opening areas of the panel. Utilization of the shear properties of the epoxy matrix proved to be an efficient means of distributing the load from the boron fibers to the basic titanium face sheet. The excellent correlation between predicted and actual test results obtained for the vertical bending design load case served to establish a high degree of confidence in the finite-element analysis program. This correlation, combined with a 21% margin in the ultimate failure load and a significant weight saving (33.2%), develops confidence in the panel design and in the probability of meeting the predicted structural performance under the critical combined load cases.

This discrepancy between predicted and actual weight may be attributed in part to the additional adhesive layers required by the drape form bonding process, peel plies, and the use of heavier grade adhesive than normally required in critical bond line areas. This conservative approach to fabrication was adopted to ensure successful fabrication of the single window belt panel.

Design refinements with the potential for additional weight savings exist. Areas of particular interest are discussed below:

- With the adoption of the drape form bonding concept it would have been practical to sculpture the reinforcing laminates to conform with the predicted strain distribution. Sculpturing was minimal due to the anticipated problems of machining the core to fit a complex contour.

- Optimization of both the fiber orientation and composite-to-metal area ratios would result in some additional weight saving. However, because of the multidirectional nature of the applied loads this is not considered to be a high-payoff area.

APPENDIX A

TEST SPECIMEN MATERIALS

Aluminum sheet and formed sections were alloy 7075-T6 per QQ-A-250/13.

Titanium sheet and formed sections were alloy 6Al-4V per MIL-T-9046F, type III, composition C, annealed or type III, composition C, solution treated and aged.

Aluminum honeycomb was per MIL-C-7438. Various densities and cell sizes were used.

Boron filaments were obtained from the Hamilton Standard Division of United Aircraft. These were 0.004-in. (0.010-cm) diameter filaments of boron vapor-deposited onto a tungsten wire substrate.

BP-907 adhesive was obtained from the Bloomingdale Department of American Cyanamid Company. This is a film adhesive of epoxy resin impregnated into a scrim of type 104 glass fabric. The material thickness is 0.003 in. (0.0076 cm). This is a latent cure material and has a shelf life of 6 months at room temperature. It is used primarily for drum winding with boron filament to form sheets of uncured boron-epoxy material. When used in adhesive bonding, liquid primer EC 2320 is used on all faying surfaces. The cure temperature cycle for the BP-907 adhesive system is shown in figure A-1.

AF 126 adhesive was obtained from the Minnesota Mining and Manufacturing Company. This is a film adhesive of epoxy resin impregnated into a dacron fiber mat or veil. The material thickness is 0.005 in. (0.013 cm) for bonding plane surfaces or 0.015 in. (0.038 cm) for bonding honeycomb surfaces. Liquid primer EC 2320 is used on all faying surfaces. The cure temperature cycle for the AF 126 adhesive system is shown in figure A-2.

Epon 933 adhesive was obtained from the Shell Chemical Company. This is the same epoxy resin used to manufacture Epon 927, but it is filled with a mixture of chopped fiberglass and asbestos to form a viscous material suitable for knife application to fill irregular bond surfaces.

The test specimen material properties used in analysis are listed in tables A-1 and A-2. Unless otherwise noted, values were obtained from MIL-HDBK-5 (ref. 11).

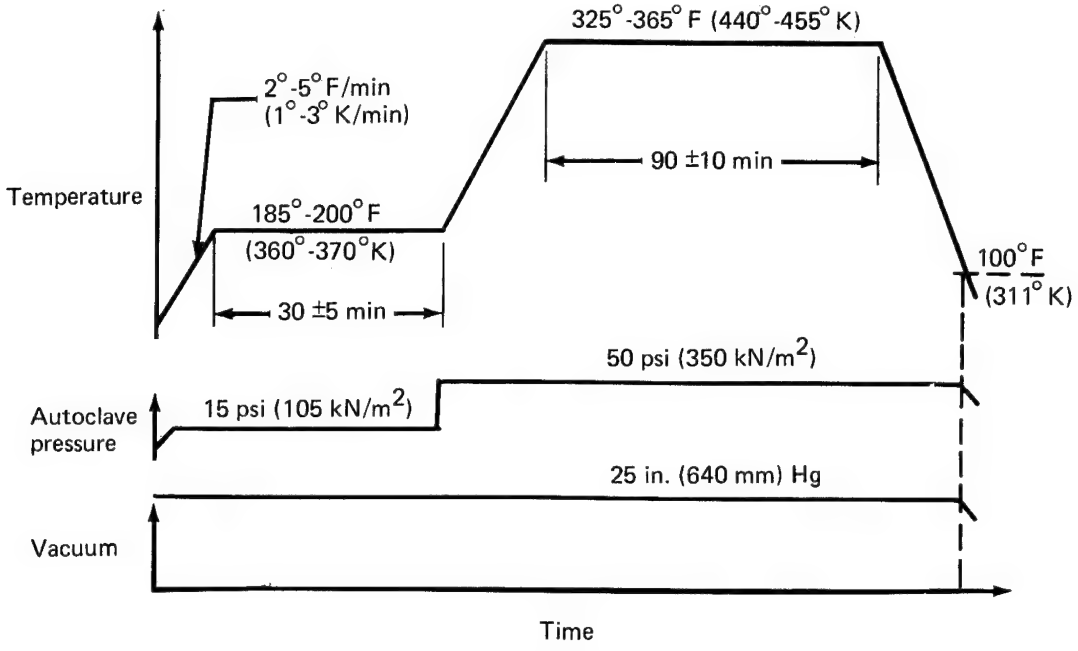

FIGURE A-1.—CURE CYCLE FOR BP-907 ADHESIVE SYSTEM

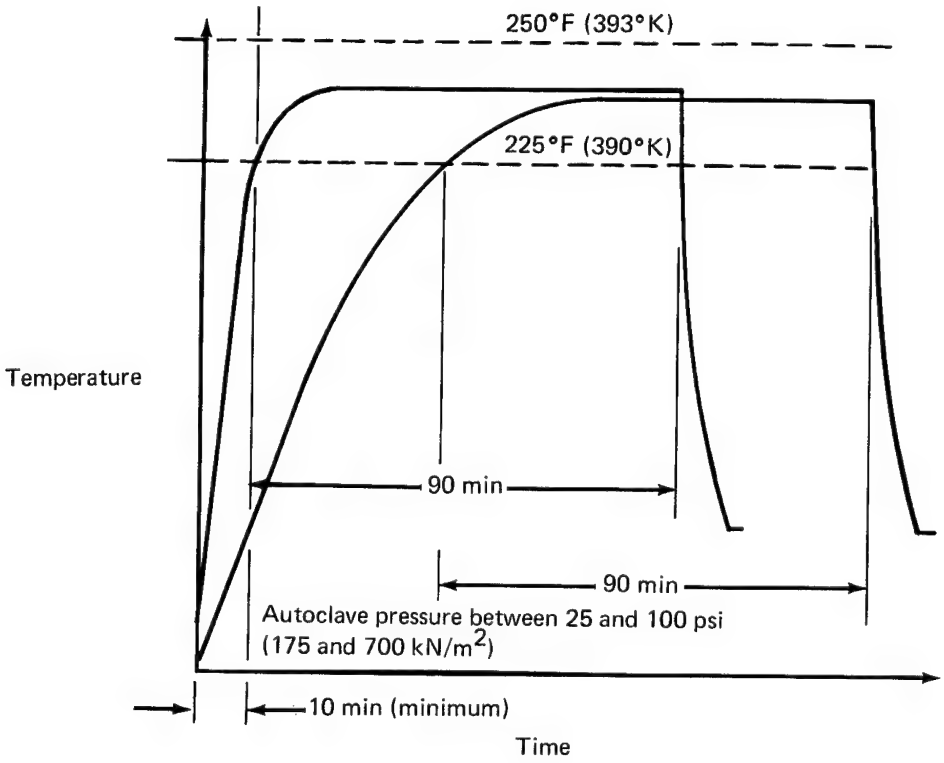

FIGURE A-2.—CURE CYCLE FOR AF-126 ADHESIVE SYSTEM

Table A-1.–Room Temperature Properties of Metal and Boron

Property	Ti-6Al-4V		Aluminum 7075-T6	Boron filament
	Annealed	Heat treated and aged		
Tensile ultimate ksi (MN/m^2)	134(923)	157(1081)	76(523)	450(3100)
Tensile yield ksi (MN/m^2)	126(868)	143(985)	65(447)	–
Compressive yield ksi (MN/m^2)	132(909)	152(1047)	67(461)	–
Shear ultimate ksi (MN/m^2)	79(544)	98(675)	46(317)	–
Elongation %	8	3	7	–
Modulus of elasticity psi x 10^6 (N/m^2 x 10^9)	16.0(110.2)	16.0(110.2)	10.3(70.9)	60(413)
Compressive modulus psi x 10^6 (N/m^2 x 10^9)	16.4(113.0)	16.4(113.0)	10.5(72.3)	60(413)
Shear modulus psi x 10^6 (N/m^2 x 10^9)	6.2(42.7)	6.2(42.7)	3.9(26.8)	25(172)
Poisson's ratio	0.30	0.30	0.33	0.20
Coefficient of thermal expansion in./in. x 10^{-6} per °F (cm/cm x 10^{-6} per °K)	5.3(9.9)	5.3(9.9)	12.9(23.2)	2.7(4.9)

Table A-2.—Room Temperature Properties of Boron-Resin Composites and Resin

Property	Material	
	Boron/BP-907	BP-907[a]
Boron volume/composite volume	0.485	–
Tensile modulus longitudinal psi x 10^6 (N/m^2 x 10^9)	29.1(201)	1.17(8.1)
Tensile modulus transverse psi x 10^6 (N/m^2 x 10^9	2.34(16.1)	1.17(8.1)
Compressive modulus longitudinal psi x 10^6 (N/m^2 x 10^9)	29.1(201)	1.17(8.1)
Compressive modulus transverse psi x 10^6 (N/m^2 x 10^9)	2.34(16.1)	1.17(8.1)
Shear modulus psi x 10^6 (N/m^2 x 10^9)	1.22(8.38)	0.452(3.11)
Poisson's ratio	0.246	0.30
Coefficient of thermal expansion in./in. x 10^{-6} per°F (cm/cm x 10^{-6} per°K)	3.1(5.8)	15.0(28.0)

[a]Includes scrim

APPENDIX B

CONVERSION OF U.S. CUSTOMARY UNITS TO SI UNITS

The international system of units (SI) was adopted by the Eleventh General Conference on Weights and Measures, Paris, October 1960 (ref. 8). Conversion factors for the units used herein are given in Table B-1.

Table B-1.—Conversion of U.S. Customary Units to SI Units

Physical quantity	U.S. customary unit	Conversion factor[a]	SI unit
Length	Inch (in.)	0.0254	Meter (m)
Mass	Pound mass (lbm)	0.4536	Kilogram (kg)
Load	Pound force (lbf)	4.448	Newton (N)
Density	Pound mass/inch^3 (lbm/in.^{3})	27,680	Kilogram/meter^3 (kg/m^3)
	Pound mass/foot^3 (lbm/ft^3)	16.02	Kilogram/meter^3 (kg/m^3)
Load intensity	Pound force/inch (lbf/in.)	175.13	Newton/meter (N/m)
Modulus, stress, pressure	Pound force/inch^2 [psi (lbf/in.^{2})]	6,895	Newton/meter^2 (N/m^2)
Temperature	Fahrenheit degree (°F)	$(t_F + 460)5/9$	Kelvin degree (°K)

[a]Multiply the value in U.S. customary units by the conversion factor to obtain the value in SI units.

Prefixes to indicate multiples of units are as follows:

centi	(c)	10^{-2}
kilo	(k)	10^3
mega	(M)	10^6
giga	(G)	10^9

APPENDIX C

TEST SPECIMEN FABRICATION

Manufacturing procedures and processes common to the fabrication of the three test components are presented in a general discussion. Subsequent sections present a detailed description of the fabrication and assembly procedures pertinent to each test component.

Manufacturing Processes

The following special manufacturing processes were required for completion of the test components.

Chemical milling.—Steps were chemically milled into the titanium load transfer fittings. This process was controlled by Boeing process specifications. The titanium was cleaned, rinsed, and dried. Masking material was applied in the desired step configuration and cured. The masking material was removed from the first step area and the exposed surface chemically milled by submersion in a nitric-fluoride solution followed by a rinse to stop the chemical action. Repeated dips and rinses were used to remove specific thicknesses of material. The masking material was removed from each successive step and the procedure repeated until the required step configuration remained. Step thickness tolerances of ±0.001 in. (0.00254 cm) were maintained.

Surface preparation.—Surface preparation of all components was essential to attain an acceptable structural adhesive bond. The surface preparation operations were controlled by Boeing process specifications. The process for each material is summarized briefly as follows:

- Titanium-epoxy bonding: Emulsion or solvent clean, alkaline clean, deoxidize phosphate fluoride conversion coat, apply protective wrap, and coat with adhesive primer within 16 hours.

- Aluminum-epoxy bonding: Vapor degrease, alkaline clean, deoxidize, apply protective wrap, and prime within 16 hours.

- Aluminum core: Vapor degrease, oven dry, apply protective wrap, and assemble within 16 hours.

- Second-stage bond assemblies: No satisfactory surface preparation process was available for second-stage bonding. Techniques have been developed for maintaining clean surfaces through first-stage bond cycles. These include:

  - Nylon peel ply—one layer of BP 907 epoxy adhesive and fine-weave nylon cloth is bonded to the exposed surfaces during the first-stage bond. Prior to second-stage bonding the nylon cloth is peeled from the detail, exposing a clean adhesive surface.

  - Protective tapes—several noncontaminating protective tapes are commercially available which may be applied to primed metal surfaces to maintain a clean surface.

Structural adhesive bonding.—The bonding process employed throughout the fabrication phase of the program conformed to established production bonding processes and was controlled by Boeing process specifications for moderate- and elevated-temperature-curing epoxy adhesives. Both adhesive systems, BP 907 and AF 126, required a 90-minute cure cycle at a minimum pressure of 35 psig (241.3 kN/m^2). The BP 907 system required a cure temperature of 350° F (450° K), compared to 250° F (394° K) for the AF 126 system. Bond cycles using both adhesive systems were conducted at the higher temperature. The positive-pressure, air-heated autoclaves were used for bonding. Lap shear and honeycomb peel control panels, as applicable, were processed with each bond cycle.

Boron-epoxy tape preparation.—Boron-epoxy materials were fabricated by a drum winding process. Tapes approximately 10 in. (25.4 cm) wide by 96 in. (244 cm) long were wound four at a time on a cylindrical mandrel. The boron filaments were wound at an average of 208 filaments per inch (82/cm) on a 3-mil (0.0076-cm) thick BP 907 adhesive film. After winding, the tapes were cut across the width, removed from the mandrel, individually packaged in plastic film, and refrigerated at 0° F for future use in fabrication of the composite reinforcement straps and laminates.

Fuselage Damage Containment Panel

A brief description of the fabrication and assembly procedures used for the manufacture of the damage containment panel is presented.

Tooling.—The panel curvature [128 in. (325 cm)] necessitated the use of the contoured bond assembly jig shown in figure C-1. This represents a hard tooling concept, and the sandwich panel was cure formed to the radius of curvature of the concave surface of the tool. The female tool permits bonding of the frames to the inside face sheet during the panel assembly cure cycle.

Load transfer fittings.—Stepped load transfer fittings were fabricated from titanium sheet (Ti-6Al-4V, condition III) by the chemical milling process described previously.

Boron-epoxy reinforcement laminates.—The boron-epoxy reinforcement was laid up and precured as a two-ply, flat, laminated sheet 120 in. (305 cm) long by 48 in. (122 cm) wide. The fiber orientation was parallel to the 48-in. (122-cm) dimension. The filaments were terminated on the two step load transfer fittings. Nylon peel ply was applied to both sides of the laminate to maintain clean surfaces for the final assembly. The layup of the composite reinforcement laminate is shown in figure C-2.

Face sheet and tang detail.—The face sheets were fabricated from 0.032-in. (0.081-cm) 7075-T6 aluminum alloy clad sheet and roll formed to the 128-in. (325-cm) radius. The edge attachments or tang members were fabricated from 0.080-in. (0.203-cm) 2024-T3 aluminum alloy sheet material. These details were also roll formed to curvature.

Frames.—The panel frames were fabricated in two sections. The outer chord was made by modifying an aluminum 7075-T651 extruded tee section. The web and inner chord, which were riveted to the outstanding leg of the tee after bonding the tee to the panel, were formed

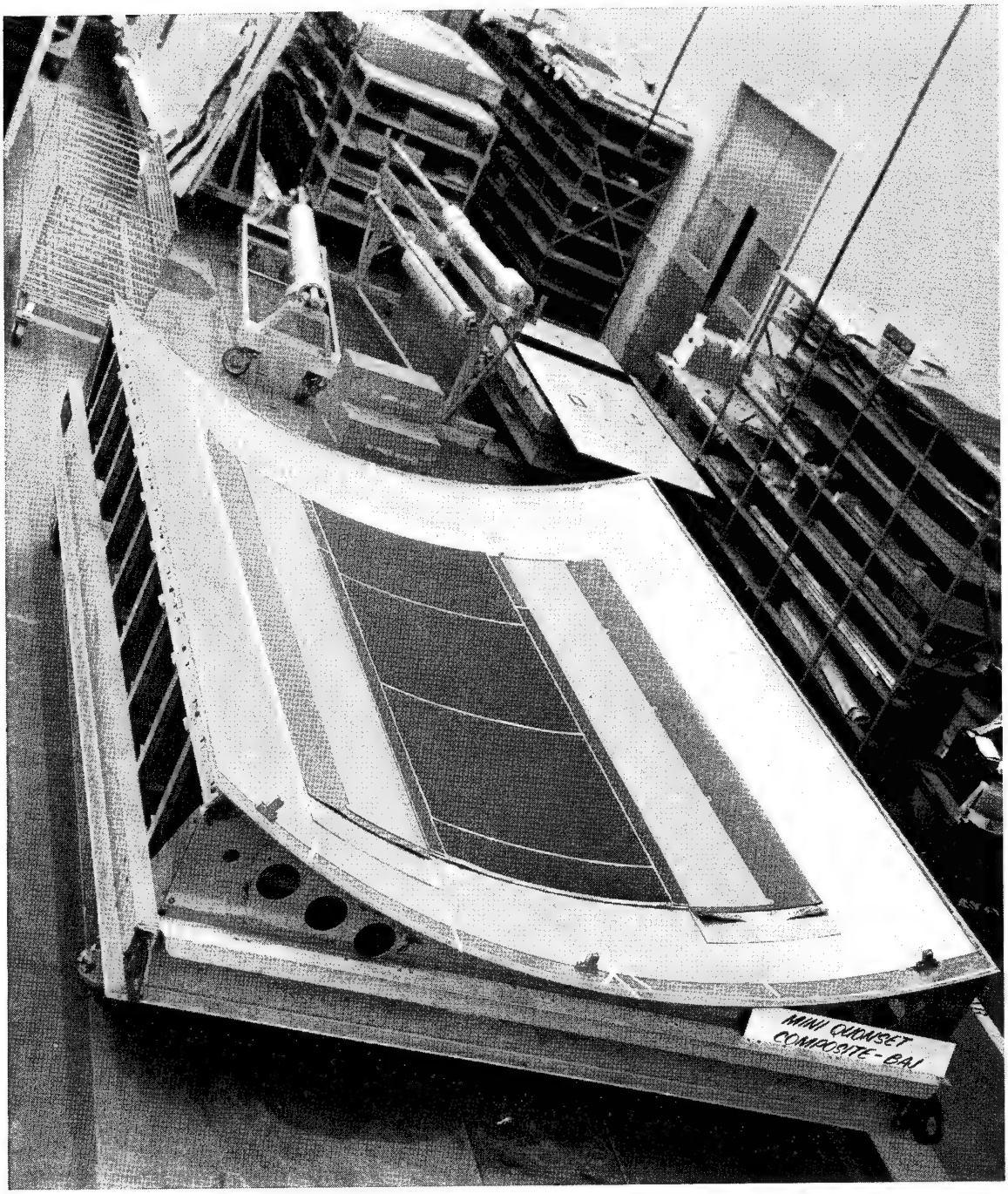

FIGURE C-1.—FUSELAGE DAMAGE CONTAINMENT PANEL—BOND ASSEMBLY JIG

FIGURE C-2.—LAYUP OF BORON-EPOXY REINFORCEMENT LAMINATES

from 0.056-in. (0.142-cm) 7075-T6 clad aluminum sheet. The web was reduced to a thickness of 0.035 in. (0.089 cm) by chemical milling. The frame sections (fig. C-3) were roll formed to conform to the inside curvature of the panel.

Core details.—The blanket core details were made from a 0.75-in. (1.9-cm) thick sheet of 3.1 lb/ft^3 (49.5 kg/m^3) density aluminum core roll formed to the 128-in. (325-cm) radius. The core ribbon was placed in the longitudinal direction. The core splices were made at a 30° angle and were located under frames 2, 4, and 6. The core details in the edge attachment area were made from 0.335-in. (0.85-cm) thick, 12-lb/ft^3 (192-kg/m^3) density aluminum core, also roll formed to curvature.

Panel assembly.—The final assembly of the damage containment test panel was accomplished in a single-stage bonding operation. Prior to assembly all details were prefit in the bond assembly tool. The aluminum sheet and extrusion detail surfaces were prepared and primed with AF 126 type I liquid adhesive primer. The peel ply was removed from the precured boron-epoxy laminates and both surfaces of these details primed. AF 126 type II film adhesive was applied to all faying surfaces in accordance with the following schedule:

- 5-mil (0.0127-cm) adhesive was used for all metal-to-metal and metal-to-composite laminate bond applications in the basic sandwich panel.
- 10-mil (0.0254-cm) adhesive was used for bonding the frame tees to the inside face sheet.
- 15-mil (0.0381-cm) adhesive was used for all metal-to-core and composite-to-core bond applications.

The assembly sequence was as follows. The external face sheet and the precured, two-ply composite laminate were positioned in the bond assembly tool. Proper positioning was ensured by tooling pins installed during prefit. The blanket core details were then positioned and the split core and edge member tang assembled. A spacer shim placed between the tool surface and the tang held this member in the correct elevation. All core splices were made at 30° with 100-mil (0.254-cm) AF 3012 foam adhesive. The second precured composite laminate and inside face sheet were positioned on the core using the tooling pins to ensure correct alignment. The frame tees were positioned at 20-in. (50.8-cm) centers and held in place with tape. The assembly was bagged and cured in the autoclave for 90 min at 35-psi (242-kN/m^2) pressure and 250° F (394° K) temperature. Following the cure cycle the bond assembly was inspected by ultrasonic through-transmission techniques (fig. C-4). Final assembly consisted of riveting the roll-formed web and inner chord member to the frame tee.

Repair.—A structural repair technique was required to facilitate repair of the panel following each blade penetration. The repair scheme illustrated in figure C-5 was implemented. The damaged area of the convex face was removed by cutting a 3- by 14-in. (7.63- by 35.6-cm) rectangular hole in the face sheet. A similar procedure was followed to remove an 8- by 16-in. (20.4- by 40.7-cm) portion of the concave face sheet. The honeycomb core was routed from the panel to conform with the 8- by 16-in. (20.4- by 40.7-cm) opening, exposing an area of the inside surface of the convex face. This was done to provide for an internal doubler.

(a) Modified BAC 1506-2577
7075-T651 Tee Section

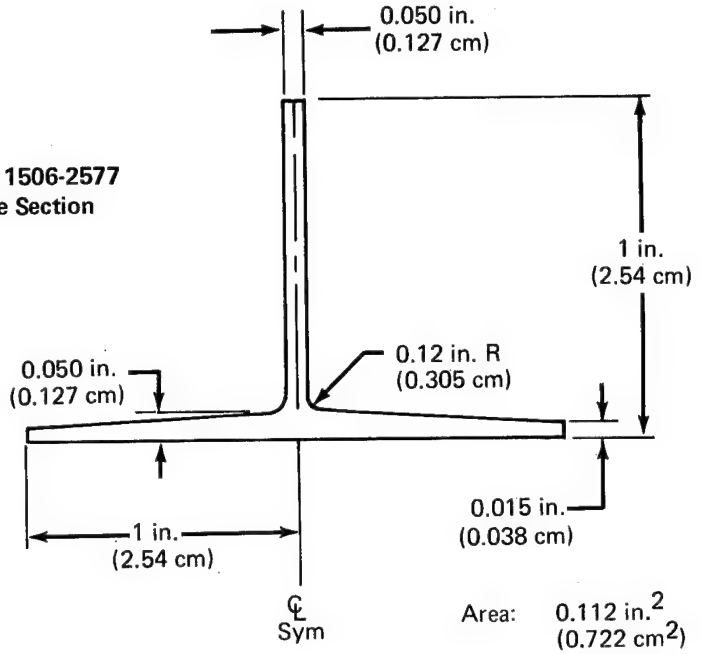

(b) 7075-T6 Frame Section

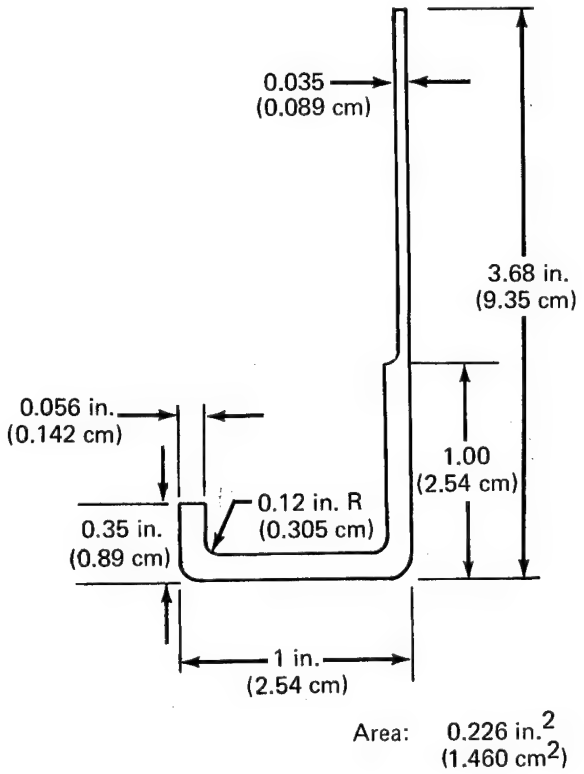

FIGURE C-3.—TYPICAL FRAME SECTIONS

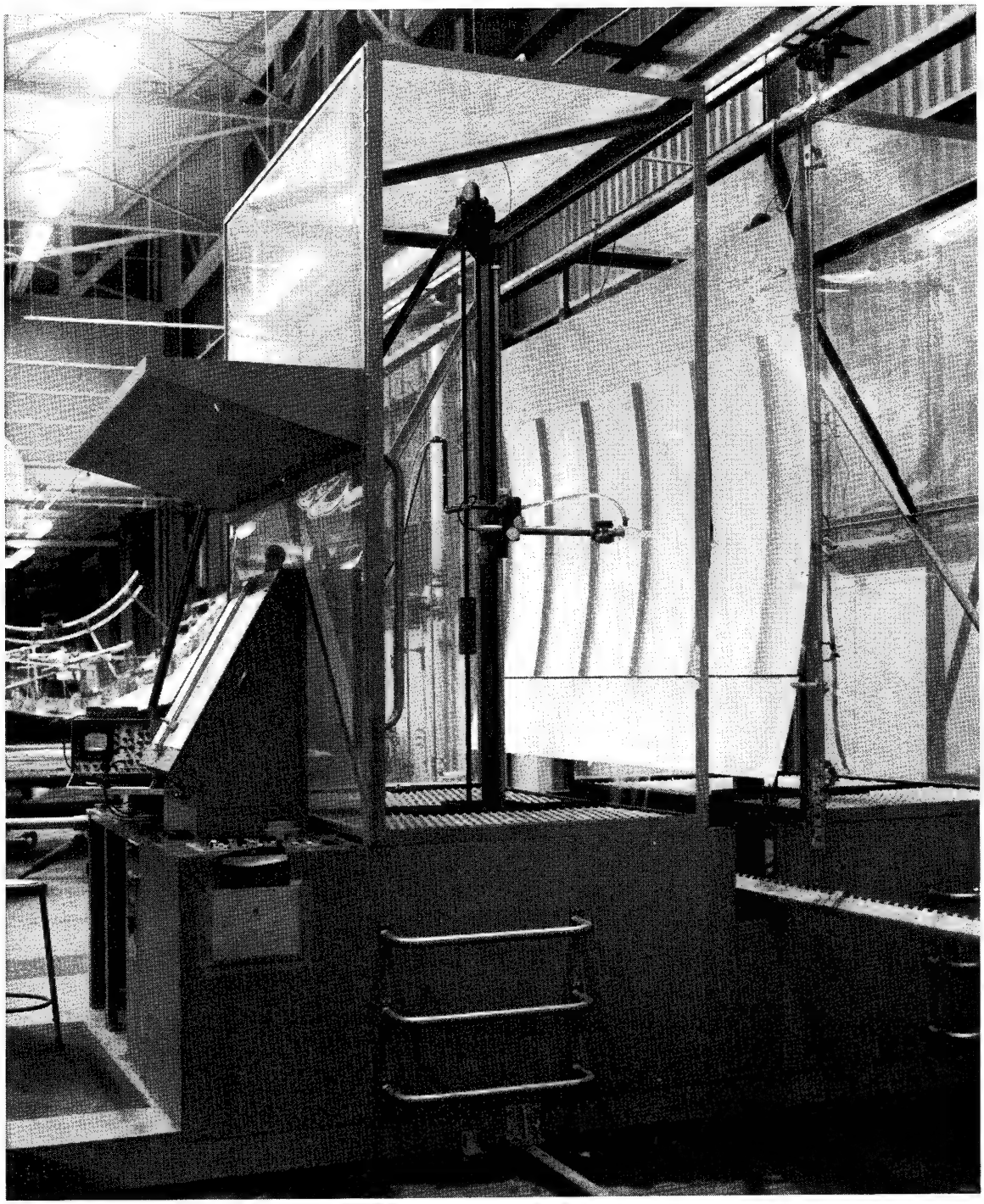

FIGURE C-4.—ULTRASONIC THROUGH-TRANSMISSION INSPECTION OF FUSELAGE DAMAGE CONTAINMENT PANEL

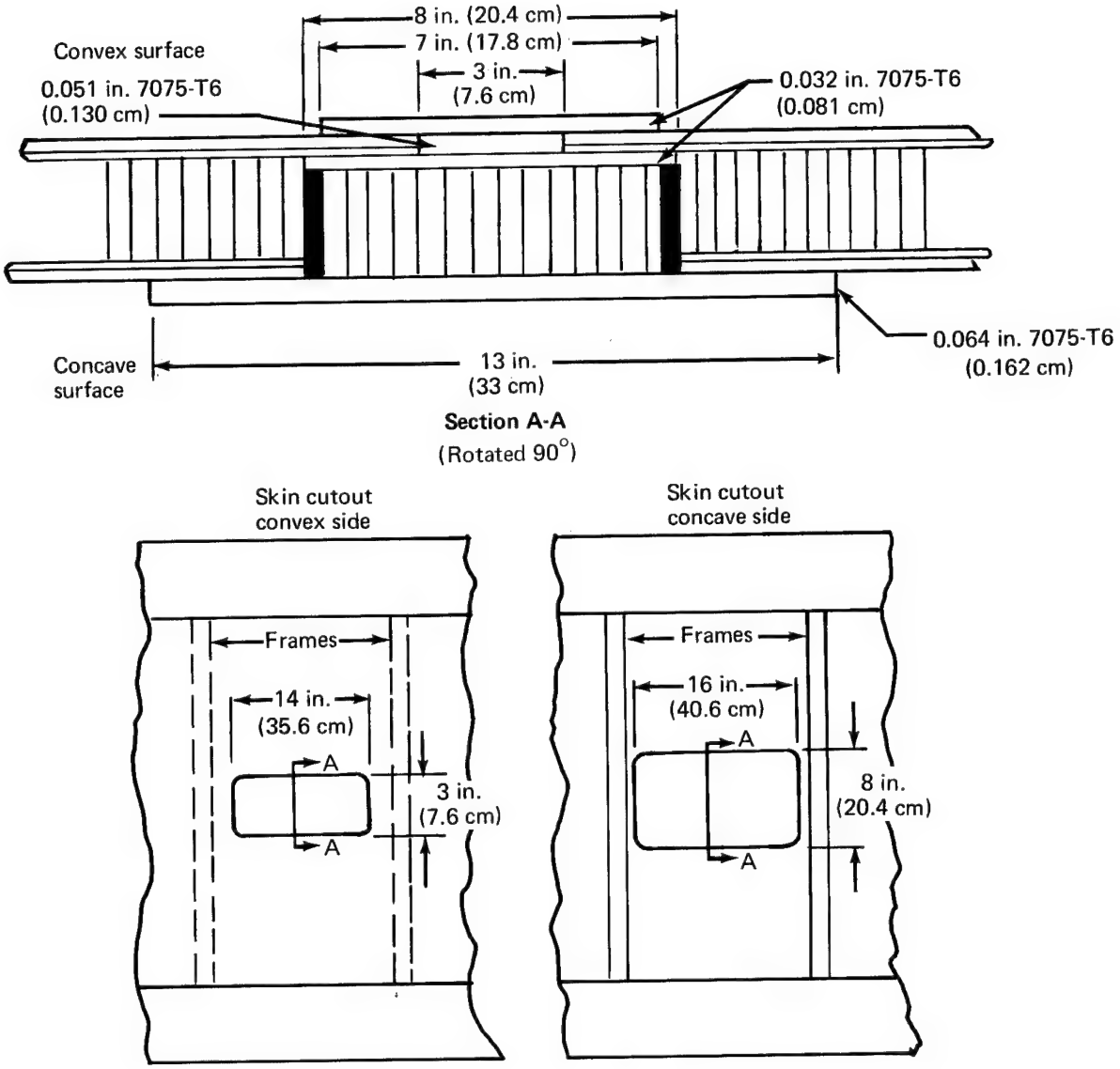

FIGURE C-5.—DAMAGE REPAIR SCHEME

A core plug was machined to the prescribed thickness, allowing for the doubler and bond line thicknesses. Both surfaces of the core were stabilized with 10-mil (0.025-cm) AF 126 adhesive and then roll formed to contour.

Two 0.032-in. (0.081-cm) 7075-T6 aluminum doublers and a 0.051-in. (0.130-cm) 7075-T6 aluminum filler plate were fabricated for the convex face and a 0.064-in. (0.163-cm) 7076-T6 aluminum doubler was fabricated for the concave face sheet. The prepared area of the panel and the doubler and core details are shown in their assembly positions in figure C-6.

The metal detail surfaces were prepared and primed with Desoto 513-707 primer. The faying surfaces on the panel were treated with a hand preparation and alodine 1200 applied, followed by adhesive primer. EC 2216, a room-temperature-curing adhesive, was applied to the bonding surfaces and the details assembled. A vacuum bag was applied to each side of the panel, enclosing the repair area. A 36-hr cure cycle under full vacuum pressure was required to accomplish the repair. The repair was inspected by ultrasonic through-transmission, and all critical metal-to-metal bonds were determined to be void free. Strain surveys conducted prior to the second blade penetration test verified the repair.

Multibay Skin-Stringer Compression Panels

Two reinforced, hat-stiffened, multibay compression panels were fabricated from titanium sheet and structural sections which were reinforced with boron-epoxy-laminated straps. The panels were assembled by moderate-temperature-curing structural adhesive bonding and mechanical fasteners. A brief description of the manufacturing processes, panel detail fabrication, and assembly procedures is presented in the following paragraphs.

Tooling.—A minimum tooling concept was adopted for fabrication of the panels. The basic tool consisted of a flat steel plate. Aluminum filler bars were machined to fit inside the hat sections to provide stability to the sections during the bonding cycles. Additional bars fitting between the hat stiffeners were provided to ensure positive pressure transfer to the hat flanges. Teflon locator tabs were used for positioning the composite straps on the stiffeners during bonding.

Load transfer fittings.—The load transfer fittings were fabricated from 0.040-in. (0.102-cm) Ti-6Al-4V condition I sheet, in 36-in. (91.4-cm) lengths, and then sheared to the required strap width. The steps in the fittings were formed by the chemical milling process described previously.

Boron-epoxy reinforcing straps.—To fabricate these precured, five-ply, laminated straps, boron-epoxy tapes were cut in strips 96 in. (243.8 cm) long by 0.75 in. (1.91 cm) wide and assembled in a laminated stack-up, with each end of each laminae terminating on a step of a load transfer fitting.

Face sheet.—The panel face sheet was fabricated from 0.050-in. (0.127-cm) titanium (Ti-6Al-4V condition I) alloy sheet. The face detail was fabricated in a single sheet 96 in. (243.8 cm) long by 36 in. (91.4 cm) wide.

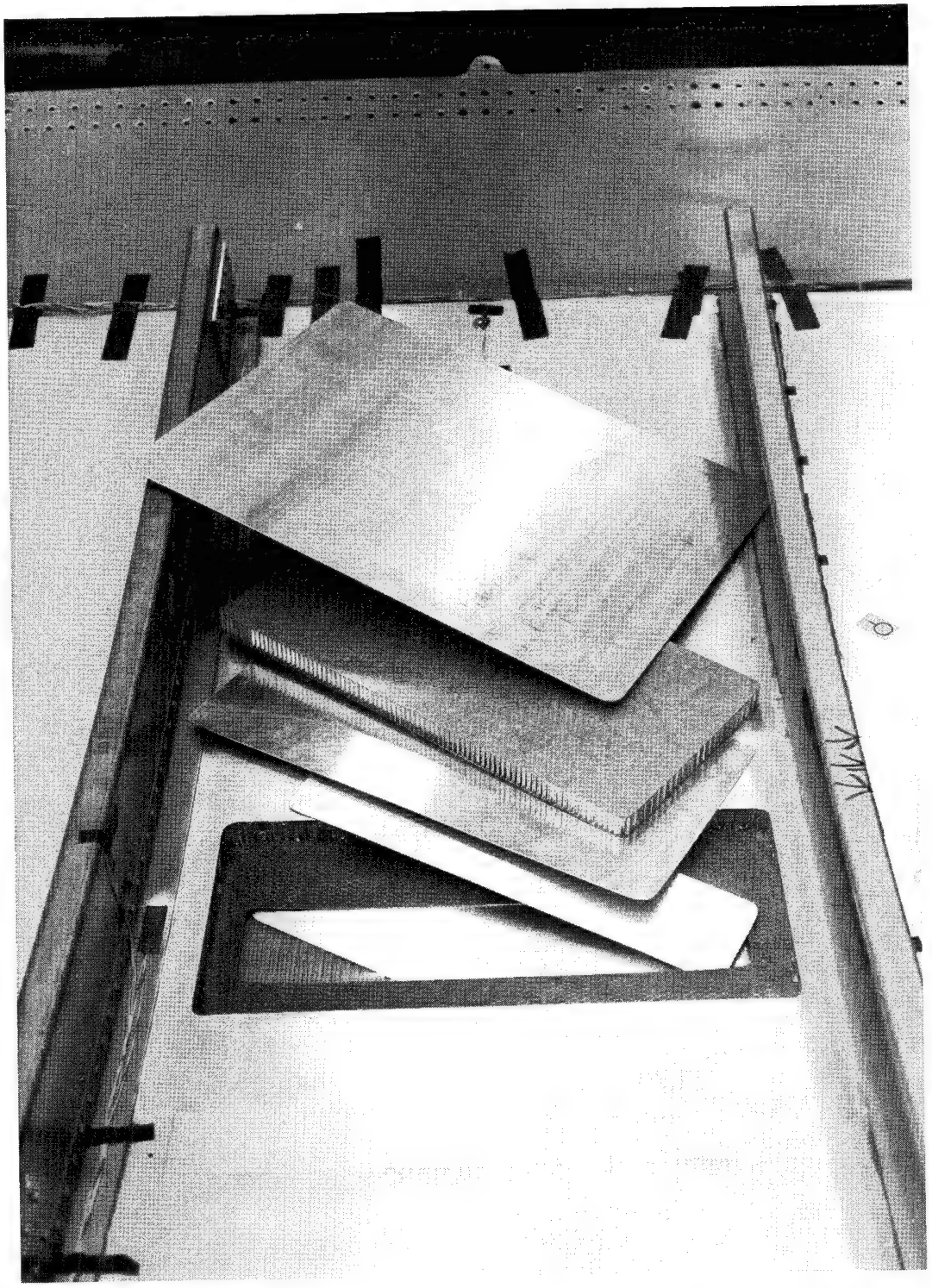

FIGURE C-6.—LAYUP SEQUENCE OF STRUCTURAL REPAIR DETAILS

Hat stiffeners.—Six hat section stiffeners 96 in. (243.8 cm) long were fabricated from titanium (Ti-6Al-4V condition I) alloy sheet. The hat section was formed by a hot-roll process. The crown and webs were reduced to a 0.040-in. (0.102-cm) thickness by chemical milling.

Frames.—The four panel frames were fabricated from 0.1-in. (0.254-cm) titanium (Ti-6Al-4V condition I) alloy sheet. The U-channel section was formed by a "hot brake" forming process.

Shear ties and clips.—The shear ties and clips for installation of the panel frames were fabricated from 0.050-in. (0.102-cm) titanium (Ti-6Al-4V condition I) alloy sheet.

Fasteners.—Solid, universal head, titanium alloy (Ti-6Al-4V) rivets, [minimum diameter 0.156 in. (0.396 cm)] were used for assembly where mechanical fastening was required.

Panel assembly.—Assembly of the multibay compression panel was achieved by a combination of structural adhesive bonding and mechanical fastening. The assembly sequence is outlined below.

A prefit of the panel details was conducted prior to final assembly. The hat section stiffeners were positioned on the face sheet and located by means of tooling pin holes. Each stiffener was identified with its respective location and this identification retained throughout the assembly operation.

Two bonding operations were required for assembly of the panels. In the first stage the precured boron-epoxy straps were bonded to the stiffener crowns. After surface preparation and priming with AF-126 type I adhesive primer the flange surfaces of the stiffeners were covered with protective tape to maintain clean surfaces for a second-stage bond. The boron-epoxy laminates were primed and a 5-mil (0.0127-cm) layer of AF-126 type II adhesive applied to one surface of each five-ply laminate. Three of the five-ply laminates were positioned on the stiffener crown to form the 15-ply reinforcing strap. The stiffeners were bagged and cured at 50-psi (345.8-kN/m^2) pressure and 250° F (395° K) temperature for 90 min in the autoclave. Two rivets were installed through the load transfer fittings at each end of the straps after bonding.

The titanium face sheet was cycled through the surface preparation process and one surface primed. The protective tape was removed from the stiffener flanges and a 5-mil (0.0127-cm) layer of AF 126 type II adhesive applied to the exposed surfaces. The stiffeners were positioned on the face sheet using the identification to ensure correct location. The tooling pins were installed and the assembly bagged and cured in the autoclave under the same conditions as outlined for the first-stage bond cycle.

On completion of the bond cycle the flange rivet pattern was laid out and drilled and the rivets installed. The U-channel frames were clamped in position and attached to the panel with mechanically fastened clips and shear ties. The frame installation is shown in figure C-7.

The panel longitudinal edges were slotted at 2.85-in. (7.24-cm) intervals to a depth of 3 in. (7.62 cm) to facilitate structural test requirements. Both ends of the panel were potted and machined flat and parallel to ensure uniform load distribution during test.

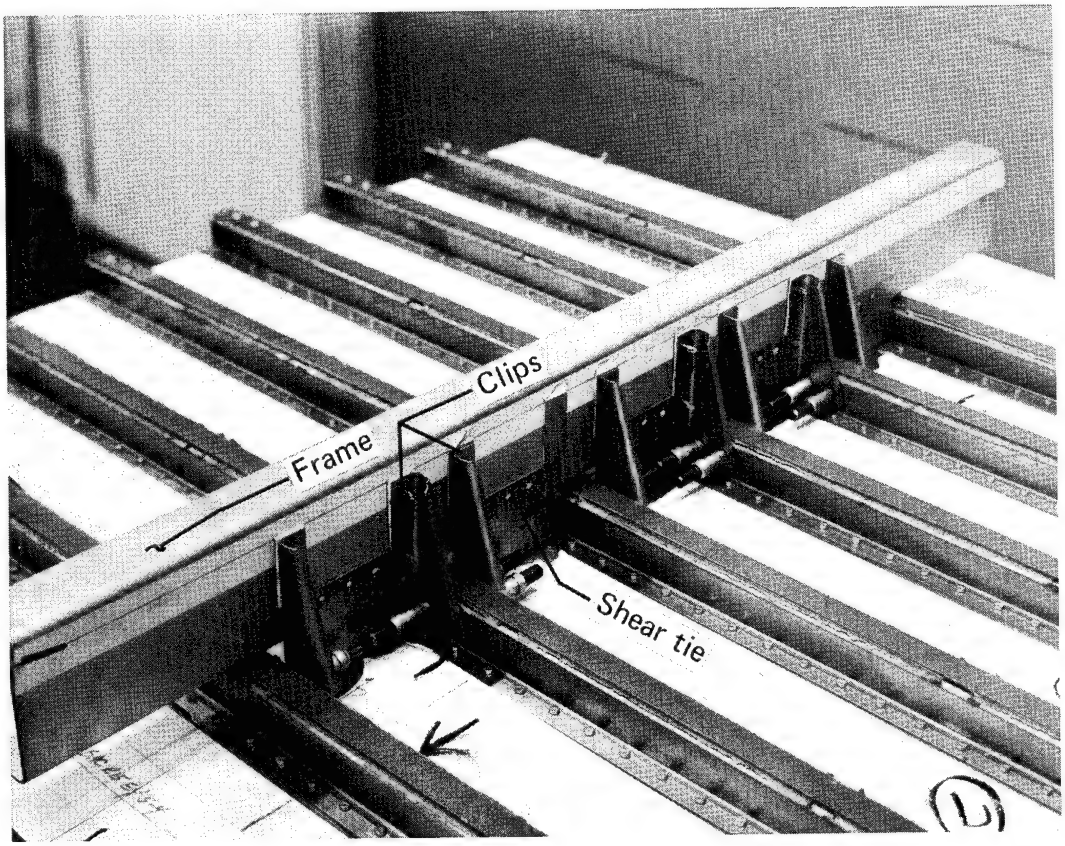

FIGURE C-7.—FRAME INSTALLATION

Panel rework.—As a result of the adhesive bond line failures between the reinforcing straps and stiffeners encountered during the first panel test, the corresponding bond lines on the second panel were inspected and determined to be of questionable quality. It was therefore decided to remove and replace the straps in an attempt to achieve a better quality specimen.

The frames, clips, and shear ties were removed from the panel. The hat stiffeners were left intact. A heat gun and knife were used to peel the bonded reinforcement straps from the stiffeners.

Possible degradation of the stiffener-to-face-sheet bond lines prevented recycling of the panel through the surface preparation process. Several hand preparation methods were therefore evaluated to determine an acceptable method for recleaning the stiffener crowns. A small process evaluation program using 24-in. (61.0-cm) long reinforced hat assemblies and lap shear specimens was conducted.

Specimens were prepared by each of the processes and bonded. The straps were peeled from the hat section to inspect the bond lines, and the lap shear specimens were tested to evaluate the bond strength. The results of this evaluation program are summarized in table C-1. The titanium surface preparation selected on the basis of this program consisted of an alumina blast followed by a silane rinse. Factors considered in this selection were:

- Good shear strength developed by the lap shear specimens
- Cohesive failures developed in both the lap shear and hat assemblies
- Ease of the procedure
- Good strength retention following environment exposure (indicated by previous test data)

New reinforcing straps were fabricated for installation on the stringer. A 100% bagging concept, which consisted of bagging each stringer individually by inserting a cylindrical bag inside the hat section and sealing the edges to an external bag placed over the composite, was used for bonding the straps to the stiffener. A vacuum was developed in the volume enclosed by the two bags. When vented to atmosphere in the autoclave, full pressure was applied to both the strap and the inside surface of the hat, thus accomplishing positive bonding pressures.

Following the bond cycle, the strap-to-stringer bond line was inspected by nondestructive testing and determined to be of good quality.

One small modification was made during the rework program. An 0.08-in. (0.203-cm) doubler was bonded to the ends of the reinforcing straps to compensate for the hole-out area left by the removed rivets.

The frames were reinstalled using the existing rivet hole patterns for the clips and shear ties and the panel prepared for test.

Table C-1.—Surface Preparation Techniques Investigated for Bonding of Replacement Boron-Epoxy Straps

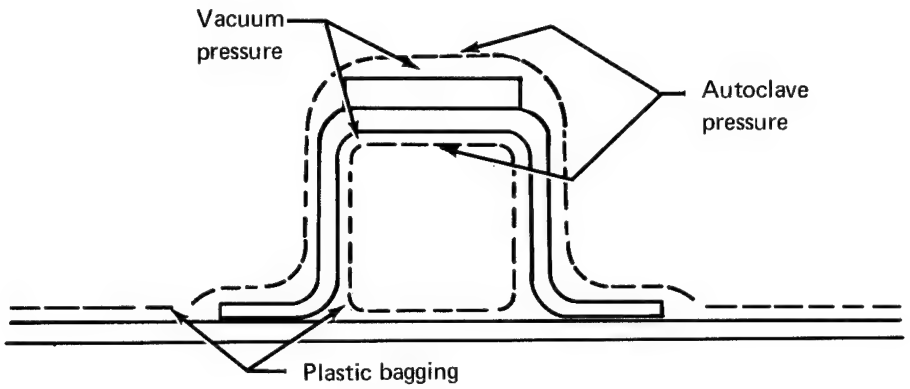

Surface preparation study results:

Surface preparation	Lap shear, psi (MN/m^2)	Failure analysis
Pasa-jel	5208 (36.0)	35% adhesive, 65% cohesive
Phosphate fluoride	4142 (28.5)	25% adhesive, 75% cohesive
Alumina blast plus MEK wipe	4920 (34.0)	100% cohesive
Alumina blast plus silane rinse (selected)	5168 (35.6)	100% cohesive
Pasa-jel plus second cure cycle	5834 (40.0)	20% adhesive, 80% cohesive

Window Belt Panel

The window belt panel was fabricated from titanium, boron-epoxy, and aluminum honeycomb core details bonded together with moderate-temperature-curing structural adhesive to form a 70- by 70-in. (177.8- by 177.8-cm) flat honeycomb sandwich panel. A description of the manufacturing processes, panel detail fabrication, and assembly procedures is contained in the following paragraphs.

Tooling.—A minimum tooling approach was adopted for the program. The flat panel design permitted the use of a flat steel "caul plate" tooling concept. A full-scale layout of the panel and pertinent detail features such as window and load transfer fitting locations were inscribed on the face of the tool. Locator devices were attached to the tool surface to accurately locate each corner of the three windows. Additional shop aid tools including window filler plugs and fairing bars were fabricated as required.

Load transfer fittings.—The load transfer fittings shown in figure C-8 were fabricated from titanium sheet (Ti-6Al-4V condition I). The steps in both the window ring and edge fittings were formed by the chemical milling process described previously. A typical cross section is shown in figure C-9.

Boron-epoxy reinforcing laminates.—The boron-epoxy reinforcement was laid up in a multidirectional precured laminate prior to bonding to the interface of the core and face sheet. The laminates were fabricated in a two-stage bonding operation.

First-stage laminate.—The first-stage bonding procedure was as follows:

- A thin, transparent separator film was placed over the inscribed surface of the tool.
- The load transfer fittings were positioned on the tool and taped in place.
- The two longitudinal (0°) boron-epoxy laminates were cut to size and laid adhesive side down, adjacent to the bottom step of the window ring fittings.
- The first (+45°) boron-epoxy cross-ply laminate was laid up in narrow strips, butt joined, and carefully trimmed to fit the first step of the load transfer fitting.
- The second (-45°) boron-epoxy cross-ply laminate was then laid up in the same manner, terminating on the second step of the fittings.
- A layer of BP-907 was placed over the stack-up and covered with the nylon peel ply. The stack-up was carefully removed from the tool and inverted, and peel ply applied to the bottom surface and then replaced in the proper position on the tool.
- A picture frame was installed around the periphery to maintain edge thickness, and the assembly bagged and cured.

The cured first-stage laminate, shown in figure C-10, was 70 in. (177.8 cm) long by 30 in. (76.2 cm) wide.

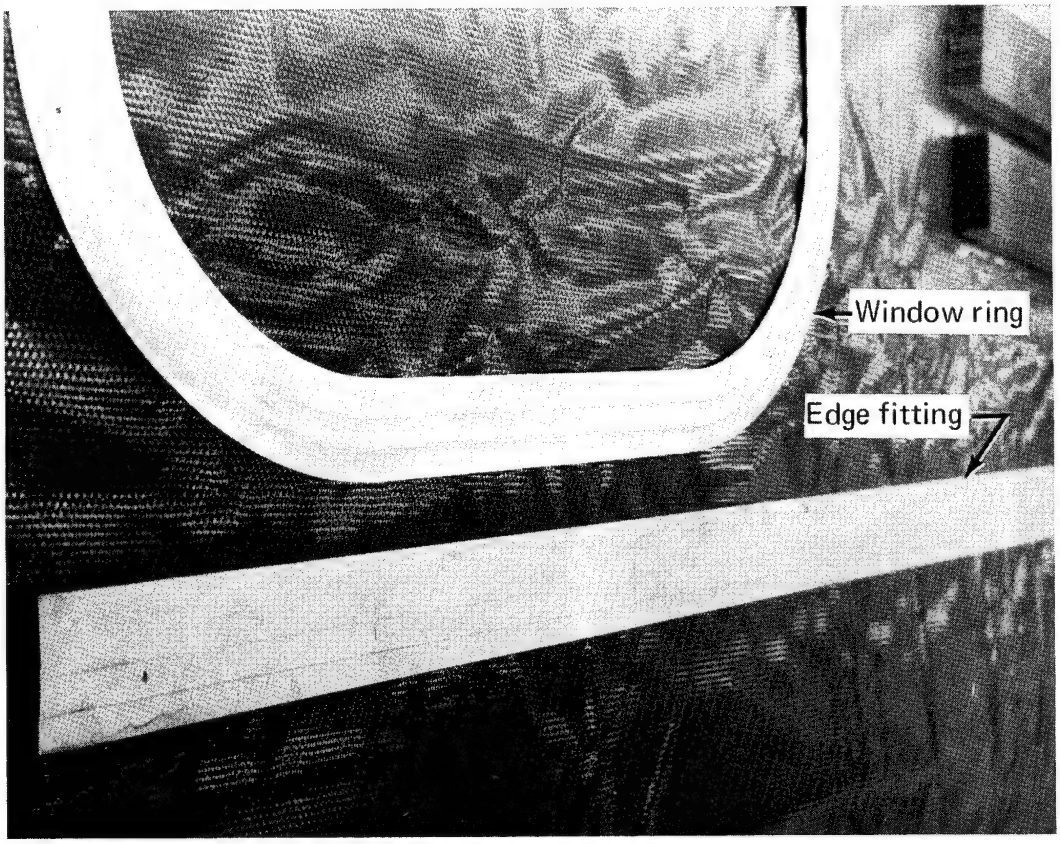

FIGURE C-8.—CHEMICALLY MILLED TITANIUM LOAD TRANSFER FITTINGS

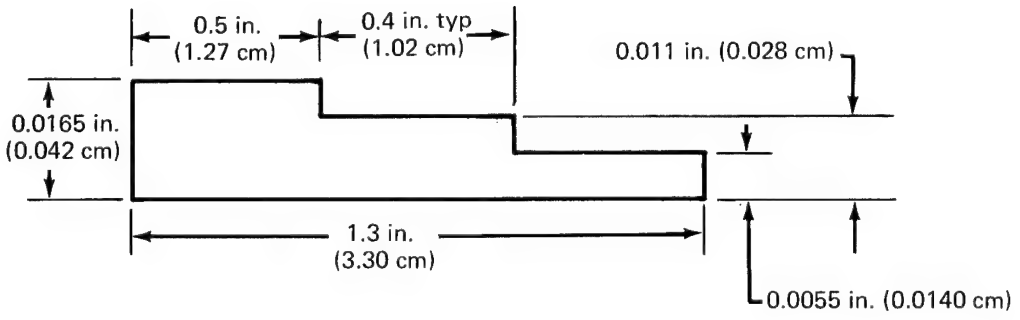

FIGURE C-9.—TYPICAL CROSS SECTION THROUGH TITANIUM LOAD TRANSFER FITTING

Second-stage laminate.—The second-stage laminate was prepared in an identical manner as the first stage, up to the point of applying the nylon peel ply. This layup, however, was 36 in. (91.5 cm) wide compared to the 30-in. (76.2-cm) width of the first-stage laminate.

- The nylon peel ply was removed from the top surface of the first-stage laminate and a 5-mil (0.127-cm) layer of AF 126 adhesive applied to the exposed surface.
- The first-stage laminate was then inverted and placed on top of the second-stage laminate, using the window locator tools for proper positioning.
- The circumferential (90°) plies were then laid up between the windows, nylon peel ply applied to the bottom surface, and the assembly bagged and cured.

The precured second-stage laminate is shown in figure C-11.

Window frames.—The three window frames were fabricated from 0.75-in. (1.91-cm) thick titanium plate (Ti-6Al-4V condition III). The heat-treated condition was selected to facilitate machining as it provided a more stable material for machining to thin gages. The frames were formed by a single machining operation, employing a numerically controlled milling machine equipped with gang cutters.

Face sheets and doublers.—The face sheets and edge doublers were fabricated from 0.020-in. (0.0508-cm) titanium (Ti-6Al-4V condition I) sheet material. Each face sheet was fabricated in three sections, to be butt joined on final assembly. The center face detail contained the three window openings. The two skin splices were located 20.5 in. (52.1 cm) from the longitudinal centerline. The external edge doublers were 2.17 in. (5.5 cm) wide and cut to length on assembly to fit the periphery of the panel.

Honeycomb core details.—Sheets of aluminum honeycomb core of the required densities were vapor degreased and stabilized by bonding a 10-mil (0.0254-cm) layer of AF 126 adhesive and nylon peel ply to one surface. Sections of core were then machined to the required thickness. The core details were cut to the net dimension on assembly.

Major subassemblies.—To facilitate fabrication and ensure a quality bond assembly, several major subassembly operations were performed.

Window frame subassembly.—The three window frames of U-channel cross section required core stabilization of the flange members. Sections of core conforming to the contours of the window frame were cut from sheets of core machined to the required thickness and stabilized on both surfaces with adhesive. These pieces of core were cut in half and Epon 933 adhesive applied to the surfaces of the core and the inside of the channel. The core sections were wedged between the flanges and the assemblies bagged and cured under vacuum in an industrial oven. After bonding the excess core was trimmed at 30° from each flange for splicing to the blanket core details.

Skin splice-core plug assembly.—Two skin splice-core plug assemblies were fabricated prior to the final panel assembly. The assembly consisted of a long, narrow sandwich panel 70 in. (177.8 cm) long and 2 in. (5.08 cm) wide. Two 0.020-in. (0.0508-cm) titanium

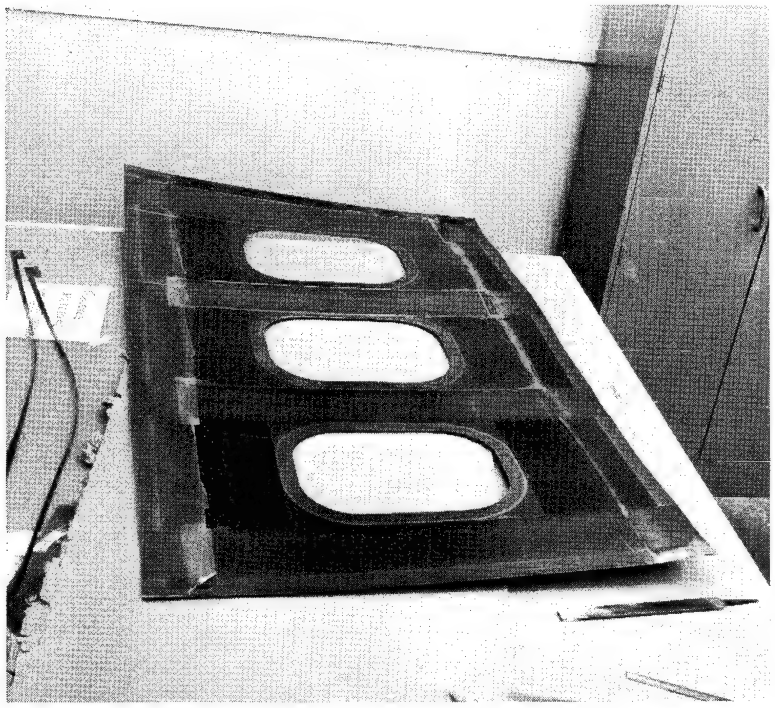

FIGURE C-10.—FIRST-STAGE BORON-EPOXY LAMINATE

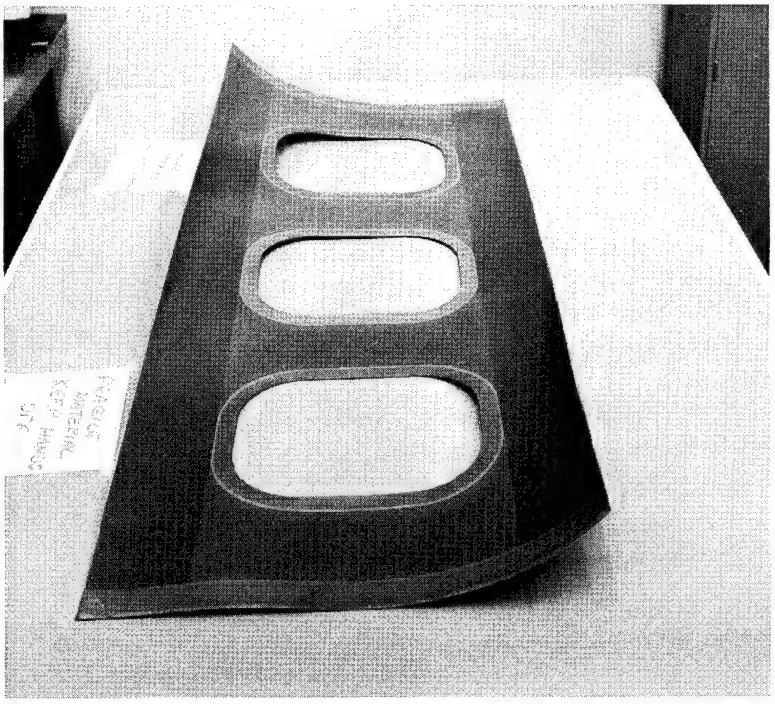

FIGURE C-11.—SECOND-STAGE BORON-EPOXY LAMINATE

(Ti-6Al-4V condition I) doublers formed the face sheets and were bonded to 8.1-lb/ft^3 (129.8-kg/m^3) aluminum honeycomb core. The core at each end of the assembly was replaced to a depth of 2.17 in. (5.5 cm) with a high-density [26.5-lb/ft^3 (425-kg/m^3)] aluminum, reinforced corrugated core. The sandwich was assembled with 15-mil (0.0381-cm) AF 126 adhesive and cured in the autoclave.

Composite skin-blanket core assembly.—Due to the irregular, terraced surface of the boron-epoxy laminate, a drape form bonding process was adopted for bonding the composite reinforcement laminate to the blanket core. This procedure was chosen as a positive means of tolerance control.

The boron-epoxy, precured laminates were prepared for bonding by removing the peel plies and protective tapes and priming the exposed surfaces. The laminate was placed in the bonding tool with the irregular surface upward. A 15-mil (0.0381-cm) layer of adhesive was applied to this surface and the blanket core detail positioned on the laminate. The assembly was bagged and cured using the autoclave pressure to drape form the core to match the irregular surface of the laminate. Following bonding the free surface of the core was machined flat to a total thickness equal to one-half the required panel thickness. The machined core surface was vapor degreased and stabilized with 10-mil (0.0254-cm) adhesive. The completed assembly is shown in figure C-12.

This fabrication procedure, selected to simplify final assembly, results in a weight increase due to the additional adhesive bond line through the center of the panel. This weight penalty was accepted as a preferable trade for the improved tolerance and ease of fabrication.

Final assembly.—The final assembly was accomplished in a single-stage bonding operation, but limited preassembly work was required. Following fabrication of the composite-laminate core subassembly, some residual deformation remained due to the unbalanced layup of the boron-epoxy plies. It was found during prefit that sufficient distortion existed to prevent proper alignment of the details. The two composite-laminate core subassemblies, together with the three window frame plugs, were preassembled by placing a layer of adhesive between the two mating stabilized core surfaces. The core splices were made at the interface of the blanket core and window frame plugs and at the high-density edge core interface. This assembly was then bagged and held under vacuum for several hours, but not cured. Sufficient bond strength was developed by the uncured adhesive to hold the assembly together and keep it flat, as shown in figure C-13.

The following layup and bonding sequence was followed for the final assembly:

- All detail parts were cleaned, peel ply and protective tapes removed, and sprayed with liquid adhesive primer.
- AF 126 film adhesive was applied to the bonding surfaces in accordance with the following schedule:
  - -- 5-mil (0.0127-cm) adhesive was used for metal-to-metal and metal-to-composite bond applications.

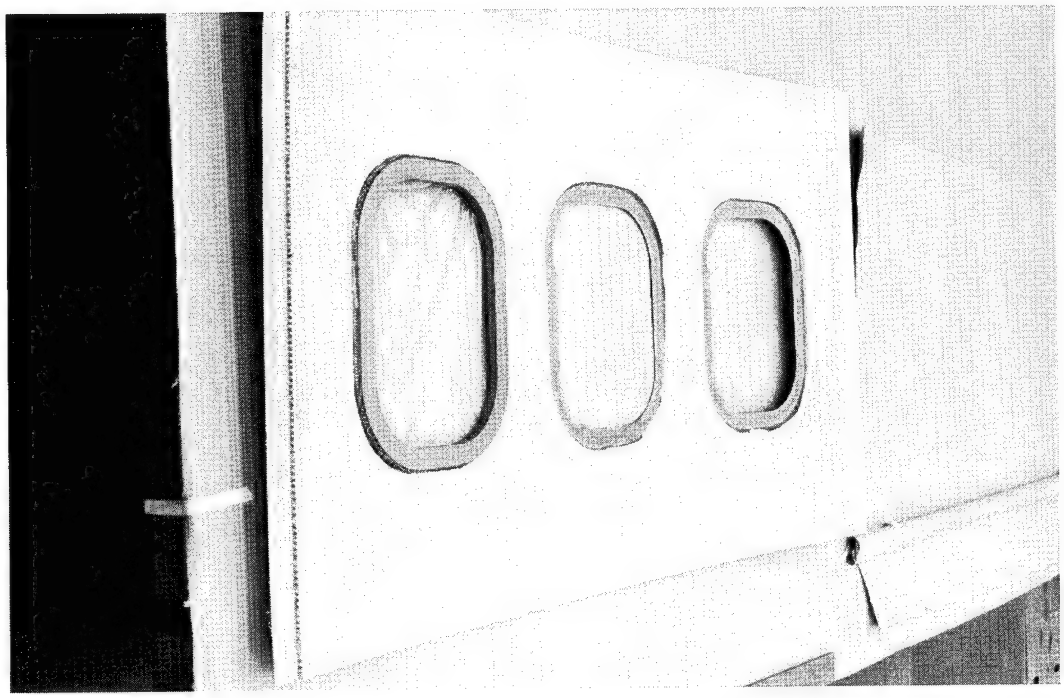

FIGURE C-12.—COMPOSITE SKIN-BLANKET CORE SUBASSEMBLY

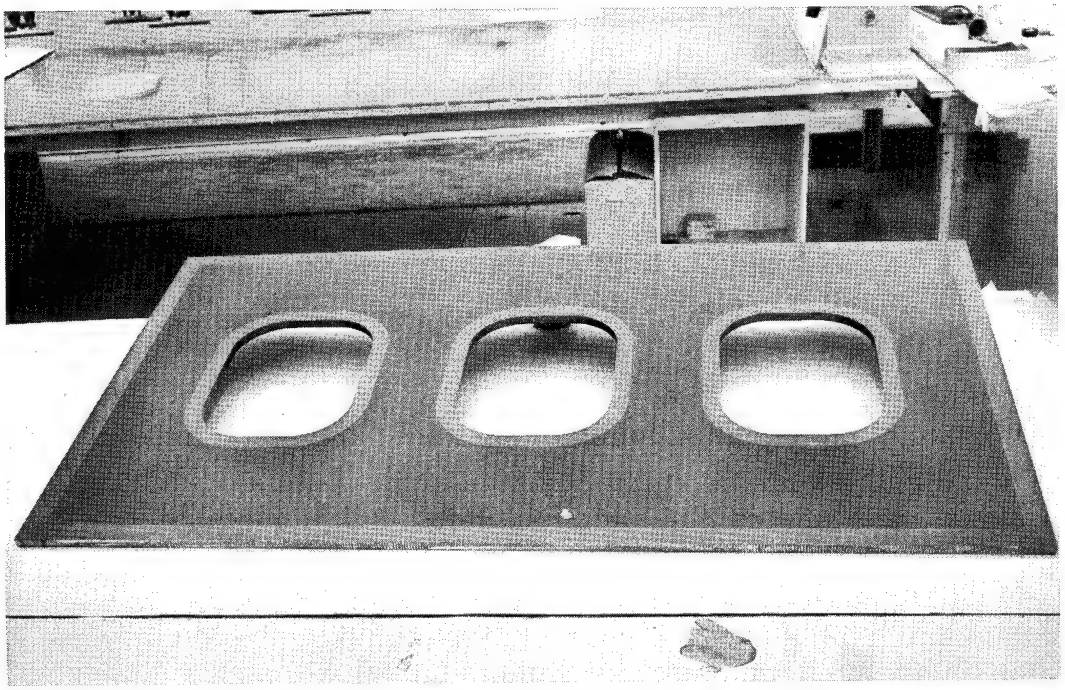

FIGURE C-13.—PREASSEMBLY OF COMPOSITE SKIN-BLANKET CORE AND WINDOW FRAME PLUG ASSEMBLY

- 10-mil (0.0254-cm) adhesive was used for forming the bond line through the center of the panel.

- 15-mil (0.0381-cm) adhesive was used in metal-to-core bond applications.

- The external doublers were positioned on the tool and a metal shim butted next to the inside edge of the doublers. A thin separator film was placed between the doublers and the tool surface and over the shim.

- The center portion of the bottom face sheet was positioned using the window locator tools. The outside portions of the face sheet were then butted to the center face sheet to form the longitudinal face sheet splice.

- The preassembled laminate core window plug assembly was then positioned on the center face sheet. Positioning film was used to reduce the tackiness of the adhesive to permit alignment of the assembly.

- The core details and face sheet splice plugs were installed and the 90° core butt splice formed. This stage of assembly is shown in figure C-14.

- The stack-up was completed with installation of the top face sheet and edge doublers. Positioning film was again used to install the top face sheet. The final assembly prior to bonding is shown in figure C-15.

- Fairing bars were installed around the periphery of the panel and the assembly bagged for the final bond cycle.

The completed window belt panel installed in the ultrasonic through-transmission inspection facility is shown in figure C-16.

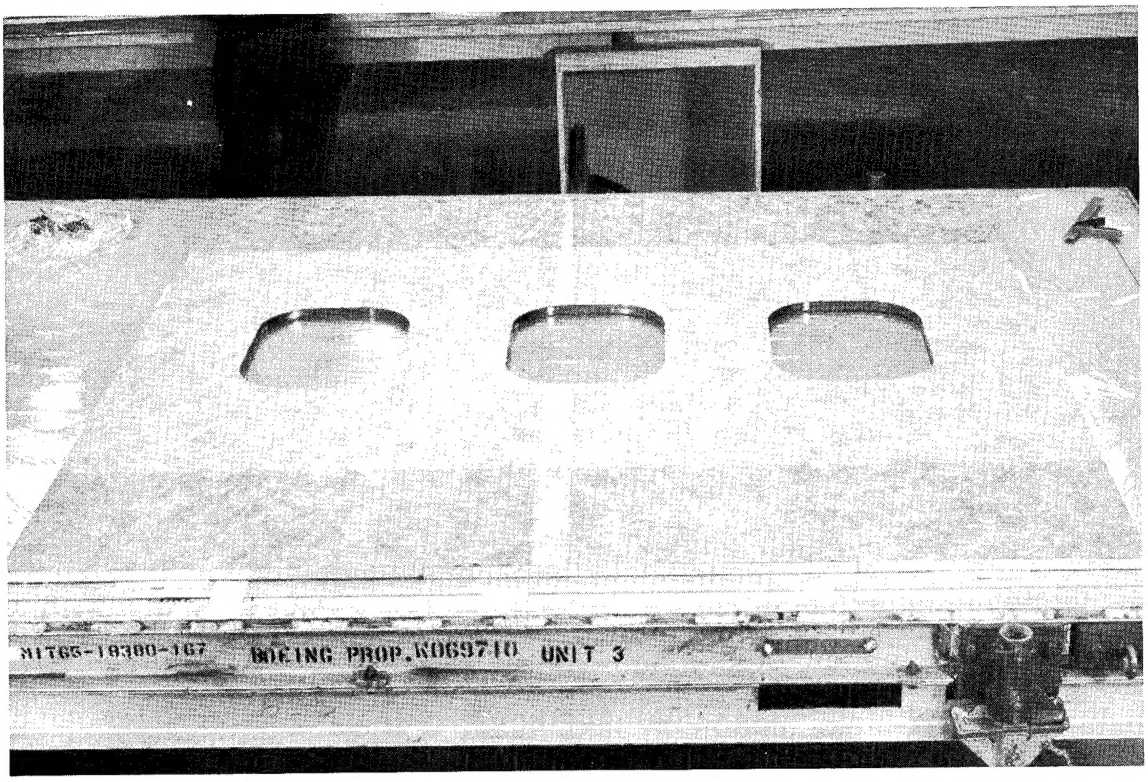

FIGURE C-14.—FINAL ASSEMBLY OF WINDOW BELT PANEL PRIOR TO TOP FACE SHEET CLOSEOUT

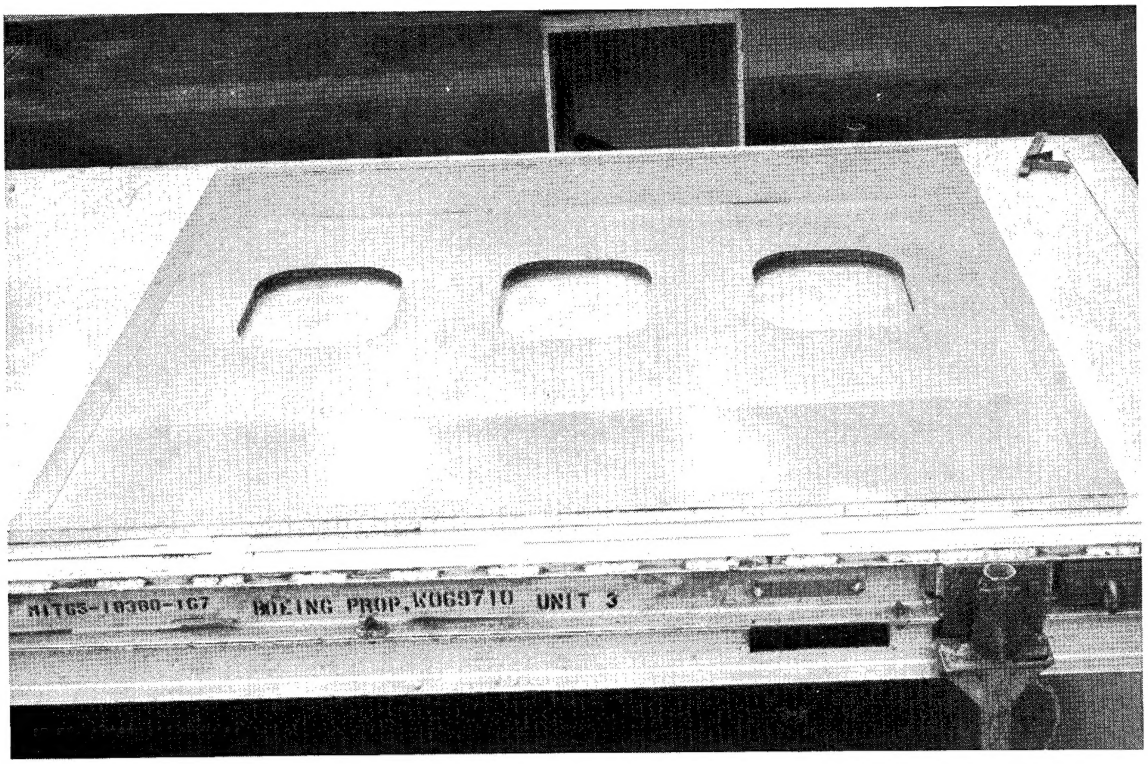

FIGURE C-15.—FINAL ASSEMBLY OF WINDOW BELT PANEL PRIOR TO BONDING

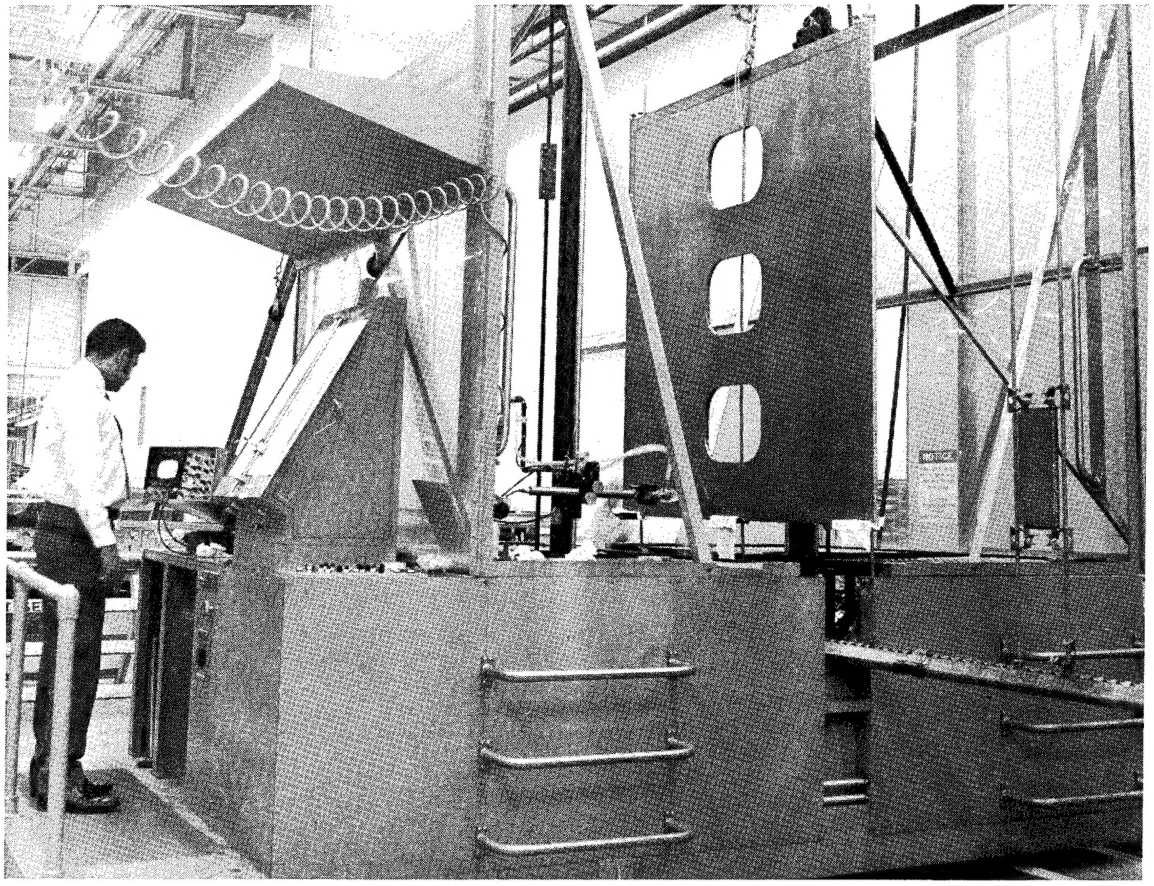

FIGURE C-16.—COMPLETED WINDOW BELT PANEL INSTALLED IN ULTRASONIC THROUGH-TRANSMISSION INSPECTION FACILITY

REFERENCES

1. Oken, S. and June, R. R.: Analytical and Experimental Investigation of Aircraft Metal Structures Reinforced with Filamentary Composites; Phase I–Concept Development and Feasibility. NASA CR-1859, December 1971.

2. Blichfeldt, B. and McCarty, J. E.: Analytical and Experimental Investigation of Aircraft Metal Structures Reinforced with Filamentary Composites; Phase II–Structural Fatigue, Thermal Cycling, Creep, and Residual Strength. NASA CR-2039, June 1972.

3. Hoffman, D. J. and June, R. R.: Cyclic Debonding of Adhesive Joints–Summary Report. NASA CR-2207, February 1973.

4. Hoffman, D. J. and June, R. R.: Cyclic Debonding of Adhesive Joints–Data Report. NASA CR-11219, February 1973.

5. Kelly, J.B. and June, R.R.: Residual Stress Alleviation of Aircraft Metal Structures Reinforced With Filamentary Composites. NASA CR-112207, January 1973.

6. Viswanathan, A. V. and Tamekuni, M.: Elastic Buckling Analysis for Composite Stiffened Panels and Other Structures Subjected to Biaxial Inplane Loads. NASA CR-2216, March 1973.

7. Viswanathan, A. V. and Tamekuni, M.: Analysis for Stresses and Buckling of Heated Composite Stiffened Panels and Other Structures. NASA CR-112227, March 1973.

8. Committee On Metric Practices: ASTM Metric Practice Guide, National Bureau of Standards Handbook 102. U.S. Department of Commerce, March 10, 1967.

9. Smith, S. H., Porter T. R., and Engstrom W. L.: Fatigue Crack Propagation Behavior and Residual Strength of Bonded Strap Reinforced, Lamellated and Sandwich Panels. Proceedings of the Air Force Conference on Fatigue and Fracture of Aircraft Structures and Materials. AFFDL TR 70-144, September 1970.

10. Tripp, L., Tamekuni, M., and Viswanathan, A. V.: A Computer Program for Instability Analysis of Biaxially Loaded Composite Stiffened Panels and Other Structures–Users Manual for BUCLASP 2. NASA CR-112226, March 1973.

11. Metallic Materials and Elements for Aerospace Vehicle Structure. Military Handbook MIL-HDBK-5B, U.S. Department of Defense, September 1, 1971.

*U.S. GOVERNMENT PRINTING OFFICE: 1973-739-154/57